HOKKAIDO UNIVERSITY

Title	Studies on the ultrastructure and growth of skeletons of the test and spines in the sea urchin,Strongylocentrotus intermedius
Author(s)	Motohiro, Shimizu
Degree Grantor	北海道大学
Degree Name	博士(水産学)
Dissertation Number	乙第4091号
Issue Date	1992-03-25
DOI	https://doi.org/10.11501/3088438
Doc URL	https://hdl.handle.net/2115/49806
Type	doctoral thesis
File Information	000000249721.pdf

Hokkaido University Collection of Scholarly and Academic Papers : HUSCAP

主論文

Studies on the ultrastructure and growth of skeletons of the test and spines in the sea urchin, *Strongylocentrotus intermedius*

（エゾバフンウニにおける殻および棘の骨格の成長に関する微細構造学的研究）

清水幹博

１９９２

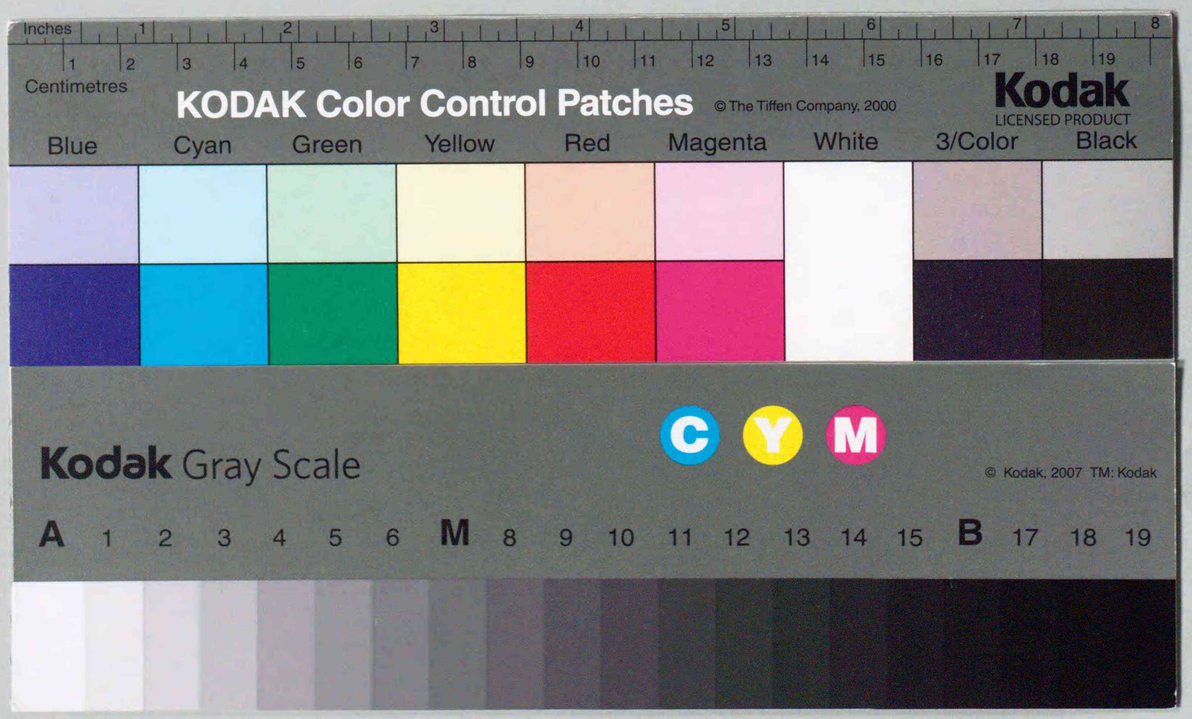

STUDIES ON THE ULTRASTRUCTURE AND GROWTH OF SKELETONS OF THE TEST AND SPINES IN THE SEA URCHIN, *STRONGYLOCENTROTUS INTERMEDIUS*.

MOTOHIRO SHIMIZU

1992

CONTENTS

I. INTRODUCTION 1

II. MATERIAL AND METHODS 6

III. SCANNING ELECTRON MICROSCOPIC CONFIGURATION OF THE SKELETAL TRABECULAE IN RELATION TO THE TEST GROWTH 7

1. MATERIAL AND METHODS 8
2. RESULTS 9
3. DISCUSSION 13

IV. HISTOTOPOGRAPHY AND HISTOCHEMICAL PROPERTIES OF COLLAGEN-LIKE FIBERS IN THE TEST PLATE AND ASSOCIATED TISSUES 17

1. MATERIAL AND METHODS 18
2. RESULTS 20
3. DISCUSSION 23

V. ULTRASTRUCTURES OF CELLULAR AND FIBROUS CONSTITUENTS OF THE ORGANIC STEREOM OF THE TEST PLATE 27

1. MATERIAL AND METHODS 28
2. RESULTS 28
3. DISCUSSION 35

VI. THREE-DIMENSIONAL ULTRASTRUCTURE OF CELLS AND COLLAGEN FIBERS IN THE TEST PLATES AND SPINES 40

1. MATERIAL AND METHODS 41
2. RESULTS 42

3. DISCUSSION 47

VII. CYTOLOGICAL AND ULTRASTRUCTURAL FEATURES AND BEHAVIOR OF COELOMOCYTES 50

1. MATERIAL AND METHODS 51

2. RESULTS 53

3. DISCUSSION 58

VIII. ULTRASTRUCTURE OF SCLEROCYTES AND ASSOCIATED TISSUES IN THE REGENERATING TEST AND SPINES 64

1. MATERIAL AND METHODS 65

2. RESULTS 66

3. DISCUSSION 74

IX. GENERAL DISCUSSION 81

SUMMARY 87

ACKNOWLEDGEMENTS 90

REFFERENCES 91

I. INTRODUCTION

The recent annual yield of sea urchin fishery in Japan has amounted to about 20000 metric tons. It is now economically one of the most important fisheries in Hokkaido; its annual amount reached about 13000 million yens in 1989. Target species for the sea urchin fishery are Strongylocentrotus intermedius, S. nudus, Hemicentrotus pulcherrimus, Anthocidaris crassispina and Pseudocentrotus depressus. Among those, S. intermedius is the most popular species in Hokkaido and is noted as an objective species for artificial propagation. Technologies for seeding and rearing of this species have been considerably developed in a few recent years and many stations for raising seedlings have been built up widely in Hokkaido. About 20 million young sea urchins were artificially produced in 1988 in these facilities.

Technological improvement for artificial propagation of sea urchins requires fundamental knowledge on the growth mechanism of the animals. However, we have little information on the physiology of body growth of this species compared with advanced knowledge on ecological traits. The greater part of the body of this species is occupied by the test composed of dermal skeleton, and therefore, the test growth is of the primary importance for the body growth. From a study of energy-dynamics of this species, Fuji(1967) proposed an excellent concept on the mutual influence between the gonad development and the test growth.

In order to elucidate the mechanism of the test growth of sea urchins, understanding of the morphology is essential. The coronal system of echinoids varies considerably among genera and even among species. Sea urchins including S. intermedius have a hemispherical test which curves strongly in the ambitus toward the apical and the oral areas (Text-fig. 1a). The oral area is nearly flat and the apical area is of a swollen architecture. The coronal system is constructed by many articulated skeletal plates, and at its apex the genital and the ocular, or the terminal, plates are arranged pentagonally around the central periproct to form a characteristic apical system (Text-fig. 1b). The coronal system consists of two types of test plates: poriferous ambulacral and non-poriferous interambulacral plates. A pair of the same type plates pile up regularly to form paired longitudinal rows from the edge of the apical system to the peristome. These rows of ambulacral and interambulacral plates are arranged alternately (Text-fig. 1c); the interambulacral rows are connected to a genital plate and the ambulacral rows to a terminal plate. Consequently, an alternate pattern of radially arranged ambulacral and interambulacral zones is apparent on the naked test surface. Two longitudinal and two latitudinal sutures are found in each test plate. The boundaries at four faces of the plate are called the interradial, adradial, adapical and adoral sutures, respectively. The interradial sutures in the interambulacral zone draw a vertical zig-zag line, because

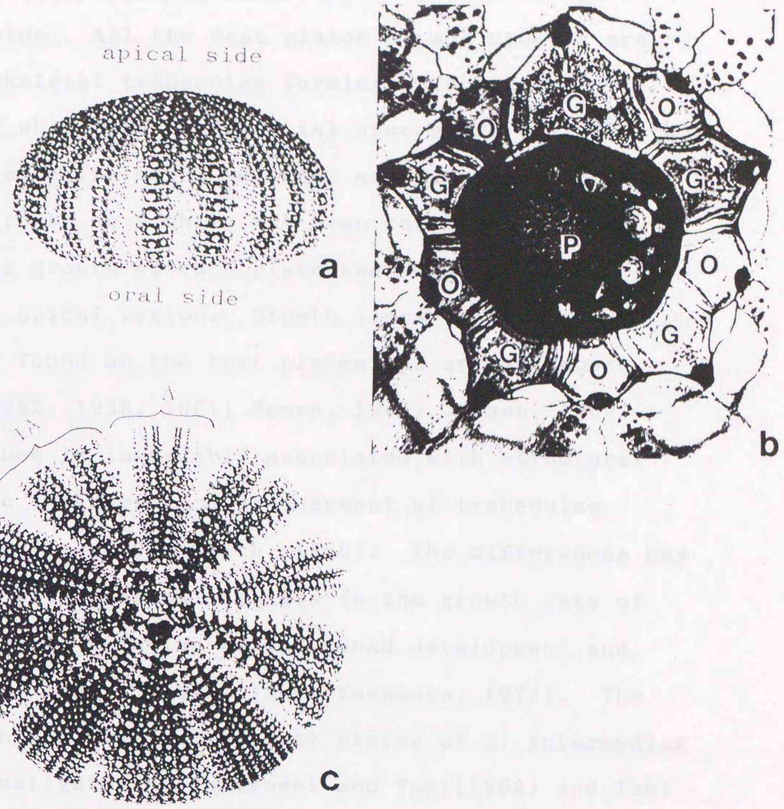

Text-fig. 1. Coronal system of Strongylocentrotus intemedius. a. Lateral view of a necked test. b. Apical system of test plates. c. Upper view of a naked test. A: ambulacral zone; IA: interambulacral zone; P: periproct; G: genital plates; O: ocular plates

each plate of this zone has an arrowhead corner at the interradial side. All the test plates of sea urchins are composed of skeletal trabeculae forming a fenestrate structure, of which the interstitial spaces are filled with an organic tissue including cellular and fibrous elements.

The test growth as a whole has been considered to be induced by the growth of each plate and addition of new plates at the apical region. Growth lines or bands have been commonly found on the test plates and spines (Moore, 1935; Swan, 1952, 1958, 1961; Moore, 1966; Jensen, 1969). Their occurrence is invariably associated with structural differences in thickness and arrangement of trabeculae (Pearse and Pearse, 1975; Smith, 1980). The differences may be correlated with seasonal changes in the growth rate of the test plates in relation to the gonad development and spawning (Fuji, 1967; Jensen, 1969; Kawamura, 1973). The growth pattern and gradient of test plates of S. intermedius have been investigated by Kobayashi and Taki(1969) and Taki (1971, 1972). They demonstrated by a tetracycline labeling method that the largest growth is at the longitudinal suture in each plate and the test growth is active in winter and ceases in summer accompanied with the change of gonadal development.

Crystallographic studies of calcareous skeletons of echinoderms have been made by many investigators (Raup, 1966; Ebert 1967, 1968; Towe, 1967; Currey and Nichols, 1967; Donnay and Pawson, 1969; Nissen, 1969; Weber, 1969;

Weber et al., 1969; Jensen, 1972; Märkel, 1975, 1976a, b, 1981). Also, cytological observations of skeletal tissues in various sea urchins are accumulating; most of the studies are concerned with larval spicules (Okazaki, 1960, 1965; Okazaki and Inoue, 1976; Okazaki et al., 1980), and a few with histology of test plates (Deutler, 1926; Moss and Meehan, 1967; Travis et al., 1967; Travis, 1970). These previous studies on the skeletal tissues of sea urchins were reviewed by Raup (1966) and Simkiss and Wilbur (1985). More recently, several observations of intact and regenerating skeletal tissues of sea urchins were made by electron microscopy to provide further information as to cell participation in the initiation of mineralization in these tissues (Heatfield and Travis, 1975a, b; Märkel and Röser, 1983; Märkel et al., 1986, 1989). Also, a biochemical approach to the spicule formation in a culture system has presented detailed informatin on the role of glycosaminoglycans in the matrix (reviewed by Decker and Lennarz, 1988). In spite of these previous studies on the mineralization of various skeletal tissues of sea urchins, we do not have clear answers to the following questions; (1) in which of the intra- or extracellular space does the mineralization of skeletal trabeculae initiate and proceed ?, (2) how do we identify the sclerocyte in the test plate ?, (3) where do the sclerocytes come from ?, and (4) by what mechanisms are the skeletal trabeculae formed and maintained?

The present study aimed at obtaining detailed

morphological bases to understand mechanisms of the test growth in S. intermedius. The following investigations were conducted:(1) light and scanning electron microscope observations of the skeletal trabeculae of the test plate; (2) histotopographic and histochemical observations of the organic constituents of the test plates; (3) ultrastructural observations of the organic elements of the test plate and coelomocytes; (4) histological and ultrastructural observations of the regenerating test plates and spines.

II. MATERIAL AND METHODS

Hundreds of individuals of a sea urchin, Strongylocentrotus intermedius, ranging from about 5 mm to 72 mm in test diameter, were used in the present study. They were mostly collected from the coastal waters at Usujiri and Toi near Hakodate, southern Hokkaido, Japan. Some of them were reared in a tank with running sea water in the Usujiri Fisheries Laboratory of Hokkaido University at Minamikayabe and others were brought into the laboratory and reared in aquaria equipped with an air-circulating apparatus. Sea water was changed once a month. A sufficient amount of seaweeds, mostly Laminaria, was given as food. Young individuals smaller than 10 mm in test diameter were supplied from the Fisheries Seedling Center of Shakotan-Cho near Yoichi. Water temperature was kept at about 15 °C but the lighting condition was not controlled. Observations were mostly made by light microscopy (LM), scanning electron microscopy (SEM) and transmission electron microscopy (TEM).

Procedures for preparing tissue specimens for microscopic observations (LM, SEM and TEM) are described in each chapter.

III. SCANNING ELECTRON MICROSCOPIC CONFIGURATION OF THE SKELETAL TRABECULAE IN RELATION TO THE TEST GROWTH

In general, echinoids are known to achieve their test growth by both the growth of individual plates at their margins and the addition of new plates toward the adoral side at the apical region (Becher, S.,1914; Becher, E.,1924; Deutler, 1926; Kobayashi and Taki, 1969;Jensen, 1969, 1972; Märkel, 1975, 1976a). Deutler (1926) reported that the interambulacral and ambulacral plates of Echinus esculentus grow by adding new zones along the lateral sides of the plate. Moore(1935) found the presence of dark and light growth zones in ground genital plates of E. esculentus and showed that the dark zones are formed in summer and the light zones in winter. By treating unground plates with xylene and methyl benzoate, Jensen (1969) showed a clear growth pattern composed of alternation of dark and light zones in several sea urchins including Strongylocentrotus, and she supported that the alternate dark and light zones are formed relative to a slow growth in summer and a fast growth in winter, respectively. In S. intermedius, Kawamura (1973) found similar growth zones in ground sections of the genital plates by a similar method, and used the zones for age determination of this species. Kobayashi and Taki (1969) demonstrated a growth gradient of the test of this species by a tetracycline labeling method. Using a similar labeling method, Märkel(1975, 1976a) presented very detailed evidence of the growth pattern in the coronal system in

Paracentrotus lividus and Arbacia lixula.

Admitting that the dark and light zones represent a change in the growth rate of the test plate (Jensen, 1969), and that the growth gradient differs in four directions of the plate (Kobayashi and Taki, 1969), it is presumed that there could be local differences of the stereomal structure of the plate corresponding to changes in the growth rate.

In this chapter, three-dimensional features of the internal structure of the test skeleton of S. intermedius are described based on SEM observations of fractured surfaces. X-ray micrography (microradiograpghy) of ground sections of test plates was performed to examine mineralizing conditions in relation to the growth activity.

1. MATERIAL AND METHODS

About fifty individuals of young and adult S. intermedius, ranging from 5 mm to 65 mm in test diameter, were used. The entire test and fractured fragments were fixed with a modified Karnovsky's (1965) fixative for 2-24 h at 4 °C. The fixative used was 2% paraformaldehyde-2.5% glutaraldehyde in a mixture of 0.1 M cacodylate buffer solution and sea water (1:1), pH 7.6. The fixed test was cut into blocks of 3-5 plates or pieces smaller than one-half of a plate, and then bleached with 5% sodium hypochlorite to remove organic elements from the skeleton. The dried specimen mounted on a stub was coated with

particles of an alloy of platinum-paradium using a sputter coater (JEOL JFC-100). Specimens were examined by scanning electron microscopes (JEOL JSM-25 and Hitachi S-1000) mostly at 25 kV.

Some sea urchins were fixed with 10% neutral formalin-sea water. Some test plates were treated with xylene and methyl benzoate (Jensen, 1969) to observe growth zones, and others were ground into about 50-100μm thick sections for microradiography. An X-ray micrograph apparatus (Sofron, SRO-M 50, Soken Co. Ltd.) was operated mostly at 30 KV, 3 mA. The time of exposure was about 10 min.

2. RESULTS

(A) Microradiography of ground sections of the test plate

Unground test plates of S. intermedius after treated by the Jensen's (1969) method showed alternating dark and light growth zones; they were particularly evident at the marginal area of the plate. Ground sections after the same treatment revealed a clearer pattern of light and dark zones in the entire plate under a light microscope with reflective light. Plates around the ambitus showed the largest zone number as well as plates of the apical system, of which the genital or the ocular (terminal) plates had narrower bands in a more distinct pattern compared with other plates (Fig. 1). Usually, the light zones were wider than the dark zones.

X-ray micrographs of ground sections of the plates showed some more details of the growth zones. In most plates

ground tangentially (Fig. 2) or vertically (Fig. 3), each zone was composed of several bands of alternately arranged dense and loose meshworks of calcified trabeculae. However, thin ground sections (less than 100μm thick) used for X-ray micrography showed a decreased number of zones because some of the zones became indistinct and, therefore, it was not possible to find accurate correspondence in position of the zones and meshwork bands. The apical plates showed a clearer banding pattern of meshworks compared with other plates (Figs. 4, 5). The dense meshwork was seen less porous and constructed of thick compact trabeculae, whereas the loose meshwork appeared as a more porous skeleton made up of thinner trabeculae. The growth direction of the trabeculae in a plate was easily observed in the microradiograph (Fig. 6).

A new test plate is attended at the apical region of each row as the test grows. Text-figure 2 represents the plate number at a row of interambulacral (IA) zone of S. intermedius of various test diameters. Individuals of test diameters 65-71 mm had 25-32 plates in a row, whereas those around 10 mm had about 10 plates. The regression indicates that the plate number of this species increases rapidly among 5 mm-20 mm in test diameter. X-ray micrographs clearly revealed the addition of new plates occurring at the site between the genital system and the adjacent plates (Fig. 7).

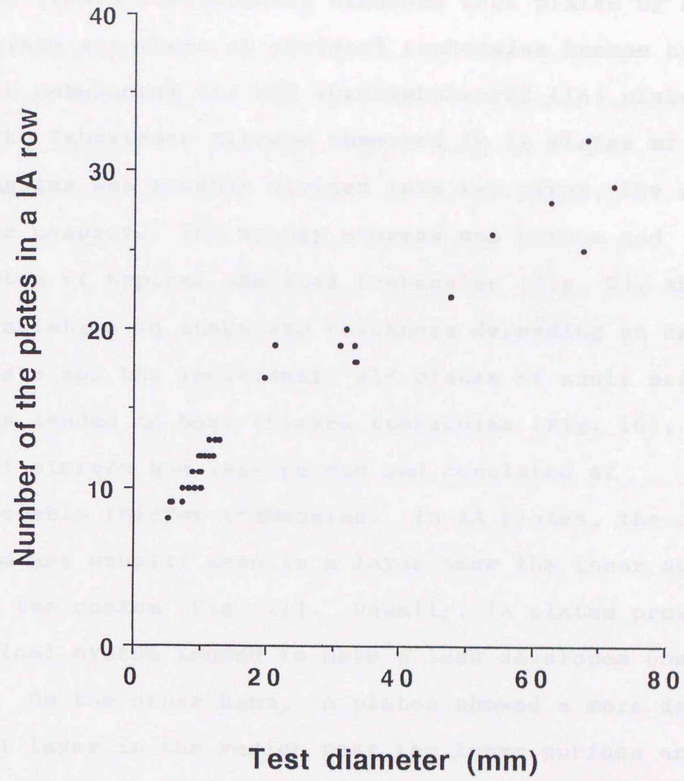

Text-fig. 2. Relationship between the number of the plates in a row of IA zone and the test diameter in *S. intermedius*

(B) Three-dimensional ultrastructure of the skeletal trabeculae of the test plates

When viewed sufficiently bleached test plates by SEM, a fenestrate structure of skeletal trabeculae became apparent in both ambulacral (A) and interambulacral (IA) plates (Fig. 8). The fenestrate stereom observed in IA plates of S. intermedius was roughly divided into two types, the spongy and the compact. The spongy stereom was porous and consisted of typical skeletal trabeculae (Fig. 9), showing some varieties in shape and thickness depending on ages of the plate and the individual; old plates of adult sea urchins tended to have thicker trabeculae (Fig. 10). The compact stereom had less porous and consisted of considerably thicker trabeculae. In IA plates, the compact stereom was usually seen in a layer near the inner surface facing the coelom (Fig. 11). Usually, IA plates proximal to the apical system tended to have a less developed compact layer. On the other hand, A plates showed a more developed compact layer in the region near the inner surface and even in the interior region. Both IA and A plates proximal to the apical system tended to have less developed region of compact setreom. In young sea urchins, the spongy stereom was more conspicuous in both IA and A plates (Fig. 12), and the compact streom partially covered the inner surface of the plates (Fig. 13). However, in the interior of these young plates, small transverse areas of compact stereom were sometimes seen. The appearance of the compact stereom in

the spongy area seemed to develop to a pattern of the dense and loose meshworks observed by microradiography of the test plate.

The stereomal structure of basocoronal plates revealed a different appearance from the above two types particularly in plates proximal to the peristomial membrane (Fig. 14). The structure had less porous and was built up by thicker and sometimes irregularly shaped trabeculae (Fig. 15). The irregular stereom of this type appeared frequently also in A plates of adult sea urchins but not of young sea urchins (Fig. 16).

The trabeculae sufficiently dissolved off the organic elements by the hypochlorite treatment usually showed a smooth surface in the interior stereom as seen in Figs. 9-10. However, some trabeculae which appeared to be actively growing presented a rough surface by showing numerous small crystals of short pillars attached on it (Fig. 17). On the other hand, resorbing trabeculae exhibiting an irregularly rugged surface were also observed (Fig. 18). Sometimes, they were considerably etched by erosion and partially torn off (Fig. 19). These resorption features of trabeculae were detected near the suture of plates (Fig. 20). The resorption of trabeculae near the suture was more conspicuous in plates of young urchins (Fig. 21). Fractured surfaces of trabeculae of S. intermedius represented commonly a layered or a ripplet structure (Fig. 22).

Addition of a new plate was observed at the apical region

between an apical plate and the adjacent plate (Fig. 23). The new plate appeared at the sutural space, where numerous fibrous bundles interconnecting the new plate and the adjacent old plate were observed in a weakly bleached specimen (Fig. 24).

3.DISCUSSION

The microradiography presented a clear alternate pattern of dense and loose calcified meshworks in both light and darkgrowth zones of the test plate in S. intermedius; the dense meshwork was more calcified than the loose meshwork. It was not possible to show a precise positional relationship between the growth zones and the meshwork bands. However, accepted that the light and dark zones are formed in winter and in summer, respectively (Moore, 1935; Jensen, 1972; Kawamura, 1973), the presence of the alternate meshwork pattern in each zone may result from a rhythmic growth within the seasonal change of skeletal deposition. It also suggests that the rhythm of calcification in this species is more active in winter than in summer because the light zone was composed of much more meshworks than the dark zone. As Fuji (1967) argued, a change of energy allotted for the gonad development and the test growth in summer and winter may induce the change of calcifying activity of test plates in a gross, seasonal level. Some minor factors effective on the calcifying activity, however, may take part in the rhythmic or periodical formation of different

meshworks, though the mechanism remains unknown.

S. Becher (1914) and E. Becher (1924) showed in Heterocentrotus mammillatus and Echinus esculentus, respectively, that the latitudinally directed calcareous trabeculae grow curving toward the perradial (interradial) and adradial sides of the plates, while the orally/apically oriented ones grow in a right angle toward the adapical and adoral sides of the plates. A similar growth pattern of the test plate has been reported in several Strongylocentrotus species other than S. intermedius by scanning electron microscope studies (Jensen, 1972). The results presented by X-ray micrography and SEM in the present study showed a similar growth pattern of trabeculae also in S. intermedius.

The calcite crystals in test plates grow stereographically in three directions, forming the skeletal stereom of a three-dimensionally unique fenestrate structure. In S. intermedius, the fenestrate skeleton of both the A and IA plates presented basically two types of stereoms, the spongy and the compact. The spongy stereom was found mostly in both the interior and the peripheral sutural area of IA plates but less in those of A plates. In young urchins' plates, this structure was dominant. On the other hand, the compact stereom was dominant in a layer at the inner surface of adult urchins' plates and less developed in young urchins' plates. Modifications of compact structure appeared in the plates proximal to the peristome.

The sutural areas of test plates in adult S. intermedius

are known to be actively growing sites (Kobayashi and Taki, 1969; Taki, 1971, 1972), where the spongy stereom prevailed. In young urchins' plates, which grow more actively than those of adult urchins, the spongy streom was shown in overall areas. This suggests that the presence of spongy stereom represents an actively growing area. On the other hand, the inner surface area of every plate and older plates proximal to the peristome are known to show less growth or occasional resorption in some urchin species (Raup, 1966). The stereoms of these areas were of the compact structure. Skeletal stereoms in many species of echinoids generally are not uniform in structure among species, plates and even in a single plate. The stereoms of a single type also underwent changes as the plates became thicker (Pearse and Pearse, 1975; Smith, 1980). Simkiss and Wilbur (1985) suggested that the growth rate of the test affects the type of stereom: a fast growth is associated with a labyrinthic or more porous stereom and vice versa. The irregular compact structure observed in the basocoronal plates may have been caused by some growth inhibiting factors such as partial distotion; similar phenomena have been reported in E. tribuloides and Diadema antillarum (Märkel, 1981) and in chemically polluted Tripneustes cf. gratilla (Dafni, 1983).

Jensen (1972) described the ultrastructure of resorbing trabeculae, especially of primary tubercles in young sea urchins. In the present study, the trabecula resorption was observed often at the inner surface of sutural areas,

especially in young urchins. The trabecula resorption at the actively growing site may represent reorganization of trabecular arrangement prior to deposition of new trabeculae.

A layered or rippled structure, generally called a conchoidal fracture, was disclosed by SEM observations of fractured surface of almost all trabeculae. This shows that the trabecular skeleton is polycrystalline in nature (Towe, 1967). Some organic substances may be incorporated as calcifiable matrix in the aggregation of crystallites (Weber et al., 1969). Such organic substances have been recently reported as minor components of test plates and teeth in Paracentrotus lividus (Weiner, 1985) and Lytechinus variegatus (Veis et al., 1986).

IV. HISTOTOPOGRAPHY AND HISTOCHEMICAL PROPERTIES OF COLLAGEN-LIKE FIBERS IN THE TEST PLATE AND ASSOCIATED TISSUES

The interstitial spaces of the skeletal stereom are occupied by some organic elements which form an inverse stereomal structure, called the organic stereom. The organic stereom contains cells and fibrous elements (Moss and Meehan, 1967; Travis, 1970; Travis et al., 1967). In their tetracycline labeling study of test plates in S. intermedius, Kobayashi and Taki (1969) showed that test plates actively grow at the sutural areas, especially along longitudinal sutures, and their growing activity is different between summer and winter. They suggested that biochemical nature of the fibrous elements distributed at the sutural areas change seasonally, possibly in company with alteration of other components such as acid mucopolysaccharides associated with the fibers. Travis et al. (1967) presented ultrastructural evidence in S. droebachiensis and Lytechinus variegatus that collagen fibers similar to typical mammalian ones constitute the organic matrix of mature test plates onto which the calcification occurs. Based on histological observation in Arbacia and other echinoids, Moss and Meehan (1967) suspected the role of the sutural and other collagen-like fibers in sea urchin test as calcifiable matrix, and considered that the sutural system acts as a stress-breaker. Nichols and Currey (1968) also doubted that collagen fibers

in the test plates function as organic matrix in initiating the mineralization. However, Travis (1970) asserted that calcite crystals in sea urchin skeletons are deposited in specific regions of typical repeating periods (600-700 Å) of collagen fibrils.

Collagen fibers, acid mucopolysaccharide-protein complexes, and lipids are important organic components in initiation of mineralization of various hard tissues (Weidmann, 1963; Schiffmann et al., 1970). However, it is not clear whether those organic substances exist in the test plate and, if present, what roles they play in the test growth. In a sea urchin test, a precise distribution of these substances must be investigated to elucidate the mineralization mechanism. In this chapter, the histotopograpy and histochemical nature of fibrous elements and their associated mucosubstances are examined with decalcified test plates and associated tissues including the spine and the peristomial membrane.

1. MATERIAL AND METHODS

About sixty S. intermedius, 31-100 g in body weight and 30-70 mm in test diameter, were used. A fresh test was cut into pieces so as to include both spine and the sutural area in each pieces. The test pieces thus obtained and the simultaneously removed peristomial membrane were treated as follows for histological and histochemical observations.

The fixatives used were: 10% neutral formalin for von Kossa stain, Helly's fluid mainly for Azan stain, Carnoy's fluid for periodic acid-Schiff reaction, 1% cethylpyridinium chloride in either 5% formalin or 4% glutaraldehyde for acid mucopolysaccharides, and the McManus's method for lipids. Most of the fixed tissue pieces were sufficiently treated with a 5% EDTA solution containing 5% formalin or 4% glutaraldehyde adjusted to pH 7.4 with 0.1N sodium hydroxide. When Carnoy's fluid was used, the fixed tissues were decalcified with 5% trichloroacetic acid in 90% ethanol.

The following staining and histochemical procedures were applied to paraffin sections cut at 4-10μm thick: (1) hematoxylin and eosin stain; (2) von Kossa's stain for calcium salts; (3) stainings with Azan, Van Gieson's picro-fuchsin, Weigert's resorcin-fuchsin (Pearse, 1960), some accompanied by digestion with 1% pepsin or 1% trypsin for the connective tissue; (4) metachromatic reactions with toluidine blue, pH 2.5 (Lison, 1960) and alcian blue (pH 1.0) for acid mucopolysaccharides (Luna, 1968); some digested with 1% testicular hyaluronidase (Worth. Biochem. Co.) prior to the toluidine blue staining, and the methylation and saponification test according to Fisher and Lillie's method (Lison, 1960); metachromatic reaction with toluidine blue (pH 3.4) containing heavy metal ions (Lison, 1960); pretreatment with pyridine (60 °C, 24-48 h) in order to remove lipids in metachromatic reactions; (5) periodic

acid-Schiff (PAS) reaction accompanying the digestion test with 1% amylase and acetylation and saponification test after the McManus and Cason's method for PAS-positive materials (McManus, 1946a; Lison, 1960); (6) Sudan black B stain according to McManus (1946b) for lipids, contrasted with hot pyridine- and hot chloroform-methanol treated preparations at 60 °C for 24-48 h (Irving, 1963). Among the above-mentioned procedures, deamination and digestion were applied in some preparations to examine whether or not the mucosubstances are complexed with proteins.

2. RESULTS

(A) Histotopography of fibrous elements

The decalcified plate revealed a dermal fenestrated structure of organic constitution, or the organic stereom, which corresponds to a cast of the skeletal stereom. The organic stereom, which appeared as a reticulous structure in paraffin sections, included abundant cellular and fibrous elements, and its dermal tissue was covered with a multilayered epithelium and a monolayered coelomic epithelium at the outer and the inner surface, respectively. The fibrous elements were localized abundantly at the sutural areas of the plates and rather poorly at the outer and the inner surfaces (Fig. 25); the fibers forming thick bundles extended to the adjacent plates over the systems of both longitudinal (zig-zag) and latitudinal (straight) sutures (Fig. 26). Thick fibrous bundles were also abundant

in the non-calcified portion of the peristomial membrane (Fig. 27) and in the inner connective tissue layer supporting the spine (Fig. 25). The interior of the test plate and calcified portions (the ossicles) of a peristomial membrane were occupied by a reticulous structure without the fibrous bundles.

The fibrous elements found in the plate and associated tissues revealed similar staining behaviors to collagen fibers in vertebrates by azan and Van Gieson's picro-fuchsin stains. However, the fibers were stained slightly different from typical collagen fibers in Weigert's resorcin-fuchsin stain and they showed less resistant for pepsin digestion than typical collagen fibers (Table 1). No such collagen-like fibers were noticed in the organic phase of either the interior of the test plate (Fig. 28) or calcified islands (the ossicles) of the peristomial membrane (Fig. 29). These areas display a reticulous structure composed of thin organic substances and cellular elements, but the latter was indistinct in outline and the former showed very weak stainabilities (Table 1). A similar reticulous structure was found also in the decalcified spines (Fig. 25).

(B) Histochemical nature of collagen-like fibers and reticulous structure

The collagen-like fibers in the test plate showed metachromatic reactions with toluidine blue at low pH (Fig. 30). The metachromasia never disappeared through

Table 1. Histological characteristics of collagen-like fibers and the reticulous structure in the test plate and the associated tissues

	Test plate			Spine		Peristomial membrane	
	Suture	Inner and Outer surface	Mid-portion	Inner layer (connective tissue)	Outer layer (muscle)	Calcified area	Non-calcified area
Haematoxylin and eosin	purple	purple	weak purple -unstained	deep purple	pinkish red	weak purple -unstained	deep purple
Azan	deep blue	blue	weak blue -unstained	deep blue	red	weak blue -unstained	deep blue
Van Gieson's picro-fuchsin	bright red	red	red -weak red	bright red	yellow	weak red	bright red
Weigert's resorcin-fuchsin	weak blackish blue	weak blackish blue	unstained	weak blackish blue	unstained	unstained	weak blackish blue
Digestion							
by trypsin	relatively slow	relatively slow	rapid	relatively slow	rapid	rapid	relatively slow
by pepsin	relatively rapid*	relatively rapid	relatively slow	relatively rapid*	very slow	relatively slow	relatively rapid*

* A longer time was required for the complete digestion of fibers compared with typical mammalian fibers.

dehydration procedures. Alcian blue stained these fibers positively. As indicated in Table 2, the metachromasia with toluidine blue showed no distinct difference between treatments with and without heavy metals. The metachromasia with toluidine blue and staining with alcian blue of the fibers were recovered after a saponification procedure for methylated preparations, though the intensities were somewhat reduced compared with intact control preparations. Deamination caused a more intense reaction (Fig. 31). Digestion with hyaluronidase reduced the reactivities.

The reticulous structures in both the interior of the test plate and the ossicles of the peristomial membrane showed no positive evidence for acid mucopolysaccharides by any of the above histochemical procedures.

The collagen-like fibers were observed to react to PAS. Their PAS-positivity was relatively intense in the suture (Fig. 32), the inner connective tissue supporting the spine, and the peristomial membrane (Fig. 33). It was not affected by digestion with amylase, recovered after saponification for acethylated preparations, and reduced after deamination.

The reticulous structures in both the interior of the test plate and the peristomial membrane showed a feeble PAS-positive reaction (Figs. 32, 33). Occasionally, strong PAS-positive granules, which may be cellular elements, were found to lie scattered in the reticulous structure (Fig. 34).

Sudanophilic substances were found by staining with Sudan

Table 2. Histochemical characteristics of the collagen-like fibers and the reticulous structure in the test plate and the associated tissues

	Test plate			Spine		Peristomial membrane	
	Suture	Inner and Outer surface	Mid-portion	Inner layer (connective tissue)	Outer layer (muscle)	Calcified area	Non-calcified area
Metachromasia with TB (pH 2.5)	2	2-1	N-Ort	2	N	N	2
after M & S	1	1-N	N	1	N	N	1
H-ase	1-N	1-N	N	1-N	N	N	1
deamination	3	2	1	3	1	1	3-2
Metachromasia with TB (pH 3.4) containing							
2mEq UO2(NO3)2	2	2-1	N	2	N	N	2
2mEq Ba(NO3)2	2	2-1	N	2	N	N	2
100mEq Ba(NO3)2	2	2-1	N	2	N	N	2
Alcian blue (pH 2.5 and 1.0)	2	2-1	1-N	2	1-N	1-N	2
after M & S	1	1	N	1	N	N	2
H-ase	1	1	N	1	N	N	1
deamination	3-2	2	1	3	1	1	3-2
PAS-reaction	2	1	1	2	1-N	1	2
after A & S	2	1	1	2	1	1	2
A-ase	2	1	1	2	1	N	2
deamination	1	1-N	1-N *	1	N	1-N *	1
Sudan black B	1	1	N	1	3-2	N	1
after Py and/or C-M	1	1	N	1	1	N	1

TB: toluidine blue; M & S: methylation and subsequent saponification; H-ase: digestion with 1% testicular hyaluronidase; A & S: acetylation and subsequent saponification; A-ase: digestion with 1% amylase; Py and/or C-M: extraction with hot pyridin and/or chloroform-methanol; Ort: orthochromasia.
Intensities were indicated by: 3(strong), 2(moderate), 1(weak), or N(negative).

* Strong PAS-positive granules were occasionally found.

black B were found on both the collagen-like fibers and the outer spine muscle fibers (Fig. 35). The reticulous structure, except the cellular elements, was shown to be negative. The stainabilities of the collagen-like fibers was not reduced even after extraction of lipids by a treatment with pyridine or chloroform-methanol for 48 hours (Fig. 36).

3. DISCUSSION

The collagen-like fibers of the test plate and associated tissues showed somewhat different sensitivities for stainings and enzyme digestion from those of typical, mature collagen fibers in vertebrate (Table 1). Moss and Meehan (1967) reported an elastin-positive reaction in sutural connective tissue in Arbacia. Marks et al.(1949) showed in their X-ray diffraction study of Asterius and Arbacia the presence of a collagen-type protein that is different from the collagen of vertebrates based on its small diffraction order. Travis (1970), in an electron microscope study of S.droebachiensis, found collagen fibers very similar to typical mammalian ones in the organic matrix of the test plate. Cconsidering sensivities for stainings and enzyme digestions presented in Table 1, it is supposed that the collagen-like fibers are possibly composed of mature and immature collagen fibers with some non-collagenous fibrous proteins.

Likewise the typical collagen fibers, the collagen-like fibers in the sea urchin test would have a complicated

composition together with acid mucopolysaccharides, PAS-positive materials and sudanophilic substances. Acid mucopolysaccharides may be classified into two groups based on the metachromatic and alcianophilic nature, the non-sulfated group such as hyaluronic acid and the sulfated group such as chondroitin sulfate. The positive reactions for toluidine blue after saponification for methylated preparations and after digestion with 1% hyaluronidase prove the coexistence of both sulfated and non-sulfated acid mucopolysaccharides.

Taking the positive reactions for proteins into consideration, the amylase-resistant PAS-positive materials may be a neutral polysaccharide-protein complex (Banga and Baló, 1960; Schultz-Haudt and Eeg-Larsen, 1961). This complex may also contain acid glycoproteins such as sialic acid (Quintarelli, 1968).

Sudanophilic substances resistant to extractions with both pyridine and chloroform-methanol may not certainly be simple lipids nor phospholipids (Irving, 1963). They may be complexed with non-fibrous proteins and combined tightly to the collagen-like fibers (Melcher, 1966).

The collagen-like fibers combined with mucosubstances were detected in actively growing areas of the test plate. This topographical evidence suggests that the fibers play an important role in the test growth, but their direct participation as a calcifiable matrix in initiating the mineralization is questionable because the fibers are also

distributed in non-calcifiable tissues such as the spine connective tissue and the peristomial membrane. In general, sulfated mucopolysaccharides are known to be capable of binding calcium ions (Sobel and Burger, 1954; Kobayashi, 1971). Sudanophilic substances or lipids can also bind calcium ions (Irving, 1963). Therefore, these substances in association with collagen fibers are considered to be a nucleating entity in initiating the mineralization. Evidenced by a loss or depolymerization of sulfated mucopolysaccharides just prior to the calcification of cartilage, chondroitin sulfates have been considered to have an inhibitory effect in biological calcification (Weidmann, 1963; Poole et al., 1989). Experimental evidence indicates that the protein-polysaccharide complex permits an accumulation of calcium near the seeding site in mineralization, but does not allow its sedimentation (Kobayashi, 1971).

As suggested by previous workers (Moss and Meehan, 1967; Currey and Nichols, 1967, 1969; Nichols and Currey, 1968), the collagen-like fibers detected in the suture of test plates may not participate in the mineralization as a calcifying matrix. Possibly the protein-polysaccharide complex decomposed by some cellular activity may release attracted calcium ions, which may be deposited subsequently to form calcite crystals at spaces just contiguous to an organic framework, or the reticulous structure. Formation of the organic framework must be a prerequisite for the

growth of skeletal trabeculae. Cellular elements in the test plate and calcified islands of the peristomial membrane may participate in the formation of organic framework and in the primary deposition of calcite crystals as has been reported in the spicule formation of sea urchin larvae (Okazaki, 1960, 1965; Gibbins et al., 1969). Recent in vitro culture experiments of mesenchyme cells from sea urchin larvae suggested that the collagen fibers are essentially required in spicule formation as a compartment of the extracellular matrix indispensable for cell adhesion (Blankenship and Benson, 1984; Decker and Lennarz, 1988). The collagen-like fibers distributed in the test plate, especially at the sutural area may have a similar role in the initiation of mineralization in the skeletal growth.

V. ULTRASTRUCTURE OF CELLULAR AND FIBROUS CONSTITUENTS OF THE ORGANIC STEREOM OF THE TEST PLATE

The previous histological and histochemical observations of decalcified test plates showed that the collagen-like fibers are distributed in the actively growing sites of the plates. In addition to the collagen-like fibers, several types of cell elements, some of which were probably derived from wandering coelomocytes in the coelomic fluid, exist abundantly in the organic stereom, but their roles and cytological characteristics are not well known (Deutler, 1926; Moss and Meehan, 1967). Kindred (1924) suggested that the leucocyte, which is a kind of coelomocytes, is involved in the regeneration of the test plate. Ultrastructural studies of regenerating spines of S.purpuratus showed that several kinds of cells composed of spherule and non-spherule cells appear around the newly forming microspines and one of them may act as sclerocytes (Heatfield and Travis, 1975a, b). Recently, detailed ultrastructural observations on the sclerocytes and some other cells have been done with the spines (Märkel and Röser, 1983) and teeth (Märkel et al., 1986) of E. tribuloides. However, we have little information on cellular elements in the normal test plates of adult sea urchins. In this chapter, results of transmission electron microscope (TEM) observations on the cell elements and collagen fibers in the organic stereom are presented with reference to the skeletal growth of the test plate in S. intermedius.

1. MATERIAL AND METHODS

The interambulacral test plates of young and adult S. intermedius (10-65mm in test diameter) were used. The plates were cut into small pieces and fixed with the PG fixative for 2-24 h at room temperature. Subsequently, osmicated specimens were decalcified with a 5% EDTA solution (pH 7.6) containing 8% sucrose for one to three weeks at 4 °C or room temperature. Decalcified tissues were dehydrated with a series of 50-100% ethanol and then embedded in an epoxy resin (Epon 812 or Epok 812) through QY-1. The resin-embedded tissues were cut into semithin and ultrathin sections. Ultrathin sections were stained with uranyl acetate and lead citrate for transmission electron microscopy (HU-12 and H-6000, Hitachi). Semithin sections were stained with methylene blue and azur II (Richardson et al., 1960) or alkaline methylene blue-basic fuchsin (Huber et al., 1968) for light microscope observations.

Some decalcified tissues without osmication were embedded in JB-4 (Polyscience) through ethanol dehydration and then cut into semithin sections. Hematoxylin-eosin and azan stains were applied to JB-4 sections for examination with a light microscope.

2. RESULTS

Semithin sections of the test plate revealed the organic stereom firmly framed by a thin membranous structure

separating it from the calcareous trabeculae, which were represented by many "holes" after decalcification (Fig. 37). Numerous cells of different cytological characteristics were seen within the organic stereom. A considerable number of cells were accumulated with collagen-like fibers at the peripheral sutural area (Fig. 38). Small aggregations of cells were observed in many places throughout the decalcified plate.

In the sutural area, small basophilic cells (3-7μm, mainly about 5 μm in diameter) were observed often among the bundles of collagen fibers (Fig. 39). These cells often had an intimate association with a thin membranous structure which enclosed the holes of decalcified skeleton (Fig. 40). They had strongly basophilic cytoplasm and the nucleus which occupied a large proportion of the whole cell body and had condensed chromatin.

When viewed by TEM, the cytoplasm of cells with short or elongated processes was strongly electron dense owing to a lot of free ribosomes and an electron dense ground substance (Fig. 41). The cytoplasmic processes had small bladder-like knots and sometimes showed a complicated appearance as shown in Figure 42. The cytoplasm of the knot was usually occupied by mitochondria which had an electron dense matrix and well-developed cristae. Thin processes contained saccular cisternae of the rough endoplasmic reticulum (RER). The elongated processes extended to coat the surface of trabecular skeleton (Fig. 43). Some of the cells were

holding a vacuole by the cytoplasmic process (Figs. 44-46). The cytoplasmic processes enclosing the vacuole were seen to be torn off in places to form small intermittent vesicles. The vacuoles were correspond, though smaller in size, to the holes caused by decalcification of trabecula. These features suggest that the vacuoles enclosed by cytoplasmic processes of basophilic cells are the sites of decalcified crystals of a premature trabecula. In the large vacuolar spaces were found only a few vesicles, but in the small vacuoles were much more vesicles containing electron-dense, fibrous or amorphous materials (Fig. 47). Around small basophilic cells, many fibrous bundles and fibrils were distributed (Fig. 47), which was conspicuous especially in the sutural area (Fig. 44).

Several kinds of cells which were different from the basophilic cells and did not appear to be specifically associated with the trabeculae, were distributed in the organic stereom. Based on their cytological and ultrastructural characteristics, these cells were classified as spherule-containing cells, strongly eosinophilic cells, vacuolated cells, phagocytic cells, round uniform cells and cuboidal cells.

The spherule cells were 7-23μm long of various shapes owing to an amoeboid movement in a living state, but fixed cells were mostly round to oval (Fig. 48). The cytoplasm was characteristically occupied with many spherules of various sizes, some of which showed a reddish color in

unstained sections. The spherules revealed a variety of stainabilities to different staining procedures: they were stained reddish purple to reddish black with hematoxylin-eosin and yellowish pale brown to blackish brown with azan. In semithin sections stained with a mixture of methylene blue-azur II, they were differentially stained in three colors, yellow, green and blue. The nucleus was round to irregular in shape. When viewed by TEM, the spherule cells revealed to have three types of spherical inclusions ranging from 0.7-1.8μm (Fig. 49). Those of the first type, mostly round but some irregular in shape, contained a uniformly electron-dense material. The second ones of round shape had an electron dense core surrounded by an less-dense amorphous substance. The third ones of round to oval shape consisted of a fine fibrous material (Fig. 49). The spherules of this type were sometimes observed to be diffusing by degradation of the coating membrane. The cytoplasm of spherule cells was scarce and had a few vesicular cisternae of rough surfaced endoplasmic reticulum (RER) and some vacuoles. Fusion of these spherules was sometimes observed.

The spherule cells were distributed throughout the entire organic stereom of the plates, but were more at the peripheral area of the suture. These cells were found to infiltrate into the epidermis of the plate, especially in injured portions. In unstained sections, some spherule cells maintained reddish color of their spherules. However, such cells were rarely distinguished from other spherule

cells by TEM because the red pigments were easily lost by diffusion in the process of preparation.

The round vacuole cells were observed to be distributed in many places (Fig. 37). The cells were of stably round shape of 5-10μm diameter and the cytoplasm was occupied by numerous large vacuoles (0.4μm in mean diameter) (Fig. 50). Some vacuoles retained a strongly eosinophilic material. The cytoplasm was thin and showed eosinophilic nature. The feebly basophilic nucleus was round and had several condensed heterochromatin. In TEM images, the cytoplasm was occupied by numerous large vacuoles and the poor cytoplasm contained small vesicles and a few mitochondria (Fig. 51).

The phagocytic cells were of various irregular shapes having extensions of cytoplasmic processes, some being two to three times larger than the cell body (Fig. 52). The cytoplasm was weakly basophilic. At an ultrastructural level, the cytoplasm around the nucleus was moderately electron dense and occupied by numerous vesicular structures, which were probably of the smooth surfaced endoplasmic reticulum (SER) that existed also in the thin cytoplasmic processes (Fig. 53). Large vacuoles enclosed by the elongating processes contained some fine fibrous or amorphous material. Sometimes, these cells were observed to be ingesting other cells (Fig. 54).

The round uniform cells were 5-10 μm in diameter and had the uniform cytoplasm stained weakly basophilic (Fig. 55). The cytoplasm sometimes showed irregular distribution of

strongly basophilic, thread-like or variously shaped structures. The basophilic nature of these structures was very similar to that of the nucleus. Sometimes they were continuous to the nucleus, suggesting that their origin has been derived from the nucleus by, for example, diffusion or degradation of karyoplasm. An ultrastructural characteristic of this cell was in its cytoplasm occupied by fine fibrous elements (Fig. 56).

The strongly eosinophilic cells were observed in the organic stereom of the tubercle base and in the periphery of the suture. The cells observed in the tubercle base were stably ovoid-shaped (about 15μm in diameter) and compactly contained numerous small, strongly eosinophilic granules. On the other hand, the cells distributed near the suture showed various shapes owing to cytoplasmic extensions, which also included dispersed eosinophilic granules. Electron micrographs of these cells revealed that the cytoplasm was occupied by numerous round granules (0.1-0.2μm in diameter) which contained homogeneous, electron dense or moderately dense materials (Fig. 57). The cytoplasm had mitochondria and developed RER.

In addition to cells described above, some cuboidal cells were found in the organic stereom (Fig. 58). The cuboidal cells had a fairly large nucleus, which occupied more than half of the the whole cell. When viewed by TEM, the cytoplasm was moderately electron-dense, containing free ribosomes, mitochondria, cisternae of the RER and sometimes

a few granules (Figs. 59, 60). Oil droplets were often observed. Golgi complexes with saccules containing electron-dense material were observed near the nucleus.

Many atypical cells not identified as any of the above described cells were observed in the organic stereom. They were conspicuous at the stereom near the outer surface of test plates (Fig. 61). Some of them showed a strongly basophilic nature and some others appeared to coagulate into a large mass. Cells seemingly in degenerating phase were also observed in many places in the organic stereom, especially conspicuous near the outer surface (Fig. 62).

Bundles of typical collagen fibers were found abundantly in the sutural area (Fig. 63) but not in the interior of the stereom. These collagen fibers encircled the surface of trabeculae which were coated by small vesicles or a fine granular sheet (Figs. 64, 65). The fibers were variously thick from 0.04μm to 0.14μm, and thick fibers showed a typical banding pattern similar to typical mammalian collagen fibers (Fig. 64). No fibers were detected in decalcified holes of the skeleton.

A thin membranous and/or fine granular, electron-dense material was observed to line over the surface of decalcified trabeculae (Fig. 65). They extended over almost all the trabecular surface though not fully continuous. Over this material or directly on the trabecular surface, small vesicular structures of 0.17-0.9μm were beaded to coat throughout the trabecula surface (Fig. 66). The vesicles

contained one or more small vesicles with an interstitial homogenous substance. In the organic stereom there were numerous vesicles and indefinite materials which seemed to be cell debris.

The coelomic epithelium covering the entire inner surface of the test plate appeared to be a monolayer of cells in paraffin and in semithin plastic sections (Fig. 67a). Ultrastructural features presented clearly showed that the epithelium consists of monolayered epithelial cells, interposing nerve fibers and muscle cells (Figs. 67b, 68).

3.DISCUSSION

The present observations by light and electron microscopy presented seven types of cells: small basophilic, spherule-containing, vacuolated, strongly eosinophilic, phagocytic, round uniform and cuboidal cells. Most of these cells were accumulated near the suture which is known to be the actively growing site of the test plate, but only the small basophilic cells seemed to be intimately associated with the skeletal trabeculae. The basophilic cells had characteristically branching cytoplasmic processes with small knot-like expansions. These processes closely encircled the trabecular surface, sometimes forming a syncytial structure. These ultrastructural features of the basophilic cells showed a close resemblance to those of the sclerocytes in the spine of E. tribuloides (Märkel and Röser, 1983) and the regenerating spine of S. purpuratus

(Heatfield and Travis, 1975a, b). Therefore, the small basophilic cell can be regarded as the sclerocyte in the test plate. In growing test plates, the small basophilic cells may be accumulated as sclerocytes at the actively growing site and deposit calcite crystals at the space enclosed by their cytoplasmic processes. As the crystals grow, the sclerocytes may elongate their cytoplasmic processes to form a syncytial sheath as described by Märkel and Röser (1983).

The spherule cells were observed throughout the organic stereom of decalcfied test plates of S. intermedius. They were found in the regenerating test plates (Kindred, 1924) and spine (Heatfield and Travis, 1975b). Their characteristic intracellular spherules suggest that these cells are probably identical to the red and the colorless spherule cells known to occur in the coelomic fluid. The red spherule cell is characterized by containing red-pigmented spherules and the colorless spherule cell by non-pigmented spherules. An accumulation of coelomocytes consisted of a lot of number of spherule cells was noted at wounded sites where the spherule cells rapidly broke down and liberate spherules (Smith 1981). The function of these cells is suggested to produce collagen fibers or to release chemotactic agents for migratory cells and/or to help disinfect the area against microbial invasion (Smith, 1981). Echinochrome pigment of the red spherules is known to be involved in defense mechanisms as an antibiotic (Johnson,

1970; Vevers, 1966; Service and Wardlaw, 1984). On the other hand, Vocisano (1971) suggested that spicules originated in a syncytium which was built up of leucocytes and spherule cells grow to form trabeculae within the syncytium. This will be examined in the experiments of regenerating test and spines (Chapter VIII).

The phagocytic cells were found in organic stereoms of decalcified test plates in the present study. They had expanded cytoplasm with many vesicular structures and elongated thin cytoplasmic processes to enclose other cells by phagocytic function. Ultrastructure of these cells were very similar to those of the phagocytic leucocytes, or the phagocytic amebocytes, of coelomocytes (Smith, 1981). The phagocytic leucocytes have been reported to take part in the clot formation of coelomocyte (Endean, 1966) and regeneration of test tissues (Kindred, 1924; Smith, 1981). Johnson and Chapman (1970) described that the amebocytes have a structural similarity to the skeletogenic cells (sclerocytes) existing in echinoid spines. Heatfield and Travis (1975a), however, could not find any ultrastructural evidence for the transformation of amebocytes to sclerocytes (termed calcoblasts by Heatfield and Travis). Also in the present study, ultrastructural resemblance between the sclerocytes (small basophilic cells) and the phagocytic cells was not evident. The phagocytic cells found in the test plates may serve to remove cell debris and/or invading microorganism.

The round uniform cells often showed deformation and

degradation of the cell membrane, suggesting degeneration. Their ultrastructural characteristics are very similar to those of the vibratile cells of coelomocytes (Smith, 1981). Appearance of various inclusions together with strongly basophilic nature of the cytoplasm might be reflection of degenerating nucleus or cytoplasmic organelles. The vibratile cells are known to be easily degraded to release their inclusions and to lose their flagellum at clotting or attaching to other bodies (Smith, 1981). Therefore, the round uniform cells may be the vibratile cells and they may take part in the framework formation of the organic stereom.

The strongly eosinophilic cells, the vacuolated cells and the cuboidal cells have no corresponding cell species in the coelomocytes. Therefore, these cells may originate in situ in the test tissue or in transforming stages of the coelomocytes. Origins and functions of these cells remain to be solved.

Collagen fibers were found to localize at the sutural area and near the outer surface of the test plates. They formed also a thin layer along the basement membrane under the coelomic epithelium. In these regions, especially in the sutural area, the fibers were seen to cover directly the skeletal trabecula. Travis (1970) also found collagen fibers in both organic stereom and decalcified trabecular space of the sutural area in S. droebachiensis, and argued that the collagen fibers participate in initiating the mineralization as the calcifiable organic matrix. However,

the present observations could not show any fibers in the decalcified space. The collagen fibers in the test plate probably do not participate in the initiation of mineralization as suggested by the previous light microscopic work (Moss and Meehan, 1967; Nichols and Currey, 1968). The TEM images that they are intimately associated with the trabeculae suggest their role in the trabecula formation or its maintenance.

The framework of the organic stereom was built up by a coat of thin membranous and granular structures extending along the trabecular surface. Similar structures have been reported in the regenerating spines in Echinus esculentus and Euchidaris tribuloides (Pilkington, 1969; Märkel and Röser, 1983). Märkel and Röser (1983) called it the matrix coat or the trabecula coat. Märkel et al. (1989) described that the matrix coat consists of three membranous layers derived from sclerocytes which cover the trabeculae with elongated syncytial cytoplasmic processes to form the "synplasmic sheath".

The beaded vesicular structures lined along the trabecular surface were regarded as the distal processes of sclerocyte by Märkel and Röser (1983). The present study revealed that some of them may be cytoplasmic processes continuous to the living cell body of sclerocytes. However, some others were seen to be a series of separated vesicles or at least fragmented vesicles which were torn off from the sclerocyte or other cells to be called the "coating

vesicles". It was very difficult to distingush the distal processes from coating vesicles on TEM images. Three-dimensional features on the ultrastructural basis of cells, vesicles and collagen fibers in the test plate are needed to understand their roles in the mineralizing front.

VI. THREE-DIMENSIONAL ULTRASTRUCTURE OF CELLS AND COLLAGEN FIBERS IN THE TEST PLATES AND SPINES

Numerous investigations on the skeletal structures of various calcified tissues in many echinoids have been made from a crystallographic point of view (e.g. Raup, 1966; Weber et al., 1969; Jensen, 1972; Smith, 1980). However, we have relatively little knowledge on the organic stereom which is closely associated with the calcareous stereom (Deutler, 1926; Moss and Meehan, 1967; Travis, 1970; Travis et al., 1967). A recent TEM observation of the spine tissue of E. tribuloides presented evidence that the trabeculae or microspines are enclosed by a syncytial tissue of sclerocytes and intermittent vesicular structures of its derivatives (Märkel and Röser, 1983). Märkel and Röser (1983) considered that the vesicular structures are distal processes of the sclerocytes. These features in the spine of E. tribuloides were similar to those observed in decalcified test plates presented in the previous chapter (Chapter V). In the decalcified test plates, it was not certain whether all of the intermittent vesicles covering the trabecular surfaces are really the distal processes of sclerocytes. Together with the three-dimensional configuration of cells and collagen fibers, the ultrastructure of the organic stereom remains unknown. Therefore, the present study aimed at making clear the stereographic feature of the organic stereom with reference to the formation or maintenance of skeletons in test plates

and spines of S. intermedius.

1. MATERIAL AND METHODS

About thirty individuals of young and adult S. intermedius, ranging from 5 mm to 65 mm in test diameter, were used. The entire test and spines and their fractured fragments were fixed with the PG fixative for 2-24 h at 4 °C or room temperature. The fixed test was cut into blocks including 3-5 plates or into pieces smaller than one-half of a plate. Some spines were cut into 1/3-1/2 pieces of their full length. Some of the fixed specimens were treated for 2-6 h with 2N-NaOH for a mild removal of organic materials. Alkali-treated and non-treated specimens were dehydrated with a series of 50-95% ethanol, transferred to tributhyl alcohol and successively frozen with the medium in a refrigerator. The frozen specimens were freeze-dried by evacuation with a rotary pump according to Inoue and Osatake (1988). The dried specimens were mounted on a stub, coated with particles of an alloy of platinum-paradium using a sputter coater (JEOL JFC-100), and then examined by scanning electron microscopes (JEOL JSM-25 and Hitachi S-1000) mostly at 25 kV.

Some fixed test pieces were demineralized with a 5% EDTA solution (pH 7.6) containing 8% sucrose for 1-3 weeks at 4 °C or room temperature. The demineralized pieces were osmicated with an OsO_4 solution, washed with a cacodylate

buffer and freeze-dried by the method as described above.

2. RESULTS

(A) Test plates

Test plates treated with NaOH for several hours retained some organic elements including cells and fibrous elements adhered to the skeleton. The cells showed a variety of sizes and shapes. Based on their features by SEM, the cells were roughly divided into two types: round to ovoid cells and flat cells.

The round or oval cells of 3-6μm in diameter, temporarily referred to as the "round cells" here, were dominantly observed on the skeletal trabeculae separately or in aggregations (Figs. 69, 70). Most of the cells elongated several or numerous thin cytoplasmic processes, which were about 0.12-0.2μm thick at the proximal and less than 0.03 m at the terminal end. The processes sometimes extended at long distance to contact with other cells (Figs. 71, 72). Some other processes had a few or several small (0.6-0.9μm in diameter) bladder-like knots from which short thin processes were frequently branched. The round cells often appeared around the growing site of the trabecula, and were connected each other by a meshwork of thin processes (Fig. 73). The bladder-like knots were seen to stick directly to the growing surface of the trabecula (Figs. 74-76).

The flat cells were 10-15μm long, and were occasionally more than 20 μm long. They were observed to extend the

flattened cytoplasm over the trabecular surface (Fig. 77). Some of them were shown to aggregate in a complicated form (Fig. 78), sometimes like a bunch of grapes (Fig. 79). The flat cells elongated several cytoplasmic processes (0.08-0.2μm thick) in every direction. Some of the processes were extending across several stereomal pore spaces (Figs. 78-80). The processes were very similar to those of the round cells. The flat cells were abundant in the area where the skeletal trabeculae showed a blunt appearance (Fig. 77) or the skeletal surface was eroded (Fig. 81). The stereom on which flat cells with numerous thin processes were accumulated, demonstrated wider pore spaces (Figs. 79, 80). Occasionally, numerous fragments of thin processes were observed on the eroded trabecular surface where a sharp and smooth appearance was lost (Fig. 82). In large interstitial spaces of the test stereom, the flat cells often existed together with the round cells. The eroded trabeculae associated with the flat cells were frequently observed at the inner surface near the suture (Fig. 81). This phenomenon was conspicuous in young urchins' plates.

Another type of cells (about 10μm in diameter) having scrubbed brush-like structures on the surface were observed occasionally on the trabecular surface (Figs. 83, 84). This specific brush-like structure appeared to be formed by fusion of numerous short and thin cytoplasmic processes. These cells anchored thin cytoplasmic processes on a rough surfaced trabecula which suggested a weak skeletal

resorption.

At the suture and its vicinity, thick bundles of abundant fibers were seen occupying the interstitial spaces of the stereom, or twinning around the calcite trabeculae (Figs. 85, 86) or interconnecting the neighboring plates (Fig. 87). In the test of young urchins, the sutural area often revealed a large open space between the plates, and the trabeculae near the interradial and adradial sutures showed eroded surfaces which were coarse and porous (Fig. 88). On the eroded trabeculae and interstitial spaces around them, numerous "round" and "flat" cells were accumulated with their processes extending over the trabecular surface (Fig. 89). Numerous processes having small bladder-like knots were attached to the eroded surface (Fig. 90). A cobweb-like meshwork woven of thin cytoplasmic processes and fibrous elements (about 0.13μm thick) which may include collagen fibers, was observed to cover the trabeculae (Fig. 91). Sometimes, these processes were arranged in circles on a specific place of the trabecular surface. This peculiar feature suggests a place of initiation of budding of a new crystal (Fig. 92). In other portions, the meshwork appeared to fill a stereomal pore space together with round cells (Fig. 93). The cytoplasmic processes and fibrous elements coiled round the surface of trabeculae at the suture. These trabeculae were seen covered with some amorphous substances (Figs. 94, 95). Distant from the sutural areas, the inner surface of the plate often exhibited an eroded rough

appearance in company with an accumulation of both round and flat cells (Fig. 96). The rough trabecular surface along the stereomal hole showed a few shallow circled crevices (Fig. 97). Around such an area, abundant collagen fibers of about 0.1-0.2μm thick were observed in association with flat cells having elongated cytoplasmic processes (Fig. 98). Trabeculae near the suture were covered with a compact sheet of fibrous elements (0.05-0.16μm thick) (Figs. 99, 100). On the fibrous sheet, a gourd-shaped cell, which might be a form of the round cell, existed branching short cytoplasmic processes, some of which were torn off at the tip region (Figs. 99-101). From the tip of the branched processes, thinner processes extruded. Many vesicles of round or irregular shapes (0.1-0.5μm diameter) also were distributed on the fibrous sheet (Fig. 102).

On the other hand, trabeculae at a distance from the suture scarcely had fibers and cytoplasmic processes, but numerous round to oval vesicles of 0.1-0.4μm diameter were dotted on the trabecular surface (Fig. 103). Cytoplasmic processes and fibrous elements observed in the sutural areas were less developed on the trabeculae coated by the vesicles (Fig. 104). These features were widely seen through the interior of the plates.

The three-dimensional fine structure of the organic stereom was obtained by SEM observations of decalcified plates. A membranous sheet was spreading over the entire trabecular surface to form a wall between the trabecula and

the organic stereom (Fig. 105). The calcified side of this membrane was smoother than the organic side (Fig. 106). A high magnification of the calcified side revealed it to be somewhat rough with numerous small granular materials and occasional thin cytoplasmic processes. Weak decalcification allowed to disclose dispersed depositions of small crystals on the membranous sheet, on which fibrous and cytoplasmic process-like structures also were observed (Fig. 107).

(b)Spines

The skeletal structure of a spine consisted of large calcite crystals as "wedges" and meshwork of thin skeletal trabeculae called "microspines" (Fig. 108). In cross sections, the wedges extended radially from the center of the spine, forming the circular outline of the skeleton. Each wedge formed longitudinally a thick calcified plate (Fig. 109). The meshwork formed by microspines occupied the central area of the spine and interstices between the wedges to form "bridges" mediating them (Figs. 108, 109). On the surface of the spine skeleton numerous cytoplasmic processes and vesicles were seen as in the skeleton of the test plate (Fig. 110).

In the interstitial organic space of the trabeculae, numerous cells and fibrous elements existed to enclose the skeleton as seen in the test plates; the round cell and the flat cell were main cellular constituents (Fig. 111). Also, cells showing a complicated contour were observed (Figs. 112, 113). There cells seemed to be a form of the flat

cells. Some cells had elongated processes which interconnected them each other. Fine fibrillar elements, some of which might be thin cytoplasmic processes as seen in the test plates, existed twinning around the trabeculae. The fibrillar elements were elongated to interconnect the cells like a stretched cobweb (Fig. 114).

3. DISCUSSION

The alkali-treatment of fixed test plates and spines for several hours allowed to retain some kinds of cells and fibrous elements including collagen fibers in the stereoms of the specimens. These cells and fibrous elements are probably settled tightly on the trabecula surface. The round cells elongated thin cytoplasmic processes to attach other cells at a long distance, forming bladder-like cytoplasmic knots in places. They were often seen around the growing trabeculae. Based on their morphological features and topography, the round cells may be the small basophilic cells, which were presumed as sclerocytes in the decalcified test plates in the previous chapter. On the other hand, the flat cells showing a complicated contour with cytoplasmic extensions and elongated processes were on the eroded trabecular surfaces. Cells having a scrubbed brush-like structure also were found on lightly etched trabecular surfaces. Cells of this type and the flat cells are considered to be related to the resorption of trabecular skeleton and, therefore, may be called the resorbing cells.

Small vesicles found on the surface of spine trabeculae may be the same as those detected on the trabeculae of decalcified plates. The SEM observation suggested that some of the vesicles, especially large ones or those of a tubular form, were certainly continuous to the round cell (sclerocyte) and, therefore, can be referred to as the "distal processes" as called by Märkel and Röser (1983) in the spine of E. tribuloides. However, many single or beaded smaller vesicles widely seen in the interior stereom of the test plates and spines were in no association with the sclerocyte. Therefore, if they were derived from the cytoplasmic processes of the sclerocyte, these vesicles should be called the "coating vesicles" rather than the "distal processes".

A membranous sheet woven of thin fibrous elements coated the entire trabecular skeleton. This was particularly conspicuous on the surfaces of trabeculae around the suture. The sutural area contained abundant collagenous fibers in decalcified test plate (Chapter V), as Moss and Meehan (1967), Travis et al. (1967) and Travis (1970) have found in other sea urchins. Bundles of thick fibers (about 0.1-0.2μm thick) are probably those of collagen fibers, because a typical banding pattern was observed by TEM. On the other hand, thin fibrils (thinner than 0.1μm thick) may be of immature collagen because thin fibrils were mixed with the typical collagen fibers in TEM figures. The test plate grows at the sutural area where the formation of new

skeleton occurs. Therefore, the fibrous sheet may provide the growing site with some local factors for new skeletal trabeculae. An ultrastructural feature that the fibrous elements were firmly enclosing the trabecular surface together with the thin cytoplasmic processes derived from the sclerocytes, may represent that these elements participate in determing the trabecular form of the skeleton as a mold.

The organic stereom of the spine contained some kinds of cells similar to those of the plates. One of them, the round cell had processes with bladder-like cytoplasmic knots elongated along the trabecular surface. These features are very similar to those of the sclerocyte as reported in the spine tissue (Märkel and Röser, 1983) and the teeth (Märkel et al., 1986) of E. tribuloides. In S. intermedius, the cells identified as sclerocytes in both the spine and the test plate showed the same morphological characteristics; the process of trabecula formation in these tissues may not be much different.

VII. CYTOLOGICAL AND ULTRASTRUCTURAL FEATURES AND BEHAVIORS OF COELOMOCYTES

There is no directional circulatory fluid like "blood" in echinoids, but they have a well-developed and specialized vascular system and haemocoelomic fluid. The coelom is a perivisceral space filled with the coelomic fluid. The coelomic fluid can move freely through all the coelomic systems and also across the coelomic epithelium. The fluid ionic composition is very similar to external sea water, but more importantly it possesses a large population of circulating cells called coelomocytes.

Much information on the coelomocytes of echinoderms has been accumulated by many workers (see reviews by Endean, 1966; Smith, 1981). Thirteen distinct cell types of coelomocytes have been identified in fifteen species of echinoderms (Boolootian, 1962), and eighteen types of coelomocytes have been characterized in echinoids (Endean, 1966). In his recent review of the morphology, function and origin of coelomocytes in echinoderms including several echinoids, Smith (1981) concluded that the coelomocytes appear to fall into six main categories, phagocytic amebocytes (leucocytes), spherule cells, vibratile cells, hemocytes, crystal cells and progenitor cells. However, their classification, functions and origins are still controversial. No investigations have been carried out on the coelomocytes of S. intermedius.

The coelomocytes are known to infiltrate easily into

various tissues including dermal test plates and spines (Endean, 1966). This phenomenon is conspicuous in the regenerating tissues where the leucocytes and the spherule cells play important roles in the basic tissue formation or initiation of the calcification (Kindred, 1924; Simkiss and Wilbur, 1985).

The cell elements found in the decalcified test plates included wandering coelomocytes (Chapter V). Cytological characteristics of coelomocytes in the coelomic fluid are needed to understand what cells are involved and what their roles are in the formation of the dermal skeleton. By LM and TEM observations, morphological characteristics of coelomocytes were studied to compare with those of the intrastereomal cells.

1. MATERIAL AND METHODS

Adult sea urchins of S. intermedius (21-74 mm test diameter) were used. The coelomic fluid was sucked out from the coelomic cavity by puncturing the peristomial membrane with a syringe. For LM observations, the coelomic fluid was immediately smeared on a glass slide and fixed with vapor of 1% osmium tetroxide, and then air-dried. The cell preparations were variously stained with Giemsa for general morphology, Feulgen reagent for nucleus, PAS reagent for polysaccharides, Sudan black B for lipids and toluidine blue (pH 2.7) for metachromatic staining of mucopolysaccharides

(Lison, 1960). For detection of calcium deposits or complexes, alizarin red stain was applied to the cell preparations after fixion with ethanol according to Dahl's method (Lison, 1960).

Carbon particles (Indian ink, Merck) were injected into the coelomic cavity with a syringe. The coelomic fluid was obtained by suction 2-3 h after injection and uptake of carbon particles by coelomocytes was examined. The number of coelomocytes was counted with an Erma hemocytometer.

For TEM observations, the coelomic fluid was mixed with the same volume of a 4% paraformaldehyde-5% glutaraldehyde fixative in a 0.1 M cacodylate buffer solution (stock solution for Karnovsky's fixative), and centrifuged at 1000 g for 15 min and then kept for 2 h. After removal of the fixative, precipitates of coelomocytes, some forming a clot, were osmicated, washed with the same buffer solution and then embedded into epoxy resin (Epon 812) through dehydration with ethanol.

To facilitate identification of coelomocytes and to promote understanding of their functions, their short-term in vitro culture (several hours to two weeks) was performed. Fresh coelomic fluid was prepared for a hanging drop or dish culture of coelomocytes without additional medium. The coelomocytes survived about two weeks in the dish culture system. The cultured coelomocytes were examined with an inverted light microscope (Nikon TDM).

2. RESULTS

(A) Cytological and ultrastructural characteristics of coelomocytes

In S. intermedius, five kinds of coelomocytes, viz., phagocytic leucocytes, spherule cells, vibratile cells, hyaline cells and reniform cells, were distinguished distinctly (Table 3). These cells represented various shapes and sizes showing a variety of ultrastructural and cytochemical traits (Table 4).

Phagocytic leucocytes: Two types of leucocytes existed abundantly in the coelomic fluid: those having several bladder or petaloid-form cytoplasmic extensions, called the bladder leucocytes, and those having filopodial cytoplasm, called the filiform or the filopodia-form leucocytes. The bladder leucocyte is 15-20μm in the entire length and its cell body was about half to one-third of its whole size (Fig. 115). The filiform leucocyte was 15-25μm in length (Fig. 116). The leucocytes of both types occupied about 50-60% of the whole coelomocytes of S. intermedius (Table 5). They were found to ingest peritoneally injected carbon particles and often other coelomocytes. Therefore, the leucocytes of both types were shown to have a phagocytic function.

In the hanging drop culture, the bladder leucocytes were dominant at an early stage, whereas the filiform cells

Table 3. Classification of the coelomocytes of *S. intermedius*

Cell types	Size (μm)	Cytoplasmic inclusions
Phagocytic leucocytes		
Bladder type	15-20	little granules, red pigment, crystals
Filiform type	10-25	little fine granules
Spherule cells		
Eleocyte	8-16	numerous red spherules
Colorless	10-18	numerous colorless spherules
Vibratile cell	6-10	many hyaline spherules, having flagellum
Hyaline cell	10-12	no granules, hyaline appearance
Fusiform cell	10-20	no granules

Table 4. Cytochemical characteristics of the coelomocytes of *S. intermedius*

Cell types	Meta. (TB)	PAS	AZ	SBB
Phagocytic leucocytes				
Bladder type	-	++ or +	+	+-
Filiform type	-	++	+	+-
Spherule cells				
Eleocyte	+-	+	-	+-
Colorless	++	+	-	+-
Vibratile cell	+	+	-	+-
Hyaline cell	-	++	-	+-
Fusiform cell	-	+	-	+-

Meta. (TB): metachromasia with toluidine blue (pH 2.7); PAS: periodic acid-Schiff reaction; AZ: alizarin red stain; SBB: Sudan black B stain

Table 5. Total number of the coelomocytes and populational ratio (%) of each cell type in the coelomic fluid of *S. intermedius*

Total number (/ mm^3)	Population ratio (%)						
	Leucocytes		Spherule cells		Vibratile cell	Hyaline cell	Fusiform cell
	bladder	filiform	eleocyte	colorless			
5400	32.0	24.5	11.2	12.3	9.5	9.7	0.8
7100	32.5	16.2	26.5	6.8	12.9	5.0	0.1
5800	26.8	28.8	7.5	10.4	10.8	5.0	0.1
8800	42.1	15.1	16.3	6.1	14.1	5.7	0.2
3200	28.4	20.1	11.2	10.6	12.8	16.6	0.3
5300	40.0	20.0	5.8	10.5	16.1	6.8	0.8
5700	33.6	27.6	8.9	7.1	16.8	5.6	0.4
6200	35.8	20.2	15.4	6.8	14.5	7.1	0.3
2100	52.6	17.9	6.8	3.4	7.2	11.1	1.0
3700	29.2	22.6	10.9	3.8	18.9	12.5	2.1
3400	28.2	28.5	19.6	6.3	9.7	6.6	1.1
5500	23.2	22.5	23.4	7.1	9.1	12.4	2.3
(5183±1844)	(33.7±8.0)	(22.0±4.6)	(13.6±6.7)	(7.6±2.8)	(12.7±3.5)	(8.7±3.7)	(0.8±0.7)

(Mean ± SD)

increased to become dominant with a lapse of culture time. In the dish culture, the leucocytes which seemed to be the bladder cells were observed to spread over the dish bottom forming a monolayered cell sheet without distinct cell borders. Their nuclei were indistinct in contour. Over the monolayered cells or just on the dish bottom, some filiform cells were spreading with numerous cytoplasmic processes which were elongated in every direction to connect with each other to form a mesh stucture (Fig. 117).

By TEM, numerous cytoplasmic processes of filiform cells were shown in a variety of sizes just around the cell bodies (Fig. 118). The ground matrix of the processes consisted of a uniform substance of moderate electron-density. On the other hand, the bladder type cells elongated thin cytoplasmic extensions enclosing large vacuolar spaces assuming a bladder-like appearance (Fig. 119). Intermediate forms between the two types were often observed.

Ultrastructural features of cells of the two types were basically identical. The cytoplasm was a vacuolated structure with numerous vacuoles of various sizes (Fig. 120). Near the nucleus were mitochondria and well-developed Golgi complexes (Fig. 121). The nucleus was filled with uniform matrix and occasionally a plain nucleolus. Sometimes, the leucocytes encircled other coelomocytes such as spherule cells (Fig. 122) and even leucocytes of the same type, showing a phagocytic function by elongated cytoplasmic processes. Occasionally, some bladder leucocytes were

observed to enclose an unknown strange structure (Fig. 123).

Spherule cells: In the coelomic fluid of S. intermedius, two types of spherule cells, the red spherule cells and the colorless spherule cells were observed as the second major constituents of coelomocytes (Table 5). The two types of the spherule cells were very similar in shape and size, but the red cell was somewhat smaller than the colorless cell. They were moving actively, exhibiting an amoeboid movement, but fixed spherule cells were round to oval (Fig. 124a), especially so were the red type cells. Sometimes, they were of irregular shapes with blunt pseudopodia. The red spherule cell, or the eleocyte (Endean, 1966), was distinguished from the colorless cell by reddish coloration of its pigment in paraffin and JB-4 embedded sections, but the red pigment was easily diffused into water. When the red pigment had been diffused, it was difficult to distinguish the eleocyte from other spherule cells. This was often encountered in the observations of semithin sections of epoxy- resin embedded specimens.

When the spherule cells were viewed by TEM, they were round or elongated in shape (Fig. 124b) filled with numerous, large spherical membrane-coated inclusions (0.5-1.4μm diameter). These inclusions were divided into three types by their contents: (1) a compact mass of an electron-dense, homogenous material which sometimes revealed an amorphous, flocculent appearance, (2) fine granular compact masses of moderate electron density, and (3) coarsely dispersed fine granules of moderate electron density.

Sometimes, the last type was shown to form a fine fibrous structure. Fine granules forming a fibrous structure were detected between the contents and the coating membrane (Fig. 125). Features releasing the contents of inclusions were often observed (Fig. 126). Largely vacuolized spherule cells were often observed (Fig. 127). Their scanty cytoplasm included well-developed Golgi complexes. The nucleus was irregular in shape and eccentrically placed.

Vibratile cells: Among living coelomocytes, this cell was an only actively swimming cell by exhibiting turning movements by means of a flagellum. The flagellum, however, was easily lost when clotted or attached to the glass surface or fixed with a chemical solution. The cell body was round, 6-10μm in diameter, and the cytoplasm was packed with numerous, large membrane-coated spherules (Fig. 128). The spherule consisted of two different materials at an ultrastructural level: moderately electron-dense, fine granular material evenly distributed in the spherule and a more electron-dense and homogenous material localized in parts (Figs. 128, 129). The sparse cytoplasm with relatively homogenous ground substance contained a few mitochondria and small vesicles of SER. The nucleus was oval or irregular and located eccentrically. The cell body as well as the flagellum appeared to be easily degenerated at clotting. Degenerating features were often observed in fixed specimens.

Hyaline cells: The cells were mostly round and 10-12μm in

diameter, and appeared in a relatively small number among other coelomocytes (Table 5). These cells were difficult to distinguish from filiform cells by TEM, because both of the cells were very similar in ultrastructural characteristics (Fig. 130).

Fusiform cells: The cells were mostly about 4μm in width and 20μm in length in smear preparations. They appeared in the smallest number in the coelomic fluid. The cell body was PAS-positive, but did not show metachromasia with toluidine blue at pH 2.7 (Table 5). The ultrastructure of this cell could not be observed because it was scarcely encountered in TEM preparations.

(B)Ultrastructural features of coelomocytes at clotting

The bladder and the filiform leucocytes mainly participated in the clot formation; they agglutinated each other with their thin elongated or bladder-like extensions (Fig. 131). Some leucocytes extruded fine membranous envelopes from their thin cytoplasmic processes (Figs. 132, 133). These envelopes were connected to other coelomocytes to trap them in a delicate meshwork (Figs. 134-137). The incorporated cells were closely attached to the envelopes of the meshwork with their cell membranes (Figs. 134, 135, 137) or vacuole membranes (Fig. 136).

Numerous vesicular structures, some of which were transformed from cytoplasmic processes and some others were probably the debris of degenerated cells, were distributed in spaces of the meshwork. Almost all types of coelomocytes

were found in the spaces. Sometimes, the meshwork represented a stereom-like, compact structure (Fig. 138). A deformed vibratile cell containing degenerating spherules was occasionally found in the stereom-like structure (Fig. 139). The cell membrane of such a vibratile cell was partially connected to the envelop forming a framework of the stereom-like structure.

3. DISCUSSION

Five distinct types of coelomocytes and some minor cells were identified in the coelomic fluid of S. intermedius, viz., the phagocytic leucocyte, the spherule cell, the vibratile cell, the hyaline cell and the fusiform cell. Among these coelomocytes, those observed in the decalcified test plates were the phagocytic leucocyte, spherule cell and vibratile cell. They seemed to be involved in the formation or deformation of the skeleton.

The phagocytic amebocytes or leucocytes are known to be most common among all echinoderm coelomocytes, and to show the largest population in every species examined previously (e.g. Endean, 1966; Smith, 1981). The leucocytes in S. intermedius did not display an active amoeboid movement, but an active phagocytotic behavior, hence, these cells were termed the phagocytic leucocytes in this paper. The phagocytic leucocytes were of two types, the bladder and the filiform, as reported in many other species. In S. droebachiensis, the phagocytic amebocytes (leucocytes) are

most abundant and about 20% of them are of the petaloid (bladder) type and the rest are of the intermediate type (Bertheussen and Seljelid, 1978). In S. intermedius, the phagocytic leucocytes accounted for about 50-60%, occasionally 70%, of the total population of coelomocytes, and about 60-80% of them were of the bladder type. The proportion of the leucocytes may vary from species to species and among individuals. A transformation from the bladder type to the filiform type has been reported in many echinoderms; it occurs rapidly in a hanging drop culture and is considered to be caused by collapse of the cytoplasmic bladders after wounding, osmotic shock, and various artificial stresses (Chien et al., 1970; Edds, 1977; Fontaine and Lambert, 1977; Otto et al., 1979). However, the bladder leucocytes were shown to be relatively stable in dish culture, though they were gradually transformed into the filiform type and/or a monolayered structure in vitro by confluence of their cytoplasm. Smith (1981) described that the petaloid form is capable of strong ameboid movement and is actively phagocytic, while the filopodial stage is important in cell clotting. In S. intermedius, the ameboid movement of both the bladder and filiform cells was not so distinct in dish culture, but they actively participated in the clot formation. Only the phagocytic leucocytes of both types among other coelomocytes revealed a calcium positive reaction to alizarin red (Table 4). In the regenerating test of S. droebachiensis, similar phagocytic leucocytes

which form a stereomal structure have been found to contain skeletal crystals (Kindred, 1924). Roles of the leucocytes in regenerating skeletal tissues and in their mineralization will be discussed in the following chapter.

The spherule cells also are common in echinoderms (Kindred, 1924; Behre, 1932; Bookhout and Greenburg, 1940; Boolootian and Giese, 1958; Andrew, 1962; Johnson, 1969a; Chien et al., 1970; Vethamany and Fung, 1972). These cells have been divided into the red and the colorless spherule cells on the basis of their inclusions. These two types of spherule cells were confirmed also in S. intermedius. Smith (1981) suggested that the existence of the two different types of spherule cells represents different developing stages of a single and the same cell line. In the present TEM observations, the red spherule cells were difficult to be distinguished from the colorless cells, but some spherule cells appeared to have spherules filled with a considerably electron-dense flocculent material, which seemed to be the red pigment of red spherule cells. The red pigmentation of red spherule cells in many echinoderms is due to the presence of echinochromes which are naphthaquinone compounds. Several subclasses of echinochromes have been identified (MacMunn, 1885; Kuhn and Wallenfels, 1940; Goodwin and Srisukh, 1950; Millot, 1957; Fox and Hopkins, 1966; Vevers, 1966). A chief echinochrome located in the spherule cells is echinochrome A, which is considered to bind PAS-positive proteins (Goodwin and Srisukh, 1950;

Holland et al., 1967; Johnson, 1970). Red spherule cells of S. intermedius were also PAS-positive as seen in other species (Johnson, 1969b). The colorless spherule cells of S. intermedius showed intense metachromasia (Table 5). This suggests that their spherical inclusions contain acid mucopolysaccharides as found in other echinoderms (Hetzel 1963, Cowden 1968, Fontaine and Lambert 1977). The function of the spherule cells is still controversial. In cutaneous wound healing of a sea cucumber, Thyone briareus, Menton and Eisen(1973) suggested that morula cells, which are morphologically and cytochemically similar to the spherule cells of echinoids, provide some constituent of fibrous matrix. Smith (1981) proposed that the substances released from the spherules may act as chemotactic agents for migratory cells and help disinfection against microbial invasion.

The abundance of the vibratile cells is as large as next to that of the phagocytic amebocytes in S. purpuratus and S. franciscanus (Johnson 1969a). In S. intermedius, however, they were not so abundant and showed only 7% to 19% of the total cell population. Intense metachromasia and PAS-positivity of the vibratile cells indicate that they are rich in complexed polysaccharides. A similar cytochemical nature of the vibratile cells has been found also in other urchins (Vethamany and Fung, 1972; Johnson, 1969b). The vibratile cells in fresh coelomic fluid are known to be quite stable in vitro but some release semi-transparent veils of mucosubstances (Johnson, 1969a; Chien et al.,

1970). They degenerate to participate in clot formation. Degenerating vibratile cells were often observed in the organic stereom of the test plates (Chapter V). Therefore, these cells may provide other cells with complexed mucosubstances for an aggutination that forms the organic stereom of the test plates and spines.

The cell called "hyaline cell" in this paper did not seem to have hemoglobin. Therefore, this cell can not be identified as the "hyaline hemocyte" which was reported to have hemoglobin in holothurians (Boolootian, 1962; Hetzel, 1963; Fontaine and Lambert, 1973). Cytochemical and ultrastructural characteristics of the hyaline cell were similar to those of the phagocytic leucocytes. Therefore, the hyaline cell can be a transitional form of the phagocytic leucocyte.

The fusiform cells appeared in the smallest number, 0.1-2%, in S. intermedius. This cell was PAS-positive but showed no metachromasia; this means that the cell has non-acidic, neutral mucopolysaccharides. Function of this cell remained unknown.

Other minor coelomocytes which did not fit any of the above-described types existed in the coelomocytes of S. intermedius. Smith (1981) described that there were always some intermediate or transitional forms of major coelomocytes and some could be caused by artifact.

Ultrastructural features of clotted coelomocytes presented evidence that the phagocytic leucocytes were

mainly involved in a clot formation, as was proposed in previous light microscopic studies by Donnellon (1938) and Johnson (1969a). Accumulation of spherule cells, especially of the red type was distinctive in a clot. Their active participation in the clot formation, however, was not observed. They were trapped by a veiled network formed by the leucocytes. The network may develop to take a stereom-like configuration that is similar to the organic stereom of the test plates. It is hypothesized that the organic stereom induced by participation of phagocytic leucocytes and vibratile cells leads to the growth of skeletal stereom of the test plates and spines.

VIII. ULTRASTRUCTURE OF SCLEROCYTES AND ASSOCIATED TISSUES IN THE REGENERATING TEST AND SPINES

Skeletal tissues in echinoids are conspicuous among those of invertebrates as they are exclusively mesodermal. Owing to their structural complexity and difficulty in sectioning, only a little has been known as to the cellular contribution to the formation or growth of those fenestrated structures. In connection with the question whether they are of intra- or extracellular, the nature of the organic matrices, particularly the participation of collagen fibers which formed outside of the cell, has been controversial (Okazaki, 1960, 1965; Moss and Meehan, 1967; Travis et al., 1967; Currey and Nichols, 1967, 1969; Klein and Currey, 1970; Travis, 1970; Towe, 1972; Kniprath, 1974). Studies on the cellular basis of skeleton formation in sea urchins have dealt with the growth or regeneration of spines (Pilkington, 1969; Johnson and Chapman, 1970; Heatfield, 1971 a,b; Heatfield and Travis, 1975a, b) and teeth (Kniprath, 1974), or the development of larval spicules (see Decker and Lennarz, 1988). Recent ultrastructural investigations of intact spines, teeth and regenerating spines in E. tribuloides presented detailed information on the morphology of sclerocytes, or cells involved in the skeleton formation (Märkel and Röser, 1983; Märkel et al., 1986; Märkel, 1990). The previous TEM studies in this paper also demonstrated fine structures of the sclerocyte in the normal test plates of S. intermedius. However, it was not possible to observe

an initiation phase of crystal deposition in the decalcified tissues. In view of its greater ease of sectioning, the regenerating test and spines, which probably include various mineralizing stages, seem to be suitable materials to investigate the process of skeleton formation. The present study by LM and TEM focused observations on the mineralizing front of regenerating test plates and spines.

2. MATERIAL AND METHODS

Adult sea urchins, S. intermedius, ranging from 35 mm to 64mm test diamter, were used. Experimental regeneration of the test was induced by cutting off a small part of the interambulacral area using an engine drill (Fig. 140). Care was taken not to injure the viscera and the gonads. The rectangular openings averaged 5x5 to 5x10 mm. Regenerating spines were obtained by fracturing primary spines with a pair of scissors about 1 mm above the milled ring. Experimental animals were kept in aquaria with well aerated sea water circulated at room temperature (15-25 °C). A sufficient amount of seaweeds, mostly Laminaria, was given them as food. The regenerating test tissue in the wound area was dissected one, two and three weeks after the operation. The regenerating tissue on the spine stubs was dissected out two weeks after the fracture. Pieces of the regenerates were fixed with the PG fixative and subsequently postfixed with the osmic solution (see Chapter III). In

order to identify extracellular spaces, some regenerating spine tissues were fixed in the PG fixative containing ruthenium red at a concentration of 1 mg/ml (modified from Brooks, 1969). All specimens were embedded in epoxy resin (Epon 812) after dehydration through a graded series of ethanol and QY-1. Ultrathin and semithin sections were cut with glass or diamond knives using a Porter-Blum ultramicrotome. Most of the ultrathin sections were stained with lead citrate only, but some were doubly stained with uranyl acetate and lead citrate. Some others were observed without staining. Examinations of ultrathin sections were performed with a transmission electron microscope (Hitachi HU-12 or H-6000). The semithin sections for light microscope observations were stained with toluidine blue or a methylene blue-azur II mixture (Richardson et al., 1960) or alkaline methylene blue-basic fuchsin (Huber et al., 1968).

2. RESULTS

(A) Regenerating test tissues

(a) Formation of the blastema

The first externally observable feature of the test regeneration was the appearance of a coagulation product along the wound margin within a day or so. This coagulation product was apparently made up of a clot of coelomocytes markedly pigmented as blackish red. Within two to five days, it gradually grew into a soft membranous tissue covering the whole wound area. After two weeks, the wound

area was occupied by the blastema whose outer and inner surfaces were covered, respectively, by multilayered epidermis and the monolayered coelomic epithelium (Fig.141). The dermal connective tissue was composed of several kinds of cells and extracellular fibrous and amorphous substances. Based on the advancement of mineralization, the dermal connective tissue was tentatively subdivided into three regions, the fibrous, the prestereomal and the stereomal. The fibrous region was composed of fibroblasts, bundles of collagen fibers and thin fibrils, and covered the outer and the inner narrow areas of the dermal connective tissue, being in contact with the epidermis and the coelomic epithelium. The prestereomal region occupied the middle layer with accumulation of various cell elements. In this region, small crystals were scattered. Several stereomal regions were distributed in the prestereomal region separated by the presence of growing crystals or the trabeculae. In the fibrous region, no phases of mineralization were observed either on mature collagen fibers of about 0.1μm thick (Fig. 142) and thin fibrils of about 0.02μm thick, though some crystals were seen to deposit within cells (Fig. 143). Therefore, ultrastructural characteristics of the mineralizing tissue are described of the prestereomal and stereomal regions.

(b) The prestereomal region

The upper and the lower margins of this region still had

collagen fibers and fine fibrils, and were filled with cellular elements including red and colorless spherule cells and other cells (Fig. 144). Coelomocytes except for the spherule cells could not be identified, because most cells were so complicated in form that it was difficult to trace their outlines. They had extensive vesicular cisternae of the ER (Fig. 145). Associated with the cell bodies of spherule cells were numerous membrane-bound bodies, some of which were presumably cytoplasmic extensions of the cells but some others appeared to be isolated vesicles. In the extracellular spaces, fine fibrils were more abundant than collagen fibers.

In the area where more cellular elements were accumulated, some plasmodial cells were fusing to form a syncytium (Fig. 146). Many small crystalline structures were dispersed in this area. Von Kossa's method indicated that they were calcium, but the sites were found to be empty in semithin sections (Fig. 147). An intense azurophilia or basophilia was observed in the cytoplasm around the empty holes (Fig. 148). This staining sensitivity was considerably reduced where the crystals (holes) had grown in size and in number. The azurophilic area revealed a fine structure characterized by a number of secondary lysosomes or residual bodies scattered in the syncytial cytoplasm (Fig. 149). They contained many small vesicles, myelin-like structure and electron-dense granules. There were abundant membrane-bound bodies around the syncytium. Many electron-dense

granules were noted in these bodies (Fig. 150).

Small crystalline concretions in the form of highly electron-dense particles were frequently detected in the intracellular vacuoles of single cells and the syncytium (Figs. 151, 152). The crystallites were rectangular or polygonal in shape and varied in size ranging usually from 0.1μm to 3.5μm, occasionally 5.5 μm or more (Figs. 153, 154). They probably represent initial phases of mineralization. The crystallites usually appeared in large membrane-bound vacuoles of 3-10μm in diameter(Figs. 155-160). The number of crystallites contained in the vacuoles ranged from a dozen of small ones to one or two large ones. In a very few instances, large crystallites were left intact in sections (Fig. 154). Such large crystallites appeared to lie directly in the cytoplasm without evident vacuolar envelope. The calcifying vacuoles were found mostly in the vicinity of developing Golgi vacuoles (Fig. 158). They contained granular or amorphous material and several small vesicles which bore a close resemblance to Golgi vesicles (Figs. 153, 155-158). Some of the vesicles were contiguous to the crystallites. Round mitochondria having a few cristae and prominent dense granules very often lay in close contact with the calcifying vacuoles (Figs. 158-160). Dissolution of crystallites after sectioning sometimes left spaces filled with embedding plastic (Figs. 155, 158-160). Some membranous structures in parallel array were occasionally observed (Figs. 155, 160).

Two types of crystal bearing cells, the dark and the

light, were identified. The dark cells were characterized by their dark-toned cytoplasm due to the presence of abundant free ribosomes, glycogen granules and relatively compact ground substances (Fig. 161). Glycogen granules were sometimes aggregated covering a wide field (Fig. 162). Developed Golgi complexes were in the perinuclear region (Fig. 163). Expanded Golgi vacuoles contained a small amount of granular or amorphous material, while Golgi vesicles were filled with a moderately electron-dense homogenous substance. A number of mitochondria scattering in the cytoplasm were noted with their dense granules. Secondary lysosomes or residual bodies were also common inclusions of the cells. They contained small vesicles, myelin-like structures, and dense amorphous materials (Fig. 161). Some dark cells contained small crystallites in their vacuoles but others had no crystallites at all. The light cells always contained fewer but larger crystallites. They were characterized by a reduced number of free ribosomes and glycogen granules in the less compact ground substance (Fig. 158). Golgi complexes were well-developed, but lysosomes or residual bodies were rarely encountered.

(c) The stereomal region

Rectangular or irregular spaces in semithin sections caused by displacement of crystals represented the initial stage of trabecula formation (Figs. 164, 165). It seemed that crystals were growing inside of the syncytium. When they grew further to form trabeculae, however, it was quite

difficult to say whether or not they still remain intracellular. In three-week-old regenerates the fenestrated structure of the stereom became evident (Fig. 166). The organic phase of the stereom had been constructed of an evenly spread syncytial tissue. As compared with the normal test (Fig. 167), the regenerating stereom at this stage showed more abundant cellular elements and a less complicated structure.

(B) Regenerating spine tissues

The two-week-old regenerating spine tissues contained crystals in various developing stages, which made it possible to trace the initial process of regeneration. Light microscope observations of the regenerating spines revealed a number of small crystals in the tip region and some larger, pillar-shaped crystals in the basal region. In many instances, the crystals were dislodged by sectioning and left holes in the sections (Fig. 168).

Electron microscope observations of the spine regenerates, as well as of the regenerating test, showed initial crystallites of several microns long in the vacuoles of the sclerocytes (Fig. 169). These vacuoles were obviously involved in the initial process of crystal formation, and will be referred to as "calcifying vacuoles", hereafter. The sclerocytes having the calcifying vacuoles, or to be called the early sclerocytes, showed a very complicated cell contour with numerous elongated branches of

cytoplasmic extensions (Figs 169-170). The cytoplasm was compact and contained well-developed Golgi complexes, relatively abundant mitochondria and moderately developed cisternae of the rough endoplasmic reticulum (Fig. 170). Large lipid-like droplets were also distributed in the cytoplasm. Mitochondria frequently appeared in the cytoplasmic extensions. The Golgi vesicles were filled with amorphous or some granular materials of a moderate electron-density. The calcifying vacuoles were located near the Golgi complexes, and contained many small vesicles most of which had amorphous materials of various densities. Around the calcifying vacuoles was an accumulation of mitochondria which usually contained several electron-dense granules in the matrix. The granules presumably contained calcium because the density of granules decreased by treating the sections with an EDTA solution. Intramitochondria granules of the spine sclerocytes were less conspicuous than those of the test sclerocytes. The cytoplasm having the crystal of several microns had many vescicular structures. Some of them were multivesicular bodies and some were residual bodies (Figs. 171, 172).

When ruthenium red was introduced into the tissues during the fixation, the dye particles were never detected within the calcifying vacuoles (Fig. 173). Instead, they were found exclusively in the complicated interstitial spaces of the dermal as well as the epidermal cells.

Some larger crystals of about 20-30μm long, mostly

represented by emptied spaces in sections, were surrounded by thin cytoplasmic extensions of the sclerocytes (Figs. 174-176). Sometimes, the cytoplasmic extensions revealed a syncytial appearance (Figs. 174). The extensions and the crystals were in close contact with each other or separated by large spaces. A very thin membranous or fine granular structure coated intimately the crystal surface (Fig. 175). The cytoplasmic extensions were indistinct in some portions and covered the crystal surface only intermittently (Fig. 174). The sclerocytes enclosing the crystal with their cytoplasmic extensions showed considerably loose cytoplasm, in which numerous vesicular structures of various sizes and shapes were scattered (Fig. 176). The vesicles contained heterogeneous or granular materials of various electron-densities. Some of the vesicles showing an autophagic or a myelinated figure seemed to be a kind of residual bodies. The nuclei showed clumps of condensed chromatin along the nuclear membrane suggesting a pyknotic change. The mitochondria were relatively abundant but partially vacuolized, and had fewer granules.

The crystals developing further and attaining to a stereomal structure were surrounded by less extensive cytoplasmic envelope; thinly elongated cytoplasm limited by a membrane or only a thin membrane exclusive of cytoplasm was observed in the crystal surface (Fig. 177). Vesicles of various sizes were frequently aligned along the crystal surface where the cytoplasmic envelop was missing (Fig. 178). Ruthenium red particles were detected in contact with

the crystal surface at this position (Fig. 179). The cytoplasm of the cell extensions covering larger crystals was often characterized by coarse ground substance (Fig. 180). While the early sclerocytes containing calcifying vacuoles were transformed into the mature ones which enclosed larger crystals, a number of another type of cells were accumulated among the early sclerocytes. These cells generally exhibited a morphology similar to the early sclerocytes, but differed in holding no calcifying vacuoles and showing the more compact cytoplasm, in which lipid-like granules and multivesicular bodies were distributed (Fig. 181). This morphology suggests that they are probably the progenitor cells of the "secondary" sclerocyte, which correspond to the "precalcoblasts" in the regenerating spines of S. purpuratus (Heatfield and Travis, 1975a,b) and the "young sclerocytes" in the normal spine of E. tribuloides (Märkel and Röser, 1983).

4. DISCUSSION

A coagulation product which appearing first along the wound margin of the test plates was made up of a clot of coelomocytes including phagocytic leucocytes, spherule cells and other cells. Provided that the coagulation is the initial tissue of regenerating test, its basic components must be the phagocytic leucocytes as shown in a TEM observation on the clot formation. Leucocytes are known to become fibrogenic, or to form a syncytium when stimulated

(Kindred, 1924; Kuhl, 1965; Chien et al., 1970; Johnson and Chapman, 1970). Furthermore, it was suggested that they have an ability of forming other tissues (Theel, 1894). Kindred (1924) reported that syncytium formed by leucocytes is loosely organized and has large intersyncytial vacuolar spaces within which wandering spherule cells are embedded. He further argued that the syncytial cytoplasm contains spicules and forms a prestereomal structure which is a framework of beams with lacunar spaces. These reports suggest that the leucocytes transform into sclerocytes which build up a syncytial structure where calcite crystals deposited intrasyncytially or intracellularly. The examinations of non-decalcified semithin sections of the prestereomal region in the present study have revealed that calcite crystals deposit in spaces which seemed to correspond to the lacunar spaces described by Kindred (1924). The crystals appeared to join with each other at end to end, forming a developed trabecular stereom. The mineralization seemed to be initiated intracellularly because the crystals first appeared in the intracellular space. The TEM observations also demonstrated that initial crystallites deposited in vacuoles of the sclerocyte. The fact that no ruthenium red particles were found in the crystallite bearing vacuoles in the regenerating spine verifies that the "calcifying vacuoles" are isolated from the extracellular space.

Occurrence of crystals within a membrane-bound space in

the syncytial cytoplasm has been reported in ultrastructural studies of larval primary mesenchyme cells (Gibbins et al., 1969) or tooth odontoblasts (Kniprath, 1974; Märkel et al., 1986). Kniprath (1974) found the occurrence of the first crystals in very intimate contact with the inner coating of vacuoles, and considered that this material served as an organic matrix for crystal nucleation. Calcifying vacuoles observed in the regenerating test had many small vesicles whose size was very close to the smallest crystallites. They often appeared contiguous to growing crystallites. Very similar features were observed also in the regenerating spine. Their significance in initiating mineralization is therefore to be stressed. Implications of Golgi cisternae or vesicles in the intracellular calcification have been reported in coccolith formation in marine algae (Manton and Leedale, 1969; Outka and Williams, 1971; Pienarr, 1971), and spicule formation in the sea pansy (Dunkelberger and Watabe, 1974) and in the gorgonian (Kingsley and Watabe, 1982, 1984). Topographic evidence suggested that the calcifying vacuoles may be derived from Golgi vacuoles. The vacuoles seemed to be a structure required at least for the initiation of crystal growth, because large crystals were found not to be associated with such vacuoles.

Mitochondria in the sclerocytes were characterized by the presence of electron-dense granules. Some membrane-bound bodies outside of the cell bodies also contained similar granules. Such dense granules probably contained calcium

compounds, because they were conspicuous in unstained sections and their electron density was considerably reduced after treatment with an EDTA solution. Mitochondria containing many dense granules have been referred to as being involved in calcium and phosphate transport in cartilage and bone cells (Halstead, 1969; Martin and Matthews, 1969; Shapiro and Greenspan, 1969; Holtrop, 1972). The mitochondria may be concerned with the uptake and transport of calcium in the sclerocytes.

Dark and light cells, both having initial crystals, were identified in the prestereomal region where an active reorganization of the regenerating tissue was progressing in company with crystal deposition. The dark cell having more compact cytoplasm with more ribosomes and glycogen granules had less crystals than the light cells. Therefore, the dark cells seem to transform to the light cells. During which they involved in active seeding and growth of crystals in consumption of glycogen and other cell inclusions. Accumulation and consumption of glycogen granules accompanying a progress of mineralization are known in vertebrate osteoblasts (Scott and Glimcher, 1971) and cartilage cells (Michell and Shepard, 1970). A similar phenomenon was reported in the odontoblast of teeth in a sea urchin, E. tribuloides (Märkel et al., 1986).

In the regenerating spine, more advanced phases of the trabecula formation by sclerocytes were observed. The grown-up crystals were almost entirely enclosed by thin cytoplasmic extensions of sclerocyte, except fro some

portions coated only by small vesicles separated from the extensions. The cytoplasmic extensions sometimes revealed a syncytial structure by addition of cytoplasmic extensions of other sclerocytes. The trabeculae covered with cytoplasmic extensions or vesicles were shown to be partially exposed to the extracellular space by the presence of ruthenium red particles. Märkel and Röser (1983) reported in the spine of E. tribuloides that the growing crystals are covered by cytoplasmic extensions of syncytial sclerocytes, called the cytoplasmic sheath, and the crystal surface is coated directly and tightly by a thin membranous material, called the matrix coat or the trabecule coat. In the spine regenerates in S. intermedius, the matrix coat was observed as a thin membrane or an array of fine granules. The regenerating test showed a number of clotting coelomocytes accumulating to form the blastema, but in the regenerating spines this was less pronounced. As a matter of course, the periphery of the regenerating test tissue was entirely surrounded by the ontogenic calcified tissues, different from the spine regnerate which had such tissues only on one side. In contrast to Heatfield (1971a) who reported that the spine was regenerated by a continuous outgrowth of the microspines at the fracture plane, the skeletal stereoms of test regenerates appeared as isolated calcified islands. This difference must be due to the above situational difference of the regenerating tissues of the test and spine. Heatfield (1971) and Märkel and Röser (1983) seem to have failed to

find sclerocytes bearing calcifying vacuole, because they observed bleached spines (Heatfield, 1971a) or decalcified spines (Märkel and Röser, 1983).

Fine structural evidence presented here revealed that the regeneration of the stereomal skeleton of both the test plate and the spine takes place in essentially the same sequence of two phases, intracellular and extracellular crystal growths. No collagen fibers can be the calcifying matrix in the mineralization.

IX. GENERAL DISCUSSION

(A) Do collagen fibers participate in initiation of the mineralization of sea urchin skeletons?

Collagen fibers are known to be essential for induction of calcium deposition in bone and cartilage of vertebrates (Glimcher and Krane, 1968; Schiffmann et al., 1970; Hancox, 1972). Collagen fibers having a typical banding pattern similar to mammalian ones are abundantly distributed in the organic stereom of sutural areas in the test plates of sea urchins (Travis et al., 1967; Travis, 1970). Travis (1970) reported that the collagen fibers exist also in empty holes of decalcified skeletal trabeculae of the test plates in a sea urchin, S. droebachiensis, and argued that the collagen fibers participate in initiation of the mineralization of skeletons. However, some workers were sceptical about the Travis' hypothesis from the histological and crystallographical points of view (Moss and Meehan, 1967; Currey and Nichols, 1967; Towe, 1967; Pilkington, 1969; Klein and Currey, 1970). The present TEM observations revealed that collagen fibers are distributed in the space of organic stereom but not in the empty holes of decalcified trabeculae. Also, in sections of calcified regenerating test plates, no calcifying or calcified collagen fibers were observed, though crystal-bearing sclerocytes were around them. Benson et al. (1983) described that organic components of decalcified larval spicules of S. purpuratus

have no characteristic collagen. In the teeth of L. variegatus, Veis et al. (1986) reported that the matrix proteins show a different polyacrylamide gel electrophoretic pattern from that of collagen. These findings obtained from various skeletal tissues of sea urchins strongly suggest that no collagen fibers participate in initiation of mineralization as calcifying matrix.

Blankenship and Benson (1984) showed that cultured mesenchyme cells did not undergo the final stage of differentiation to produce spicules in the presence of inhibitors of collagen synthesis but did complete the process if exogenous collagen was added. This finding suggests that collagen is required for spicule formation probably as a component of an extracellular matrix which is necessary for cell adhesion (Decker and Lennarz, 1988).

Although the trabecular skeleton of sea urchins is crystallographically known to be a single crystal, its fractured plane does not seem to show the nature of a single crystal (Nissen, 1969; Towe, 1972). The fact that the broken trabeculae show a so-called conchoidal fractured surface suggests that the crystal is formed by an aggregation of many crystallites (Towe, 1967; Berman et al., 1988). Dubois (1991) in SEM observations of TCA-etched spine skeletons in a sea star, Asterius rubens, demonstrated that a coherent material appeared as concentric laminae bridged by radial threads and concluded that echinoderm skeletons are presumably true polycrystalline entities. In the present TEM observations of the regenerating test

plates, a membranous structure in parallel array was shown in the spaces of dissolved crystallites. These also may be an intercalative material in trabecular skeletons of test plates.

Benson et al. (1986) showed in an immunoblotting analysis that the matrix of larval spicules contains N-linked glycoproteins which are immunologically related to calcium binding proteins. In a culture of dissociated mesenchyme cells from larvae of S. purpuratus, tunicamycin, an antibiotic which inhibits N-glycosylation of proteins, blocks the spicule formation (Mintz et al., 1981). It was concluded that biosynthesis of N-linked glycoproteins is a prerequisite for $CaCO_3$ deposition in the spicule formation. These findings obtained from larval spicules suggest that glycoproteins are incorporated into the skeleton as the calcifyable matrix. Acid and neutral mucosubstances histochemically detected on the collagen fibers of the test plates of S. intermedius may include N-linked glycoproteins. Acid mucosubstances are known to be capable of binding calcium ions (Sobel and Burger, 1954). Therefore, the collagen fibers associated with such mucosubstances may be related to local accumulation of calcium ions. In addition, the collagen fibers may play a role in attracting and/or detaining sclerocytes at the site of actively growing skeleton. Collagen fibers were enclosing compactly the trabecular surface at the sutural areas together with the cytoplasmic processes of sclerocytes. They may also have

some inhibitory roles for the trabecular growth by regulating the crystal shape in the sutural area.

(B) Ultrastructural characteristics and origin of the sclerocytes

Märkel and Röser (1983) reported in E. tribuloides that the spine sclerocytes extend a number of cytoplasmic processes which enclose closely the trabecular surface to form a syncytial cytoplasmic sheath. Their elongated processes have thick cytoplasmic knots, sometimes showing a characteristically complexed form. These ultrastructural features of the spine sclerocytes were very similar to those of the test sclerocytes in S. intermedius. However, some morphological differences in cellular complexity were observed between sclerocytes of regenerating test plates and of spines in the present study in which initial mineralizing stages were examined in the regenerating test and later stages in the regenerating spines. The differences observed of the two sclerocytes could be due to the stage difference of mineralization, because the sclerocytes observed in ontogenic test plates were not different from those of the spines in morphology. This suggests that the sclerocytes participating in the initial stage of mineralization can change their features in advanced stages.

The origin of sclerocytes in sea urchins is still controversial. Earlier workers considered that a kind of coelomocytes moves into the test tissue and transforms to the sclerocytes (Theel, 1894, Kindred, 1924). Heatfield

(1971b) reported in the regenerating spine of S. droebachiensis that cells near the fractured surface rarely uptook [H^3]-labeled thymidine, though labeled cells were abundantly distributed at the dermal region proximal to the milled ring at the spine base. She supposed that the sclerocytes of spines arise near the spine base and migrate to the fractured region. This suggests that the sclerocytes may not increase by cell division at the growing site but they may come from other portions.

Phagocytic leucocytes were observed to form a stereom-like structure by trapping other coelomocytes with envelopes of their cytoplasmic processes. These leucocytes were shown to have calcium crystals. It is highly possible that the phagocytic leucocytes differentiate to the sclerocytes at needs. It is postulated that the phagocytic leucocytes are the most likely candidate as progenitor cells to be transformed to the sclerocytes.

(C) By what process do the sclerocytes initiate to grow crystals?

Sclerocytes having "calcifying vacuoles" were observed in both regenerating test plates and spines. Based on the overall observations of the regenerating and ontogenic test plates and spines, the possible general course of the trabecule formation is illustrated in Text-fig. 3.

The crystal initiates to grow intravacuolarly and then comes to be exposed to the extracellular space as the

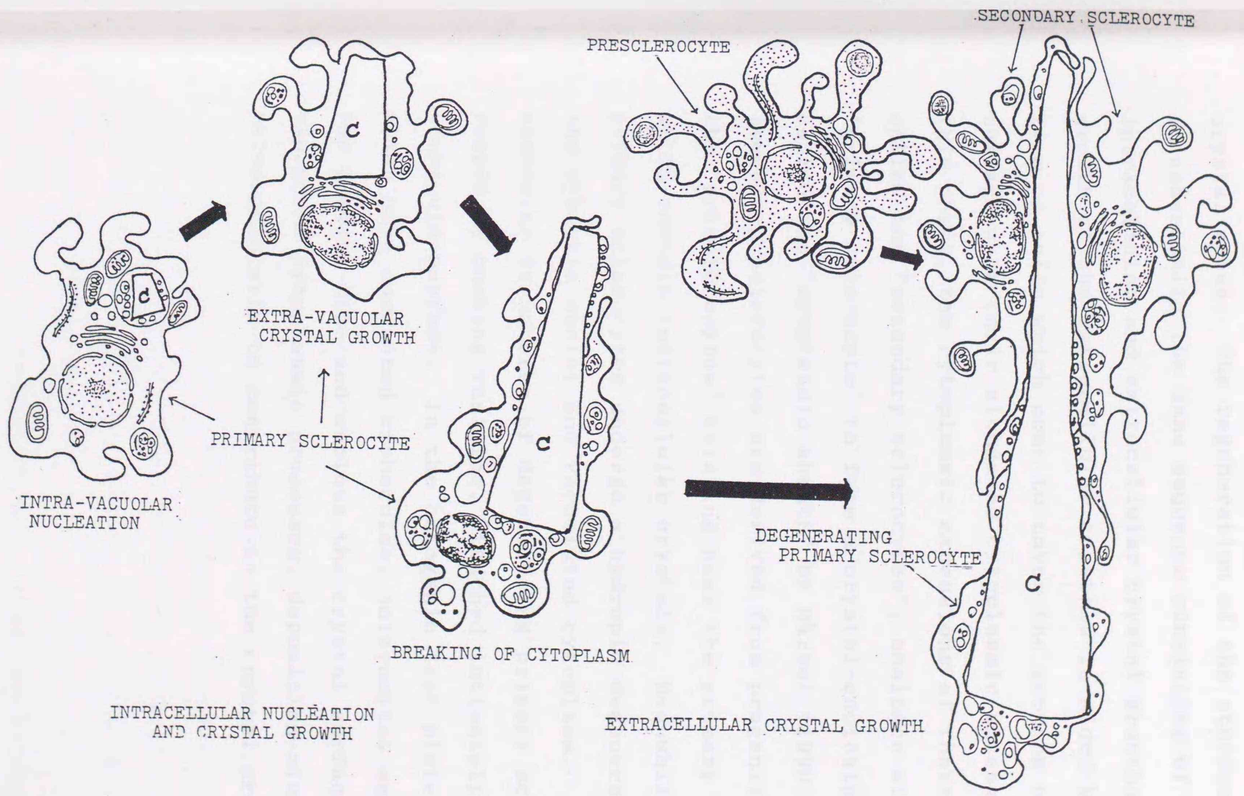

Text-fig. 3. Schematic illustration of the general course of crystal formation in regenerating test and spine
c: crystal.

crystal grows. The regeneration of the stereom takes place in essentially the same sequence consisting of two phases, intracellular and extracellular crystal growths. Further growth of the extracellular crystals is aided by another type of cells which come to cover the growing crystal surface with their elongated cytoplasmic extensions. In this phase, the cytoplasmic extensions of these cells, to be called the "secondary sclerocytes", coalesce with the "primary sclerocyte" to form a crystal-enclosing syncytium called the "synplasmic sheath" by Märkel (1990). The secondary sclerocytes are derived from progenitor cells, or the "presclerocytes" existing near the primary sclerocytes which contain intracellular crystals. Meanwhile, the primary sclerocytes undergo a hydropic degeneration showing the pyknotic nuclei and vacuolated cytoplasm. Some vesicular structures of degenerating primary sclerocytes remain as coating vesicles, attached intimately to the trabecula surface. In the ontogenic test plates and spines which have completed trabeculae, sclerocytes may gather at the growing site and enclose the crystal surface by their elongated cytoplasmic processes, depositing minerals extracellularly to contribute to the crystal growth.

SUMMARY

To investigate the growth mechanism of sea urchin dermal skeletons, the morphology and histotopography of cells and their products in intact and regenerating test plates and spines of Strongylocentrotus intermedius were examined by light and electron microscopy (TEM and SEM).

1. Fibrous elements were abundantly distributed at the sutural areas. Their histochemical characteristics showed that they were collagenous fibers combined with acidic and neutral mucopolysaccharides. By TEM observations, the fibers were shown to be composed of thick elements having a typical banding pattern of mammalian collagen fibers and thin fibrils. The collagenous fibers closely enclosed the trabecular surface. Although these fibers seemed to form a microenvironment for mineralization, they were not a constituent of the calcifying matrix. They may play an inhibitory role in the mineralization to control trabecular growth and shape.

2. Five types of cells were identified in the organic stereom of decalcified test plates. Among them, small basophilic cells having elongated cytoplasmic processes, were identified as sclerocytes. They attached closely to trace holes of decalcified trabeculae. Other cells including spherule cells, eosinophilic cells and vacuolated cells seemed to have no direct relation to the formation of skeletal trabeculae.

3. SEM observations revealed that the sclerocytes were

covering closely the trabecular surface with numerous elongated cytoplasmic processes, some of which had bladder-like cytoplasmic knots. This feature was particularly conspicuous at the periphery of growing trabeculae, where a meshwork woven by the processes was closely attached.

4. Flat cells having elongated cytoplasmic processes were observed by SEM to appear around the trabecula surface, dominantly on the portion where an erosion caused an enlargement of the stereomal pore space. The flat cells were conspicuous at the sutural areas of young urchins' plates. Also, there were cells having scrubbed brush-like projections. Together with the flat cells, they were regarded as resorbing cells.

5. Five types of coelomocytes, phagocytic leucocytes, spherule cells, vibratile cells, hyaline cells and reniform cells, were identified in the coelomic fluid of S. intermedius. At clotting in vitro, the phagocytic leucocytes formed a basic framework of envelopes derived from their cytoplasmic processes. The framework incorporated other coelomocytes to form a stereom-like structure. The vibratile cells were also observed to participate in the clot formation. By behavioral analogy, the phagocytic leucocytes were considered to migrate into the skeletal tissue as progenitor cells of the sclerocytes.

6. In regenerating test and spines, a calcifying vacuole developed in the "primary" sclerocyte was observed to take part in the initiation of mineralization. A crystal grown

in this intracellular vacuole at the primary stage was observed to be exposed to the extracellular space as the crystal grew larger. Further growth of the crystal was continued to be surrounded by syncytial cytoplasmic processes of the "secondary" sclerocytes. Grown-up trabeculae were directly coated by a continuous membrane sheet or beaded small vesicles. These structures suggested a sequential process of two phases of mineralization, intracellular and extracellular, in the regeneration of test plates and spines.

7. Histological and ultrastructural evidence obtained from the ontogenetic and the regenerating test plates and spines showed that growth of skeletal trabeculae of sea urchins may be carried out by sclerocytes transformed from phagocytic leucocytes which were accumulated at the growing site. The sclerocytes may deposit calcite crystals first in intracellular vacuoles and then liberate them in the extracellular space, where cytoplasmic processes of other sclerocytes participate in further growth of the crystals leading to a mature stereom. The assemblage of the elongated cytoplasmic processes may actively contribute to the crystal growth.

ACKNOWLEDGEMENTS

The author wishes to express his sincere thanks to Professor Juro Yamada, Faculty of Fisheries, Hokkaido University for his guidance and discussion during the course of the present study and critical readings of the manuscript. The author thanks Professor Hiroya Takahashi and Associate Professor Yasuo Mugiya for their kindness in reading the manuscript. Thanks are extended to Associate Professor Hirotoshi Yamamoto, Mr. Yoetsu Arashida and Mr. Kiyoshi Nomura for their help in rearing sea urchins at Usujiri Marine Station of Hokkaido University. Thanks are also due to Mr. Kenji Kawamata, Hokkaido Fisheries Experimental Station and the staff of Fisheries Seedling Center of Shakotan-Cho for their help in collecting material sea urchins. A debt of gratitude is also owed to graduate students, Messrs. Hiroshi Tanabe and Hiroaki Suzuki for their assistance in preparing the paper.

REFERENCES

Andrew, W. (1962) Cells of the blood and coelomic fluids of tunicates and echinoderms. Am. Zool., 2: 285-297.

Banga, I. and Baló, J. (1960) Isolation of neutral heteropolysaccharide containing mucoprotein from bovine achilles tendon with acid of collagenmucoproteinase. Biochem. J., 74: 388-393.

Becher, E. (1924) Über den feineren Bau der Skelettsubstanz bei Echinoideen, insbesondere über statische Strukturen in derselben. Zool. J. Abt. fur Allgemeine Zoologie und Physiologie der Tiere, 41: 179-244.

Becher, S. (1914) Über statische Strukturen und kristalloptische Eigentumlichkeiten des Echinodermenskeletts. Verh. dt. zool. Ges., 23-24: 307-327.

Behre, E. (1932) A preliminary report on the histology of the body fluid in Mellita quinquiesperforata (Leske). Anat. Rec., 54 (suppl.): 92.

Benson, S., Jones, E. M. E., Benson, N. C. and Wilt, F. (1983) Morphology of the organic matrix of the spicule of sea urchin larvae. Exp. Cell Res., 148: 249-253.

Benson, S. C., Benson, N. C. and Wilt, F. (1986) The organic matrix of the skeletal spicule of sea urchin embryos. J. Cell Biol., 102: 1878-1886.

Berman, A., Addadi, L. and Weiner, S. (1988) Interactions of sea-urchin skeleton macromolecules with growing calcite crystals- a study of intracrystalline protein. Nature, 331: 546-548.

Berman, A., Addadi, L., Kvick, A., Leiserowitz, L., Nelson, M. and Weiner, S. (1990) Intercalation of sea urchin proteins in calcite: Study of a crystalline composite material. Science, 250: 664-667.

Bertheussen, K. and Seljelid, R. (1978) Echinoid phagocytes in vitro. Exp. Cell Res., 111: 401-412.

Blankenship, J. and Benson, S. (1984) Collagen metabolism and spicule formation in sea urchin micromeres. Expl. Cell Res., 152: 98-104.

Bookhout, C. G. and Greenburg, N. D. (1940) Cell types and clotting reactions in echinoid, Mellita quinquiesperforata. Biol. Bull., 79: 309-320.

Boolootian, R. A. (1962) The perivisceral elements of echinoderm body fluid. Am. Zool., 2: 275-284.

Boolootian, R. A. and Giese, A. C. (1958) Coelomic corpuscles of echinoderms. Biol. Bull., 115: 53-63.

Brooks, R. E. (1969) Ruthenium red stainable surface layer of lung alveolar cells; electron microscopic interpretation. Stain Technol., 44: 173-177.

Chien, P. K., Johnson, P. T., Holland, N.D. and Chapman, F. A. (1970) The coelomic elements of sea urchins (Strongylocentrotus). IV. Ultrastructure of the coelomocyte. Protoplasma, 71: 419-442.

Cowden, R. R. (1968) Cytological and histochemical observations on connective tissue cells and cutaneous wound healing in the sea cucumber Stichopus badionotus. J. Invert. Path., 10: 151-159.

Currey, J. D. and Nichols, D. (1967) Abscence of organic phase in echinoderm calcite. Nature, 214: 51-83.

Currey, J. D. and Nichols, D. (1969) The question of the organic matrix of echinoderm skeletons. Proc. Malac. Soc., 38: 546-547.

Dafni, J. (1983) Aboral depressions in the tests of the sea urchin Tripneustes cf. gratilla (L.) in the gulf of Eilat, Red Sea. J. Exp. Mar. Biol. Ecol., 1983: 1-15.

Decker, G. L. and Lennarz, W. J. (1988) Skeletogenesis in the sea urchin embryo. Develop., 103: 231-247.

Deutler, F. (1926) Uber das Wachstum des Seeigelskeletts. Zool. Jb. Abt. fur Anat. und Ontog. der Tiere, 48: 119-200.

Donnellon, J. A. (1938) An experimental study of clot formation in the perivisceral fluid of Arbacia.

Physiol. Zool., 11: 389-397.

Donnay, G. and Pawson, D. L. (1969) X-ray diffraction studies of echinoderm plates. Science, 166: 1147-1150.

Dubois, P. (1991) Morphological evidence of wherent organic material within the stereom of postmetamorphic echinoderms. In: Mechanisms and Phylogeny of Mineralization in Biological Systems (Suga, S. and Nakahara, H., eds.) pp. 41-45, Springer-Verlag, Tokyo.

Dunkerberger, D. G. and Watabe, N. (1974) An ultrastructural study on spicule formation in the pennatulid colony Renilla reniformis. Tiss. and Cell, 6: 575-586.

Ebert, T. A. (1967) Negative growth and longevity in the purple sea urchin Strongylocentrotus purpuratus (Stimpson). Science, 157: 557-558.

Ebert, T. A. (1968) Growth rates of the sea urchin Strongylocentrotus purpuratus related to food availability and spine abrasion. Ecology, 49: 1075-1091.

Endean, R. (1966) The coelomocytes and coelomic fluids. In: Physiology of Echinodermata (Boolootian, R. A., ed.) pp. 301-328, John Wiley and Sons, New York.

Edds, K. T. (1977) Microfilament bundles I. Formation with uniform polarity. Exp Cell Res., 108: 452-456.

Fontaine, A. R. and Lambert, P. (1973) The fine structure of

the haemocyte of the holothurian Cucumaria miniata (Brandt). Can. J. Zool., 51: 323-332.

Forntaine, A. R. and Lambert, P. (1977) The fine structure of the leucocytes of the holothurian, Cucumaria miniata. Can. J. Zool., 55: 1530-1544.

Fox, D. L. and Hopkins, T. S. (1966) The comparative biochemistry of pigments. In: Physiology of Echinodermata (Boolootian, R. A., ed.) pp. 277-300, John Wiley and Sons, New York.

Fuji, A. (1967) Ecological studies on the growth and food consumption of Japanese common littoral sea urchin, Strongylocentrotus intermedius (A. Agassiz). Mem. Fac. Fish. Hokkaido Univ., 15: 83-160.

Gibbins, J. R., Tilney, L. G. and Porter, K. R. (1969) Microtubules in the formation and development of the primary mesenchyme in Arbacia punctulata. I. The distribution of microtubules. J. Cell Biol., 41: 201-226.

Glimcher, M. J. and Krane, S. M. (1968) Organization and tructure of bone. In: Treatise on Collagen., 2B (Gould, B. S., ed.) pp. 65-251, Academic Press, New York.

Goodwin, T. W. and Srisukh, S. (1950) A study of the pigments of the sea urchins, Echinus esculentus L. and Paracentrotus lividus Lamarck. Biochem. J., 47: 69-76.

Halstead, L. B. (1969) Are mitochondria directly involved in

biological mineralization? The mitochondria and the origin of bone. Calcif. Tiss. Res., 3: 103-104.

Hancox, N.M. (1972) Biology of Bone. Cambridge Univ. New York.

Heatfield, B. M. (1971a) Growth of the calcareous skeleton during regeneration of spines of the sea urchin, Strongylocentrotus intermedius (Stimpson): a light and scanning electron microscopic study. J. Morphol., 134: 57-90.

Heatfield, B. M. (1971b) Origin of calcified tissue in regenerating spines of the sea urchin, Strongylocentrotus purpuratus (Stimpson): a quantitative radioautographic study with tritiated thymidine. J. Exp. Zool., 178: 233-246.

Heatfield, B. M. and Travis, D. F. (1975a) Ultrastructural studies of regenerating spines of the sea urchin Strongylocentrotus purpuratus. I. Cell types without spherules. J. Morph., 145: 13-50.

Heatfield, B. M. and Travid, D. F. (1975b) Ultrastructural studies of regenerating spines of the sea urchin Strongylocentrotus purpuratus. II. Cell types with spherules. J. Morph., 145: 51-72.

Hetzel, H. R.(1963) Studies on holothurian coelomocytes. I. A survey of coelomocyte types. Biol. Bull., 125: 289-301.

Holland, L. Z., Giese, A. C. and Phillips, J. H. (1967)

Studies on the perivisceral coelomic fluid concentration during seasonal and nutritional changes in the purple sea urchin. Comp. Biochem. Physiol., 37: 289-300.

Holtrop, M. E. (1972) The ultrastructure of the epiphyseal plate. II. The hypertrophic chondrocyte. Calcif. Tiss. Res., 9: 140-151.

Huber, J. D., Parker, F. and Odland, G. E. (1968) A basic fuchsin and alkalinized methylene blue rapid stain for epoxy-embedded tissue. Stain Technol., 43: 83-87.

Inoue, T. and Osatake, H. (1988) A new drying method of biological specimens for scanning electron microscopy: The t-butyl alcohol freeze-drying method. Arch. Histol. Cytol., 51: 53-59.

Irving, J. T. (1963) The sudanophil material at sites of calcification. Arch. Oral Biol., 8: 735-745.

Jensen, M. (1969) Age determination of echinoids. Sarsia, 37: 41-44.

Jensen, M. (1972) The ultrastructure of the echinoid skeleton. Sarsia, 48: 39-48.

Johnson, P. T. (1969a) The coelomic elements of sea urchins (Strongylocentrotus) I. The normal coelomocytes; their morphology and dynamics in hanging drops. J. Inverteb. Pathol., 13: 25-41.

Johnson, P. T. (1969b) The coelomic elements of sea

urchins (Strongylocentrotus) II. Cytochemistry of the coelomocytes. Histochemie, 17: 213-231.

Johnson, P. T. (1970) The coelomic elements of sea urchins (Strongylocentrotus and Centrostephorus) VI. Cellulose acetate membrane electrophoresis. Comp. Biochem. Physiol., 37: 289-300.

Johnson, P. T. and Chapman, F. A. (1970) Infection with diatoms and other microorganisms in sea urchin spines (Strongylocentrotus franciscanus). J. Inverteb. Pathol., 16: 268-276.

Kawamura, K. (1973) Fishery biological studies on a sea urchin, Strongylocentrotus intermedius (A.Agassiz). Sci. Rep. Hokkaido Fish. Exp. Stat., (16): 1-54. (In Japanese)

Karnovsky, M. J. (1965) A formaldehyde-glutaraldehyde fixative of high osmolarity for use in electron microscopy. J. Cell Biol., 27: 137.

Kindred, J. E. (1924) The cellular elements in the perivisceral fluid of echinoderms. Biol. Bull., 46: 228-251.

Kingsley, R. J. and Watabe, N. (1982) Ultrastructural investigation of spicule formation in the gorgonian Leptogorgia virgulata (Lamarck) (Coelenterata:

Gorgonacea). Cell Tiss. Res., 223: 325-334.

Kingsley, R. J. and Watabe, N. (1984) Synthesis and transport of the organic matrix of the spicules in the gorgonian Leptogorgia virgulata (Lamarck) (Coelenterata: Gorgonacea). Cell Tiss. Res., 235: 533-538.

Klein, L. and Currey, J. D. (1970) Echinoid skeleton: absence of a collagenous matrix. Science, 169: 1209-1210.

Kniprath, E. (1974) Ultrastructure and growth of the sea urchin tooth. Calcif. Tiss. Res., 14: 211-228.

Kobayashi, S. (1971) Acid mucopolysaccharides in calcified tissues. Internat. Rev. Cytol., 30: 257-371.

Kobayashi, S. and Taki, J. (1969) Calcification in sea urchins I. A tetracycline investigation of growth of the mature test in Strongylocentrotus intermedius. Calc. Tiss. Res., 4: 210-223.

Kuhl, W. (1965) Das Bewegungsverhalten der Coelomzellen von Psammechinus miliaris bei der Wundheilung (Echinodermata). Helgolander wiss. Meeresunters., 12: 424-443.

Kuhn, R. and Wallenfels, K. (1940) Echinochrome als prosthetische Gruppen hochmolekularer Symplexe in den Eiern von Arbacia pustulosa. Ber. dt. chem. Ges., 73: 458-464.

Lison, L. (1960) Histochimie et Cytochimie Animales, 3e ed.,

Gauthier-Villars & Co. Paris. (Translated to Japanese by Imaizumi, T. in 1962, Hakusuisha, Tokyo)

Luna, L. G. (1968) Histological Staining Methods of the Armed Forces Institute of Pathology. 3rd ed. McGraw Book Camp., New York.

MacMunn, C. A. (1885) On the chromatography of the blood of some invertebrates. Q. Jl. Microsco. Sci., 25: 469-490.

Manton, I. and Leedale, G. F. (1969) Observation of the microanatomy of Coccolithus pelagicus and Cricosphaera carterae, with special reference to the origin and nature of coccoliths and scales. J. Mar. Biol. Ass. U.K., 49: 1-16.

Marks, M., Baer, R. S. and Blake, C. H. (1949) X-ray diffraction evidence of collagen type protein fibers in the Echinodermata, Coelenterata and Porifera. J. Exp. Zool., 111: 55-78.

Märkel, K. (1975) Wachstum des Coronarskeletes von Paracentrotus lividus Lmk. (Echinodermata, Echinoidea). Zoomorph., 82: 259-280.

Märkel, K. (1976a) Struktur und Wachstum des Coronarskeletes von Arbacia lixula Linné (Echodermata, Echinoidea). Zoomorph., 84: 279-299.

Märkel, K. (1976b) Das Wachstum der "Laterne des Aristoteles" und seine Anpassung and die Funktion der Laterne

(Echinodermata, Echinoidea). Zoomorph., 86: 25-40.

Märkel, K. (1981) Experimental morphology of coronar growth in regular echinoids. Zoomorph., 97: 31-52.

Märkel, K. (1990) Biomineralization in echinoderms. In: Echinoderm Research (De Ridder, C., Dubois, P., Lahaye, M-C and Jangoux, M., eds.) pp. 277-282, A. A. Balkema, Rotterdam.

Märkel, K. and Röser, U. (1983) The spine tissues in the echinoid Eucidaris tribuloides. Zoomorph., 103: 25-41.

Märkel, K., Röser, U., Mackenstedt, U. and Klostermann, M. (1986) Ultrastructural investigation of matrix-mediatd biomineralization in echinoids (Echinodermata, Echinoidea). Zoomorph., 106: 232-243.

Märkel, K., Röser, U. and Stauber, M. (1989) On the ultrastructure and the supposed function of the mineralizing matrix coat of sea urchins (Echinodermata, Echinoidea). Zoomorph., 109: 79-87.

Martin, J. H. and Matthews, J. L. (1969) Mitochondrial granules in chondrocytes. Calcif. Tiss. Res., 3: 184-193.

McManus, J. F. A. (1946a) The demonstration of certain fatty substances in paraffin sections. J. Pathol. Bact., 58: 93-95.

McManus, J. F. A. (1946b) Histological demonstration of

mucin after periodic acid. Nature, 158: 202.

Melcher, A. H. (1966) On sudan black positive material in connective tissue. Nature, 211:593-595.

Menton, D. N. and Eisen, A. Z. (1973) Cutaneus wound healing in the sea cucumber, Thyone briareus. J. Morph., 141: 185-204.

Michell, N. and Shepard, N. (1970) The ultrastructure of articular cartilage in rheumatoid arthritis. J. Bone Jt. Surg., 52A: 1405-1423.

Millot, N. (1957) Naphthaquinone pigment in the tropical sea urchin Diadema antillarumPhilipi. Proc. Zool. Soc. Lond., 129: 263-272.

Mintz, G. R., De Francesco, S. and Lennarz, W. J. (1981) Spicule formation by cultured embryonic cells from the sea urchin. J. Biol. Chem., 256: 13105-13111.

Moore, H.B. (1935) A comparison of the biology of Echinus esculentus in different habitats. Part II. J. Mar. Biol. Ass. U. K., 20: 109-128.

Moore, G. P. (1966) The use of trabecular bands as growth indicators in spines of sea urchin Heliocidaris erythrogramma. Aust. J. Sci., 29: 52-54.

Moss, M. L. and Meehan, M. M.(1967) Sutural connective

tissues in the test of an echinoid Arbacia punctulata. Acta Anat., 66: 279-304.

Nissen, H-U. (1969) Crystal orientation and plate structure in echinoid skeletal units. Science, 166: 1150-1152.

Nichols, D. and Currey, J. D. (1968) The secretion, structure, and strength of echinoderm calcite. In: Cell Structure and Its Interpretation. (McGee-Russell, S. M. and Ross, K. F. A., eds.) pp. 251-261, Edward Arnold Ltd. London.

Okazaki, K. (1960) Skeletal formation of sea urchin larvae. II. Organic matrix of the spicule. Embryologia, 5: 283-320.

Okazaki, K. (1965) Skeletal formation of sea urchin larvae. V. Continuous observation of the process of matrix formation. Exp. Cell Res., 40: 585-596.

Okazaki, K. and Inoue, S. (1976) Crystal property of the larval sea urchin spicule. Develop. Growth Differ., 18: 413-434.

Okazaki, K., McDonald, K. and Inoue, S. (1980) Sea urchin larval spicule observed with the scanning electron microscope. In: The Mechanisms of Biomineralization in Animals and Plants. (Omori, M. and Watabe, N., eds.) pp. 159-168. Tokai Univ. Press, Tokyo.

Otto, J. J., Kane, R. E. and Bryan, J. (1979) Formation of filopodia in coelomocytes: localization of fascin, a 58000

dalton actin cross-linking protein. Cell, 17: 285-293.

Outka, D. and Williams, D. (1971) Sequential coccolith morphogenesis in Hymenomonas carterae. J. Protozool. 18: 285-297.

Pearce, A. G. E. (1960) Histochemistry, 2nd ed. J. & A. Churchill Ltd. London.

Pearse, J. S. and Pearse, V. B. (1975) Growth zones in the echinoid skeleton. Amer. Zool., 15: 735-753.

Pienarr, R. N. (1971) Coccolith production in Hymenomonas carterae. Protoplasma, 73: 217-224.

Pilkington, J. B. (1969) The organization of skeletal tissues in the spines of Echinus esculentus. J. Mar. Biol. Ass. U.K., 49: 857-877.

Poole, A. R., Matsui, Y., Hinek, A. and Lee, E. R. (1989) Cartilage macromolecules and the calcification of cartilage matrix. Anat. Rec., 224: 167-179.

Quintarelli, G. (1968) The Chemical Physiology of Mucopolysaccharides. Little Brown, Boston, Massachusetts.

Raup, D. M. (1966) The endoskeleton. In: Physiology of Echinodermata (Boolootian, R. A., ed.) pp 379-395, John Wiley and Sons, New York.

Richardson, K. C., Jarett, L. and Finke, E. H. (1960) Embedding in epoxy resins for ultrathin sectioning in electron microscopy. Stain Technol., 35: 313-323.

Schiffmann, E., Martin, G. R. and Miller, E. J. (1970) Matrices that calcify. In: Biological Calcification: Cellular and Molecular Aspects. (Scharer, H., ed.) pp. 27-67, Appleton-Century-Crofts, New York.

Schultz-Haudt, S. D. and Eeg-Larsen, N. (1961) Isolation of radioactive hydroxyproline from an apparent heteropolysaccharide-protein complex of animal skin after the administration of [^{14}C] proline. Biochim. Biophys. Acta, 51: 560-566.

Scott, B. L. and Glimcher, M. J. (1971) Distribution of glycogen in osteoblasts of the fetal rat. J. Ultrastruct. Res., 36: 565-586.

Service, M. and Wardlaw, A. C. (1984) Echinochrome-A as a bactericidal substance in the coelomic fluid of Echinus esculentus (L.). Comp. Biochem. Physiol., 79B: 161-165.

Shapiro, I. M. and Greenspan, J. S. (1969) Are mitochondria directly involved in biological mineralization? Calcif. Tiss. Res., 3: 100-102.

Simkiss, K. and Wilbur, K. M.(1985) Biomineralization. Cell Biology and Mineral Deposition, pp 146-170, Academic Press, New York.

Smith, A. B. (1980) Stereom microstructure of the echinoid

test. Special Pap. Palaeontology, 25: 1-81.

Smith, V. J. (1981) The echinoderms. In: Invertebrate Blood Cells (Ratcliffe, N. A. and Rowley, A. F. eds.), Vol. 2, pp. 513-562, Academic Press, London.

Sobel, A. E. and Burger, M.(1954) Calcification. XIV. Investigation of the role of chondroitin sulfate in the calcifying mechanism. Proc. Soc. Exp. Biol. Med., 87: 7-13.

Swan, E. F. (1952) Regeneration of spines by sea urchins of genus Strongylocentrotus. Growth, 16: 27-35.

Swan, E. F. (1958) Growth and variation in sea urchins of York Marine. J. Mar. Res., 17: 505-522.

Swan, E. F. (1961) Some observations on the growth rate of sea urchins in the genus Strongylocentrotus. Biol. Bull., 120: 420-427.

Taki, J. (1971) Tetracycline labelling of test plates in Strongylocentrotus intermedius. Sci. Rep. Hokkaido Fish. Exp. Stat., (13): 19-29. (In Japanese)

Taki, J. (1972) A tetracycline labelling observation on growth zones in test plate of Strongylocentrotus intermedius. Bull. Jap. Soc. Sci. Fish., 38: 117-125. (In Japanese)

Theel, H. (1894) Notes on the formation and absorption of the skeleton in the Echinoderms. Svensk. Vet. Akad. Forhandl.,

(8): 345-354.

Towe, K. M. (1967) Echinoderm calcite: single crystal or polycrystalline aggregate. Science, 157: 1048-1050.

Towe, K. M. (1972) Invertebrate shell structure and the organic matrix concept. Biomineral. Res. rep., 4: 1-14.

Travis, D. F. (1970) The comparative ultrastructure and organization of five calcified tissues. In: Biological Calcification. Cellular and Molecular Aspects. (Schraer, H., ed.) pp. 203-312, Appleton-Century-Crofts, New York.

Travis, D. F., Francois, C., Bonar, L. C. and Glimcher, M. J. (1967) Comparative studies of the organic matrices or invertebrate mieralized tissues. J. Ultrastruct. Res., 18: 515-550.

Veis, D. J., Albinger, T. M. Clohisy, J., Rahima, M., Sabsay, B. and Veis, A.(1986) Matrix proteins of the teeth of the sea urchin Lytechinus variegatus. J. Exp. Zool., 240: 35-46.

Vethamany, V. G. and Fung, M. (1972) The fine structure of coelomocytes of the sea urchin, Strongylocentrotus droebachiensis (Muller O.F.). Can. J. Zool., 56: 77-81.

Vevers, G. (1966) Pigmentation. In: Physiology of Echinodermata (Boolootian, R. A., ed.) pp. 267-300, John

Wiley and Sons, New York.

Vocisano, R. A. (1971) Calcification in echinoderms: Regeneration of the test of the sea urchin Strongylocentrotus droebachiensis. M. Sc. Thesis, McGill Univ. cited from Wilbur (1973).

Weber, J. N. (1969) The incorporation of magnesium into the skeletal calcites of echinoderms. Amer, J. Sci., 267: 537-566.

Weber, J., Greer, R., Voight, B., White, E. and Roy, R. (1969) Unusual strength properties of echinoderm calcite related to structure. J. Ultrastr. Res., 26: 355-366.

Weidmann, S. M. (1963) Calcification of skeletal tissues. Intern. Rev. Connectiv. Tiss. Res., 1: 339-377.

Weiner, S. (1985) Organic matrix-like macromolecules associated with the mineral phase of sea urchin skeletal plates and teeth. J. Exp. Zool., 234: 7-15.

Wilbur, K. M. (1973) Mineral regeneration in echinoderms and molluscs. In: Hard Tissue Growth, Repair and Remineralization. pp.7-33, Elsevier, Excerpta Medica, Holland.

Fig. 1. Light microphotograph (LM photograph) of a ground section of a genital plate (G) under reflective light. Light and dark zones are observed distinctly. X 20.

Figs. 2-6. Microradiographs of ground sections of test plates.

Fig. 2. Tangential section of a test plate. Dense and loose meshworks built up of calcified trabeculae are arranged alternately. X 25.

Fig. 3. Vertically ground section of a test plate. Dense and loose meshworks are observed in the interior of the test plate. X 15.

Fig. 4. Tangentially ground section of test plates of the apical system. A clear alternate pattern of dense and loose meshworks can be seen. G: genital plates; O: ocular plates; P: periproct. X 10.

Fig. 5. Tangentially ground section of an ocular plate (O). G: genital plates. X 40.

Fig. 6. Tangentially ground section of a test plate. The growing direction of the plate is shown in the trabecular arrangement. X 50.

Fig. 7. Tangential section near the apical system. A new plate (N) is developing between the apical plates and the adjacent top plate of the interambulacral zone. G: genital plate; O: ocular plate. X 45.

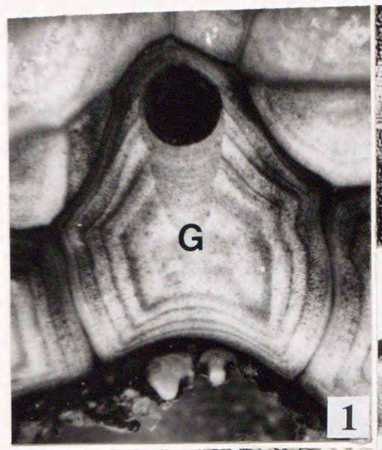

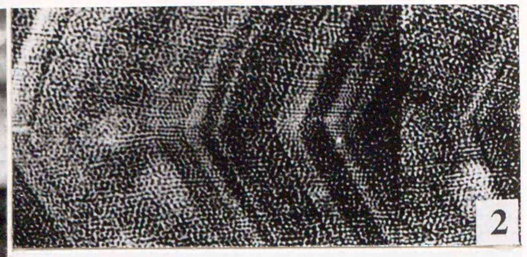

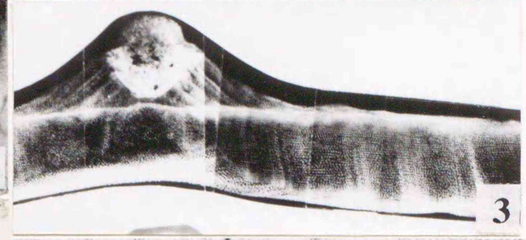

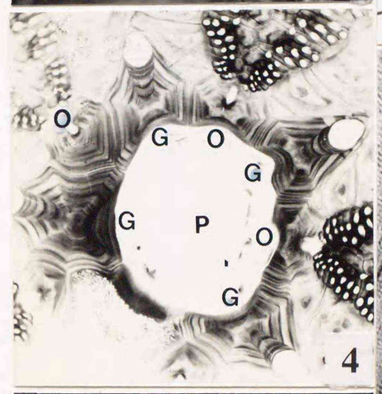

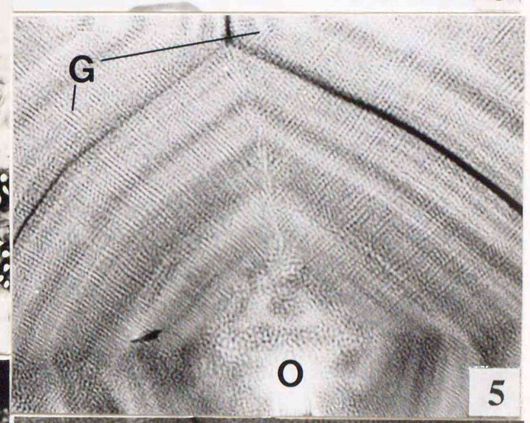

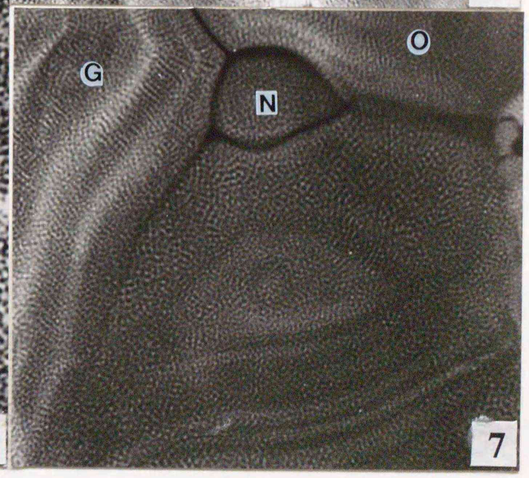

Figs. 8-13. Scanning electron micrographs (SEM photographs) of test plates bleached with hypochlorite.

Fig. 8. Interior (I) of a test plate showing fenestrate structure built up by calcified trabeculae. Tb: tubercle.

Fig. 9. Interior of a test plate showing a spongy structure of typical porous trabeculae.

Fig. 10. Spongy stereom of a test plate of a old sea urchin.

Fig. 11. Compact stereom near the inner surface of a test plate. IS: inner surface.

Fig. 12. Plate of a young sea urchin built up of the spongy structure throughout. IS: inner surface; OS: outer surface; Tb: tubercle.

Fig. 13. Inner surface of a plate of a young sea urchin. The compact structures (C) surrounded by the spongy structures (S) are seen.

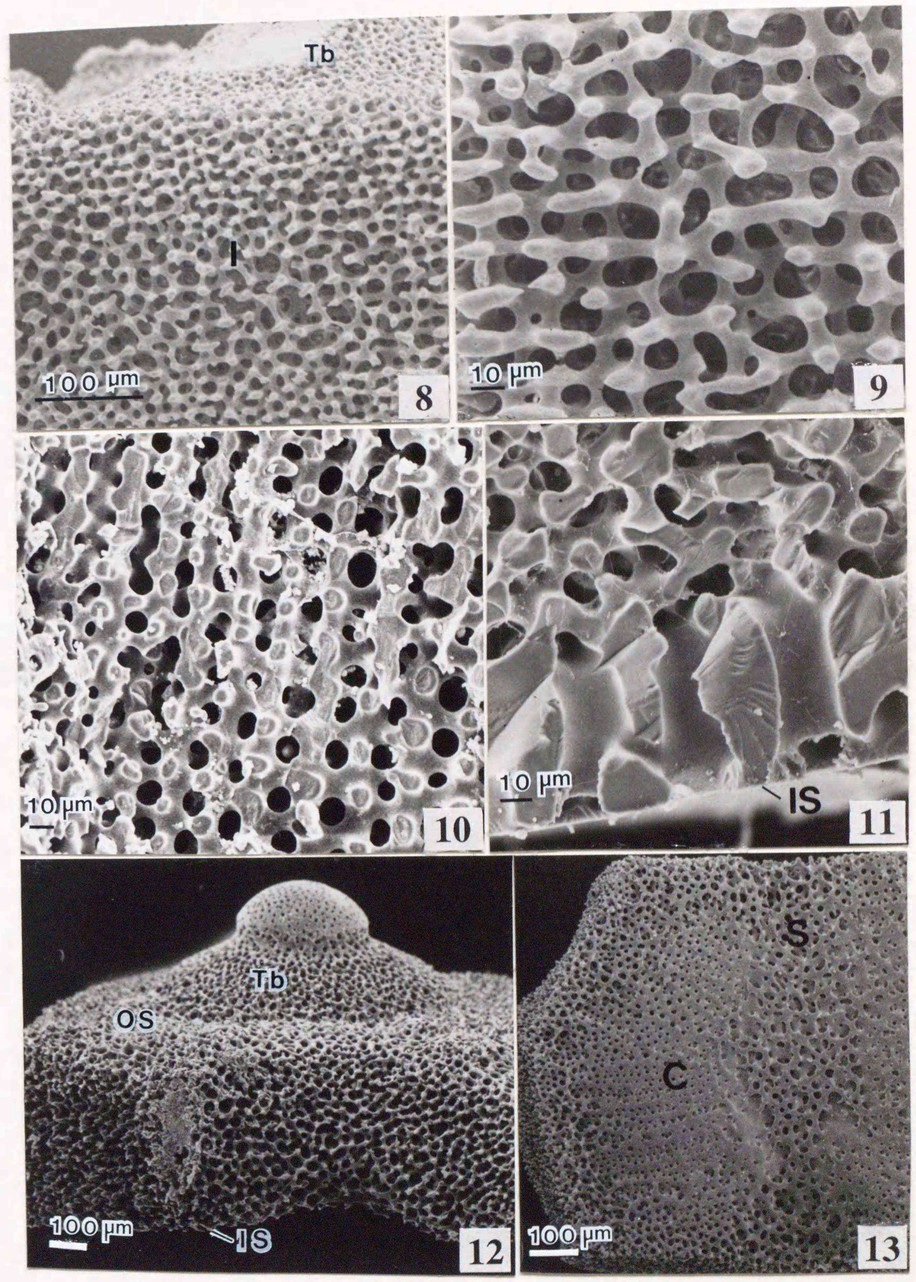

Figs. 14-17. SEM photographs of test plates.

Fig. 14. Irregular compact stereom of a basocoronal plates adjacent to the peristomial membrane. Pm: peristomial membrane side.

Fig. 15. Stereom of a basocoronal plate built up of thicker and irregularly shaped trbeculae (T) with less pores.

Fig. 16. Ambulacral plate of a young sea urchin constructed of the spongy stereom. P: pores of tube feet.

Fig. 17. Rough surfaced trabeculae (T) of a test plate having numerous small crystals (sc).

Fig. 18. Trabeculae (T) of a test plate exhibiting an irregularly rugged surface.

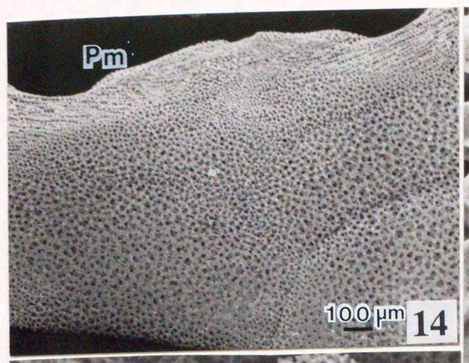

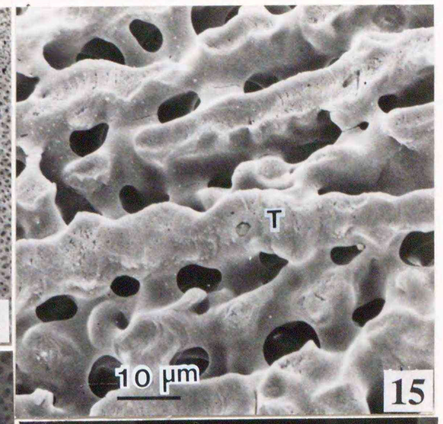

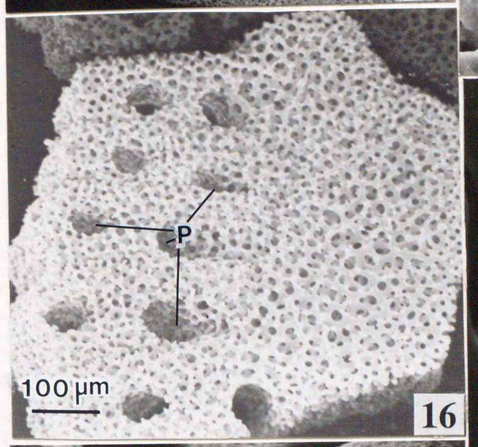

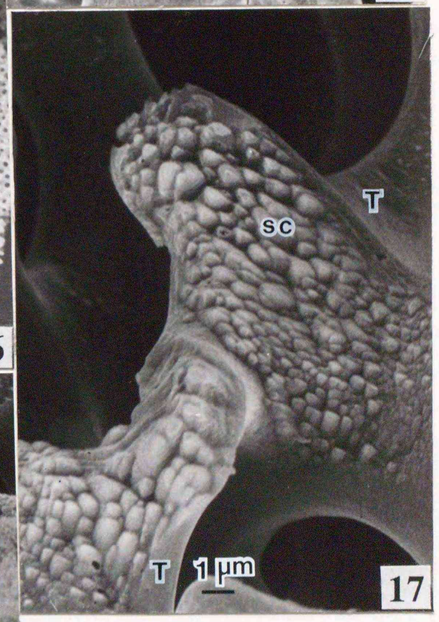

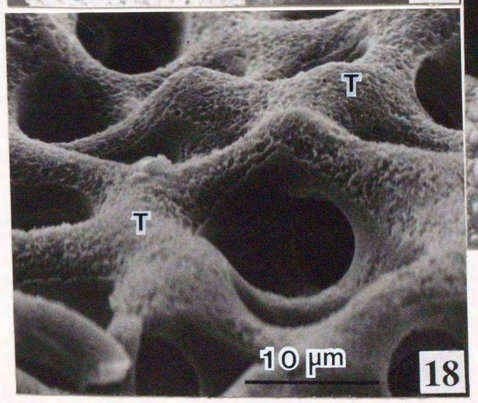

Figs. 19-22. SEM photographs of test plates.

Fig. 19. Partially broken trabeculae with eroded surfaces (arrows).

Fig. 20. Eroded trabeculae (arrows) of a plate at the inner surface near the suture.

Fig. 21. Eroded trabeculae (arrows) at the sutural area (S) of a young sea urchin plate.

Fig. 22. Fractured surface showing a layered structure.

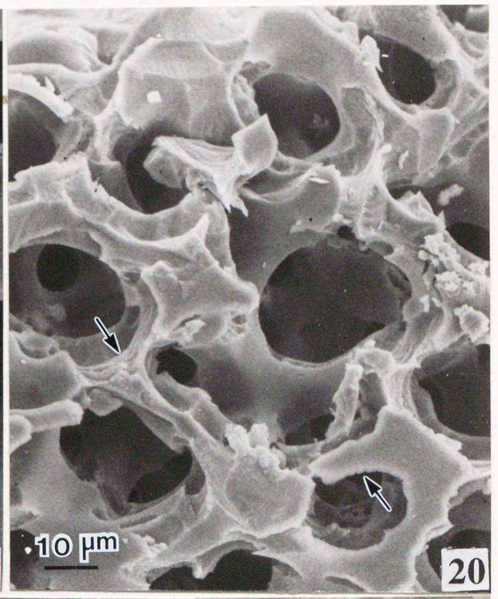

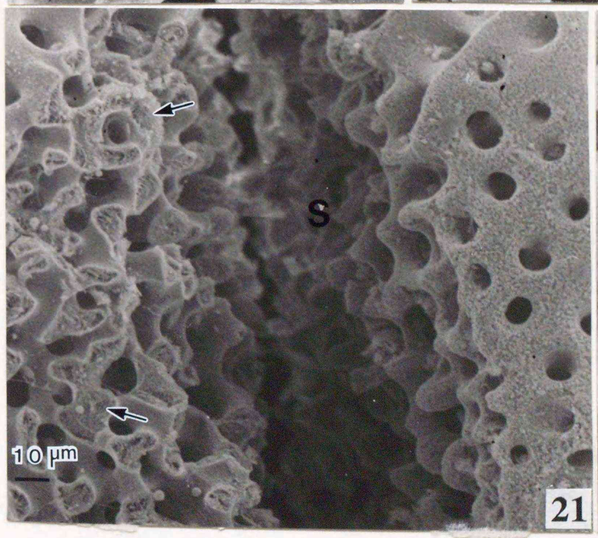

Figs. 23, 24. SEM photographs showing the formation of new plates.

Fig. 23. New plate (N) appearing between an apical plate (A) and the adjacent plate (P1) at the apical region.

Fig. 24. New plate (N) interconnected to two apical plates (A) with numerous fibrous bundles (F). P1: a plate adjacent to the apical plates.

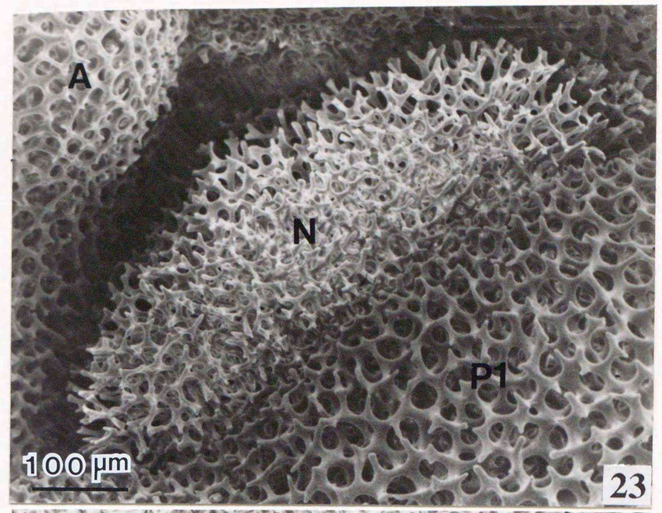

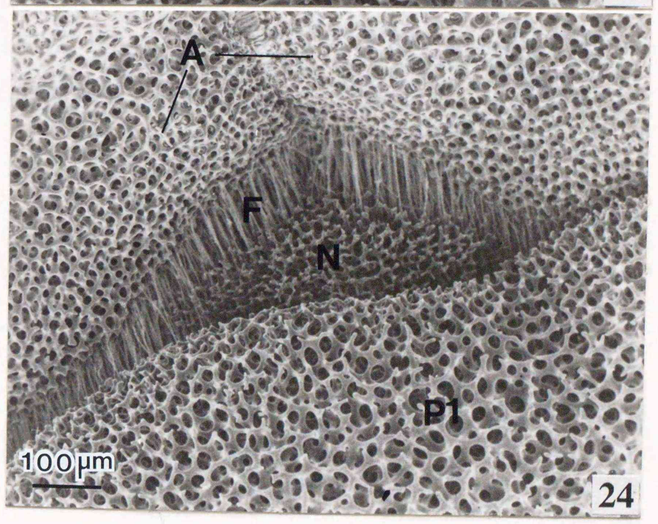

Figs. 25-31. LM photographs of decalcified test plates and the peristomial membranes. c: cellular elements; ca:calcified area of the peristomial membrane; cf: collage-like fibers; ep: epidermis, h: "holes"; ic: inner connective tissue supporting the spine; ir: interior of the test plate; is: inner surface of the test plate; nc: non-calcified connectiv tissue; om: outer muscle layer supporting the spine; os: outer surface of the test plate; s: suture; sp: spine.

Fig. 25. Longitudinal section of a decalcified test plate through the spine and the suture. Azan stain, X 80.

Fig. 26. Tangential section of a decalcified test plate showing collagen-like fibers extending over both longitudinal (sl)and latitidinal (st) sutures. Azan stain, X 100.

Fig. 27. Longitudinal section of the peristomial membrane showing abundant collagen-like fibers around the calcified area. Von Kossa, X 70.

Fig. 28. Reticulous structure of the interior of dermis in which no collaen-like fibers are found. Azan stain, X 450.

Fig. 29. Reticulous structure of the calcified area in the peristomial membrane. Azan stain, X 400.

Fig. 30. Moderate metachromasia found in collagen-like fibers of the suture and the inner connective tissue supporting the spine. Toluidine blue, X 100.

Fig. 31. Metachromasia appearing on the collagen-like fibers of the suture after deamination. Toluidine blue, X 380.

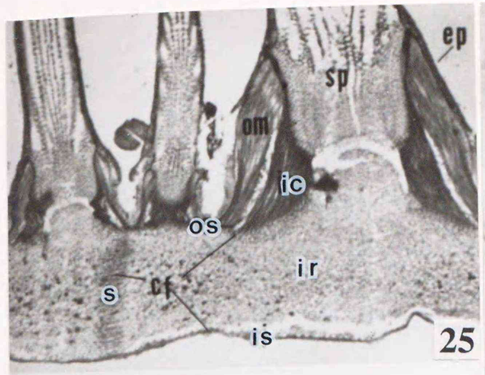

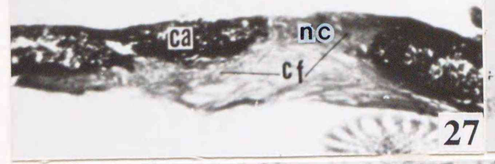

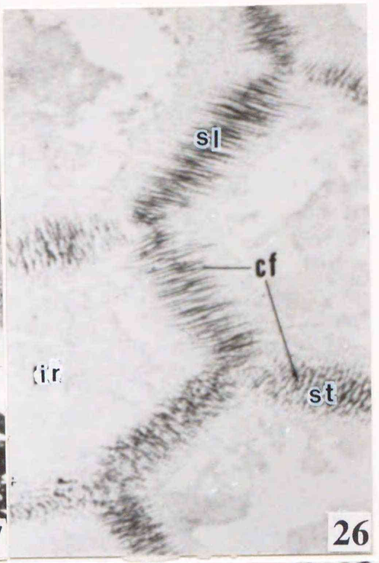

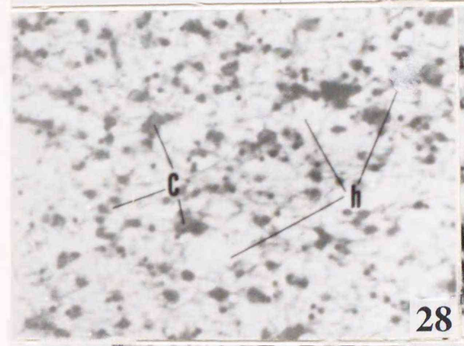

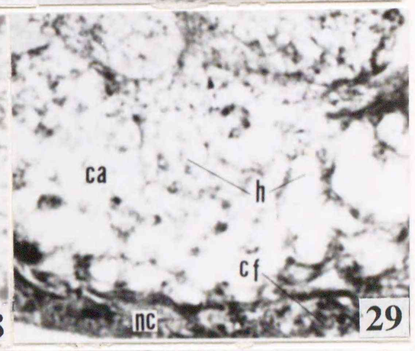

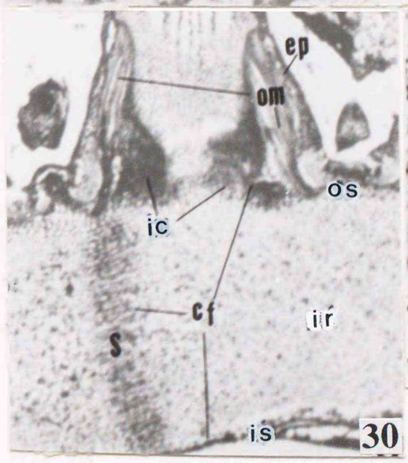

Figs. 32-36. LM photogrphs of test plates and the peristomial membrane. ca: calficied area; cf: collagen-like fibers; h: "holes"; ic: inner connective tissue supporting the spine; ir: interior of test plate; nc: non-calcified connective tissue; om: outer muscle layer of the spine supporting tissue; tb: tubercle

Fig. 32. Tangential section of a test plate showing sutural collagen-like fibers which reacted relatively intensely to PAS. X 140.

Fig. 33. Longitudinal section of the peristomial membrane. The non-calcified connective tissue reacted relatively intensely to PAS, whereas the reticuluous structure of thin organic substances of calcified area was weakly PAS-positive. PAS, X 270.

Fig. 34. Strongly PAS-positive granules (g) found in the reticulous structure of a test plate. PAS, X 200.

Fig. 35. Sudanophilic reaction found on the collagen-like fibers of the inner connective tissue supporting the spine. Sudan black B, X 95.

Fig. 36. Collagen-like fibers of the suture showing a sudanophilia after extracting lipids with hot pyridine for 24 h. Sudan black B, X 900.

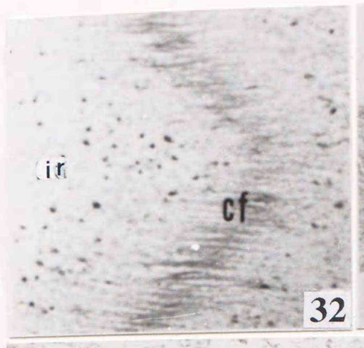

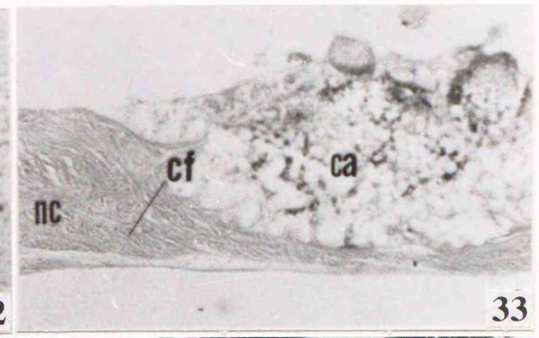

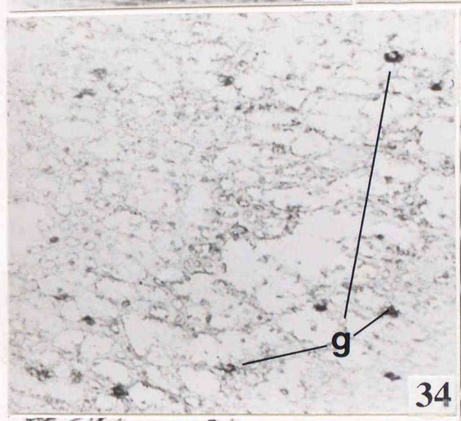

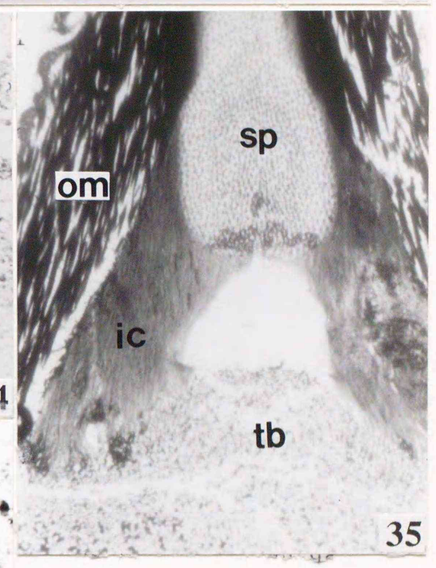

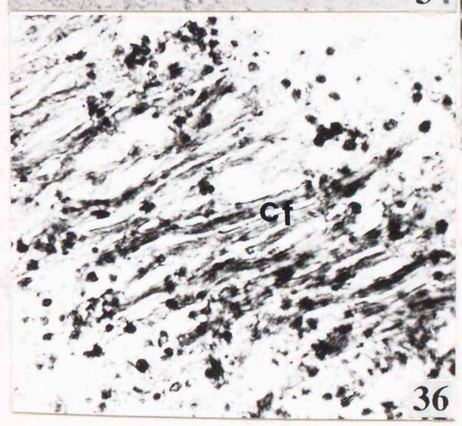

Figs. 37-39. LM photographs of semithin sections of decalcified test plates. Methylene blue-azur II.

Fig. 37. Cells of various types distributed throughout the interior organic stereom. h: decalcified trabeculae, X 800.

Fig. 38. Numerous cells of various types accumulated near the sutural area. h: decalcified trabeculae, cf: collagenous fibers. X 1000.

Fig. 39. Abundant collagenous fibers (cf) occupying the organic stereom at the sutural area. h: decalcified trabeculae, X 1000.

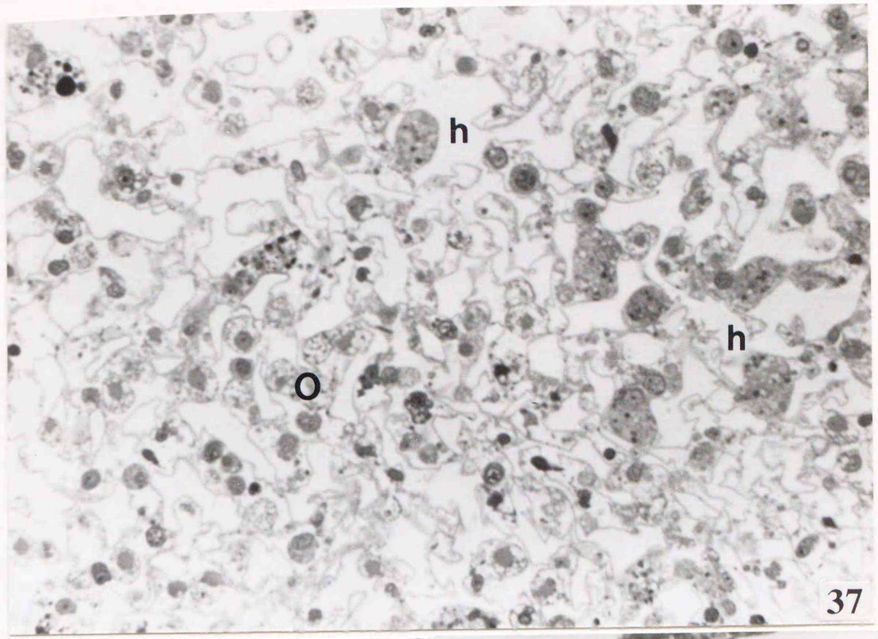

37

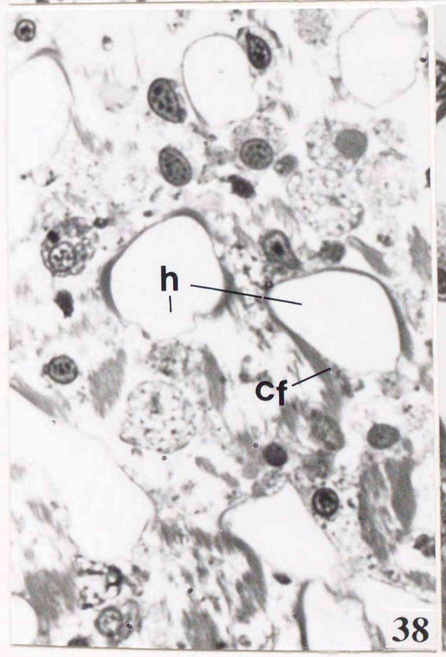

38

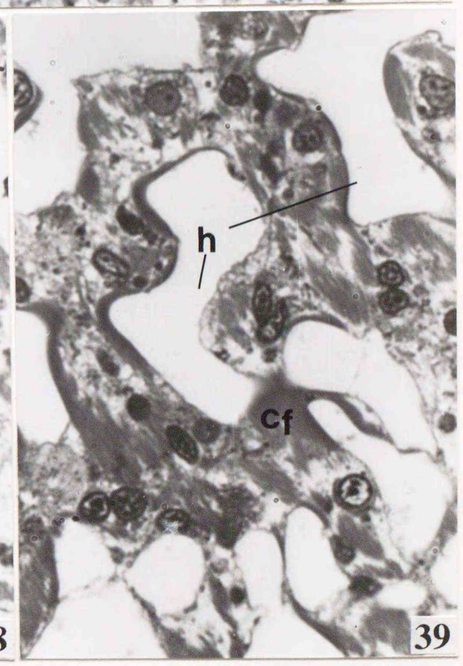

39

Figs. 40-44. LM and TEM photographs of small basophilic cells of decalcified test plate.

Fig. 40. Small basophilic cell (arrow) closely attached to a hole of decalcified trabecula (h) with the elongated processes. O: organic stereom. X 2000.

Fig. 41. Small basophilic cell (SB) characterized by a lot of free ribosomes and the electron dense ground substance. h: decalcified trabecula; O: organic stereom. X 13600.

Fig. 42. Small basophilic cell (SB) hving many cytoplasmic processes with small bladder-like knots (arrows). The cell shows a complicated form. X 19500.

Fig. 43. Elongated cytoplasmic coat (arrows) of a small basophilic cell (SB) on the surface of the trabecular skeleton (h). O: organic stereom. X 19500.

Fig. 44. Small basophilic cell (SB) having a large vacuole (V) in which are some vesicular and amorphous materials. cf: collagen fibers, X 13600.

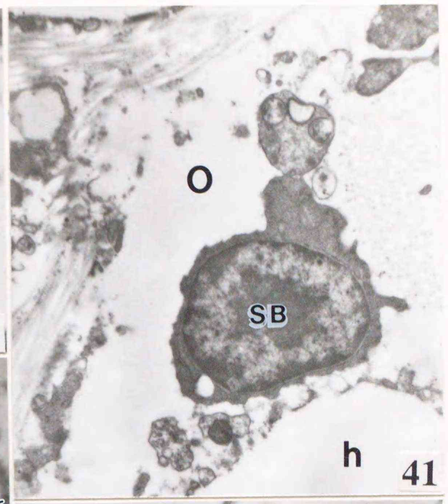

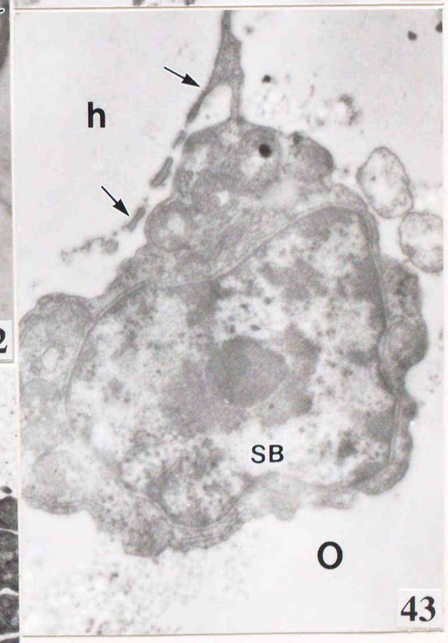

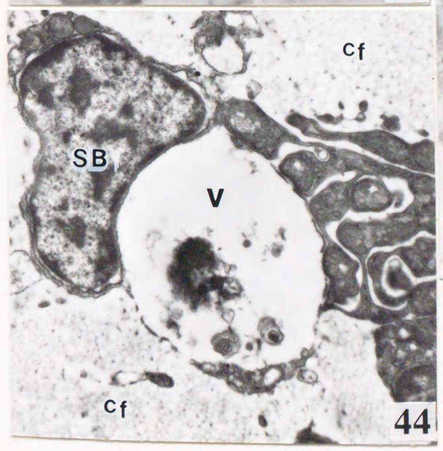

Figs. 45-47. TEM photographs of small basosphilic cells.

Fig. 45. Small basophilic cell (SB) attached to a large vacuole (V) enclosed with beaded cytoplasmic bodies (arrows). O: organic stereom. X 6800.

Fig. 46. Small basophilic cells (SB) forming a syncytium which encloses a large vacuole (V) showing an appearance similar to a decalcified trabecula. O: organic stereom. X 9100.

Fig. 47. Fine fibrils (f) and vesicles in an intracellular vacuole (V) of a small basophilic cell. O: organic stereom. X 13600.

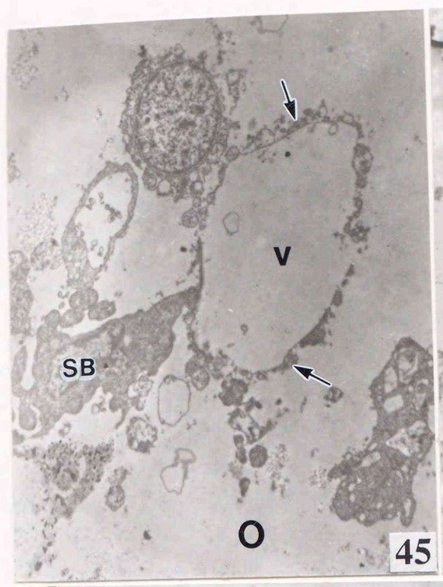

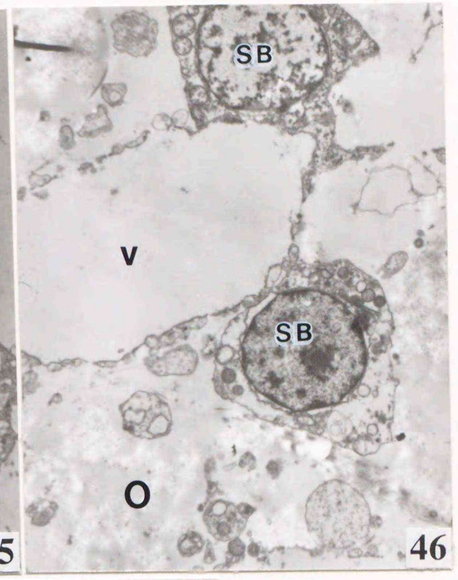

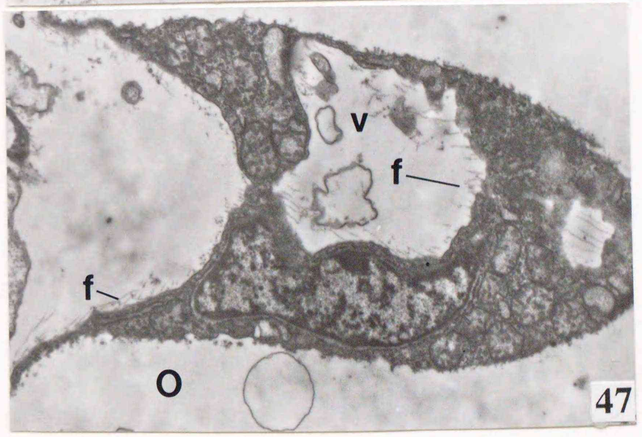

Fig. 48. LM photograph of a spherule cell (S) in a decalcified test plate. Numerous spherical inclusions are in the cytoplasm. Methylene blue-azur II, X 1250.

Fig. 49. TEM photograph of spherule cells (S) in a decalcified test plate. X 5300.

Fig. 50. LM photograph of the vacuolated cells (Vc) in a decalcified test plate. The cytoplasm is filled with many vacuoles. Methylene blue-azur II, X 1250.

Fig. 51: TEM photograph of a vacuolated cell (Vc) in a decalcified test plate. The poor cytoplasm among vacuoles has numerous small vesciles. X 15400.

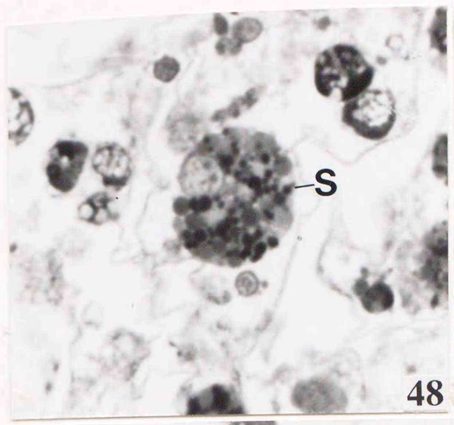

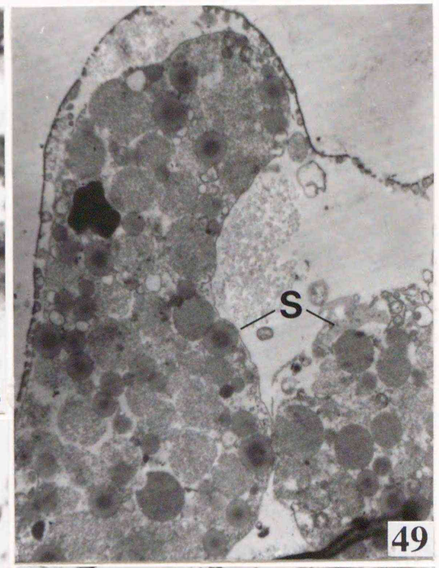

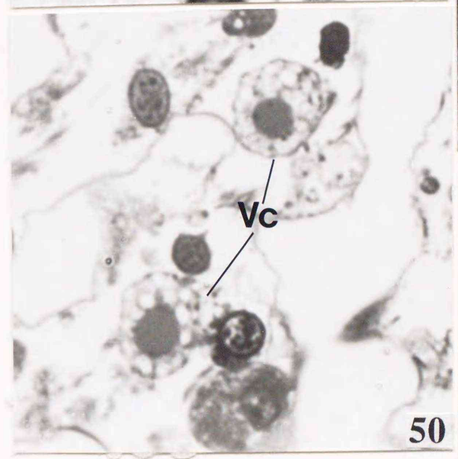

Fig. 52. LM photograph of a phagocytic leucocyte (L). Methylene blue-azur II, X 1000.

Fig. 53. TEM photograph of a phagocytic leucocyte (L) having elongated cytoplasmic processes and numerous vesicles in the cytoplasm. h: decalcified trabeculae; O: organic stereom. X 9100.

Fig. 54. TEM photograph of a phagocytic leucocyte (L) ingesting an other cell. h: decalcified trabecula; Ni: nucleus of the ingested cell; Nl: nucleus of the phagocytic leucocyte; O: organic stereom. X 10000.

Fig. 55. LM photograph of round uniform cells (Uc) in the organic stereom. h: decalcified trabecula; O: organic stereom. Methylen blue-azur II, X 800.

Fig. 56. TEM photograph of a round uniform cell (Uc). The cytoplasm is filled uniformly with fine fibrous materials and a moderately electron-dense material. h: decalcified trabecula; O: organic stereom. X 9600.

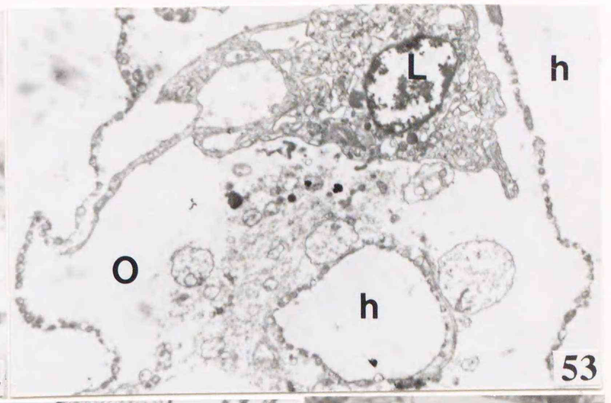

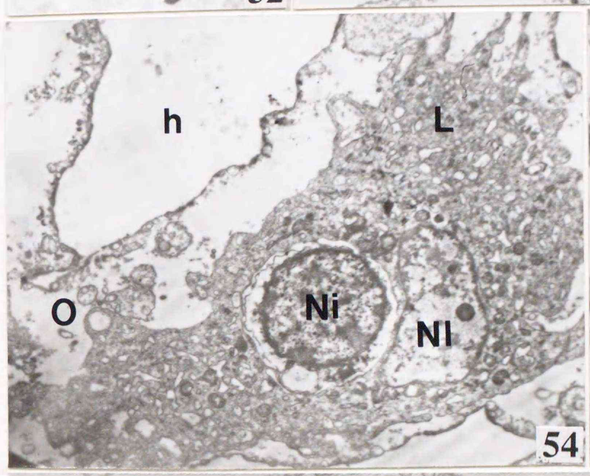

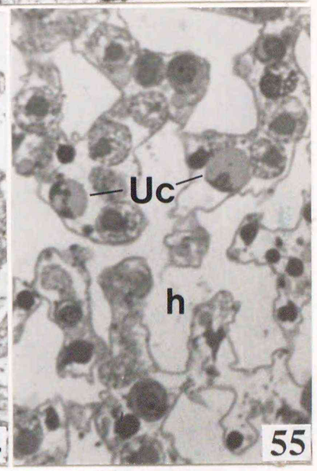

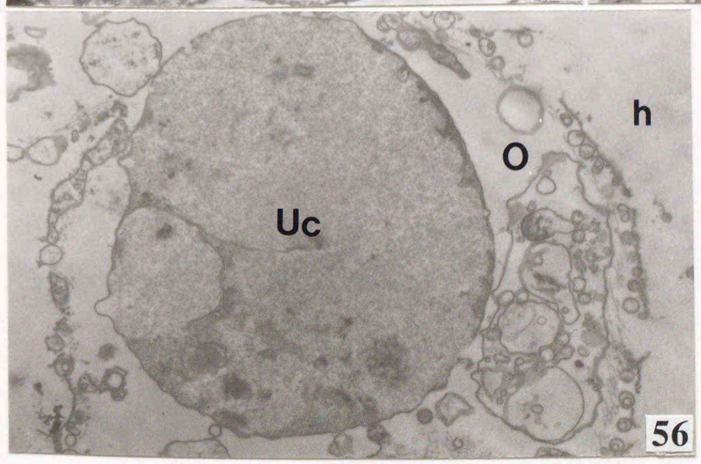

Fig. 57. TEM photograph of an eosinophilic cell (Ec) of a decalcfied test plate. The cytoplasm is filled with numerous, small electron-dense granules. h: decalcified trabeculae; O: organic stereom. X 9000.

Fig. 58. LM photograph of cuboidal cells (Cb) in a decalcified test plate. h: decalcified trabecula; O: organic stereom. Methylene blue-azur II, X 800.

Fig. 59. TEM photograph of a cuboidal cell (Cb) having a plain nucleolus and homogeneous, electron-dense compact cytoplasm. h: decalcified trabecula; O: organic stereom. X 9100.

Fig. 60. TEM photograph of a cuboidal cell (Cb) having lipid-like droplets (Lp), mitochondria and RER. X 18600.

Fig. 61. LM photograph of the organic stereom (O) near the outer surface of a test plate. Ep: epidermis; h: decalcified trabecula. Methylene blue-azur II, X 1000.

Fig. 62. TEM photograph of the organic stereom (O) near the outer surface of a plate. Many cells and their debris are present. h: decalcified trabecula. X 6000.

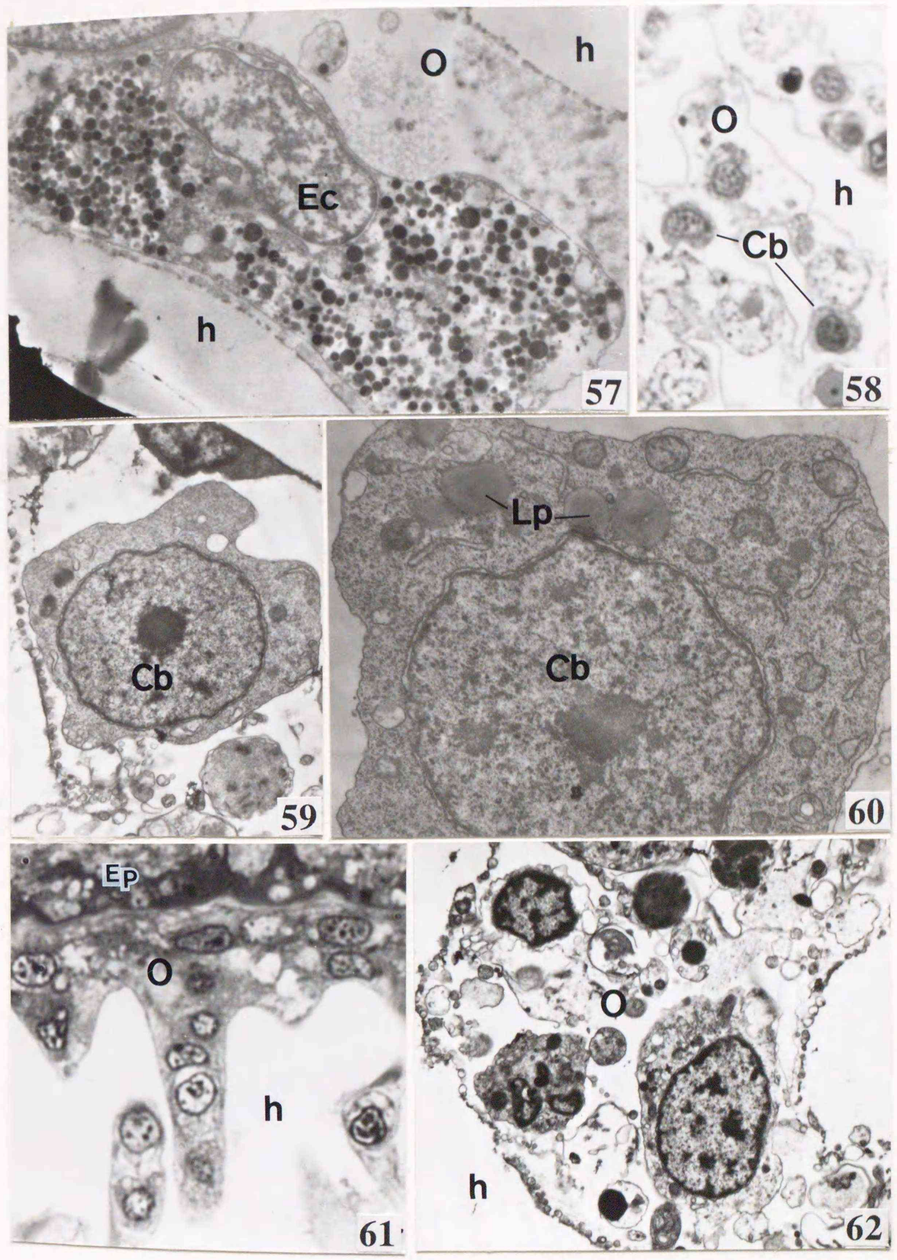

Fig. 63. TEM photograph of the organic stereom (O) at the sutural area. Abundant collagen fibers (cf) closely surround holes of decalcified trabeculae (h). The fibers are not observed in the holes. X 5400.

Fig. 64. TEM photograph of collagen fibers (cf) at the sutural area. The fibers show a banding pattern similar to that of mammalian collagen. h: decalcified trabecula; O: organic stereom. X 23000.

Fig. 65. TEM photograph of the organic stereom at the sutural area. Fine granular substances (fg) are distributed in a hole of decalcified trabecula (h) along the bundles of the collagen fibers (cf). X 10000.

Fig. 66. TEM photograph of vesicles lining along the trabecular surface. A membranous structure (arrow) or a fine granular material (arrow head) are seen directly coating the trabecular surface. h: hole of decalcified trabecula; O: organic stereom. X 24000.

Fig. 67a. LM photograph of the coelomic epithelium cells arranged in a monolayer. X 2000.

Fig. 67b. TEM photograph of the coelomic epithelium consisted of monolayered epithelial cells (CE) and interposing nerve fibers (Nv) and muscle cells (M). T: test plate. X 9000.

Fig. 68. Highly magnified TEM graph of the nerve fibers (Nv) in the coelomic epithelium. CE: coelomic epithelium cell; M: muscle cell. X 15200.

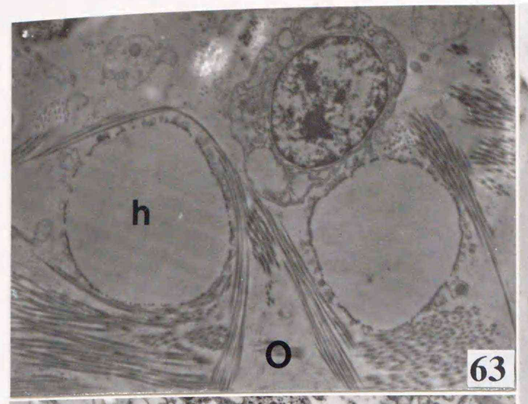

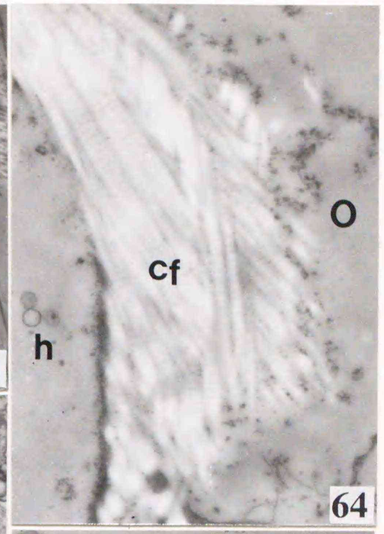

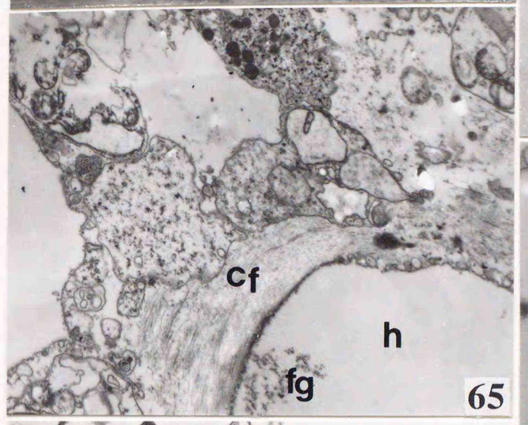

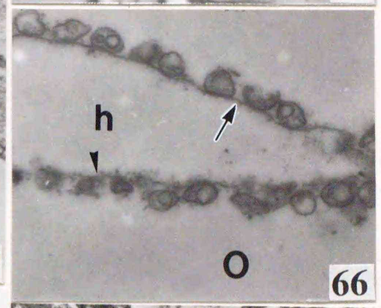

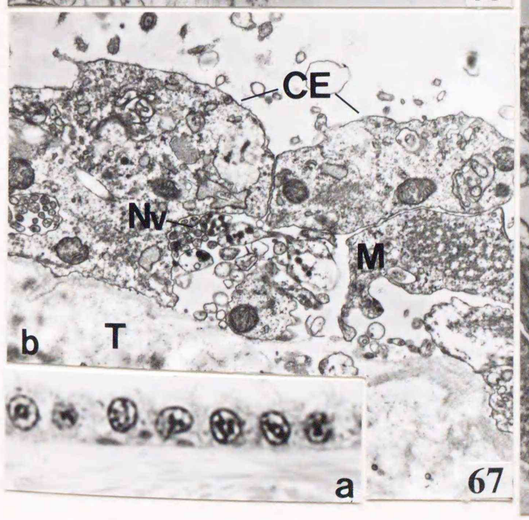

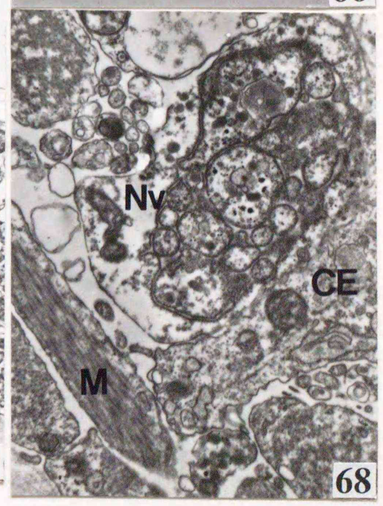

Figs. 69-72. SEM photographs of the stereom of NaOH treated test plates.

Fig. 69. Round cells (R) distributed on the trabecular surface (T).

Fig. 70. Round cells (R) dis ributed on the trabecular surface (T) separately or chained by elongated cytoplasmic processes.

Fig. 71. Round cells (R) distributed on the trabecular surface in an an aggregated form. They elongated thin cytoplasmic processes which are attched to the trabecular surface (T).

Fig. 72. Round cells (R) accumulating on a trabecula. They elongate thin cytoplasmic processes (arrows) to combine other cells.

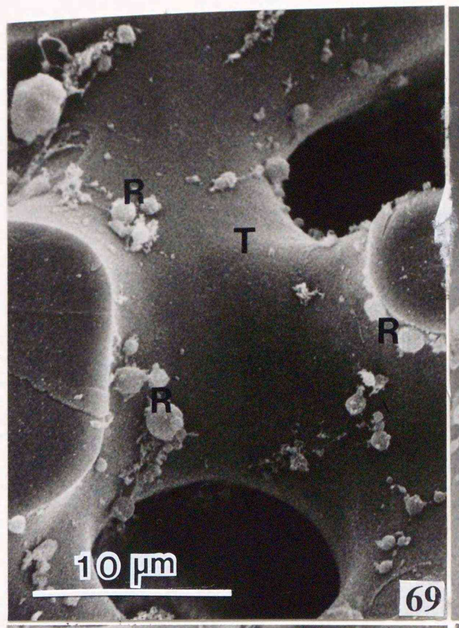

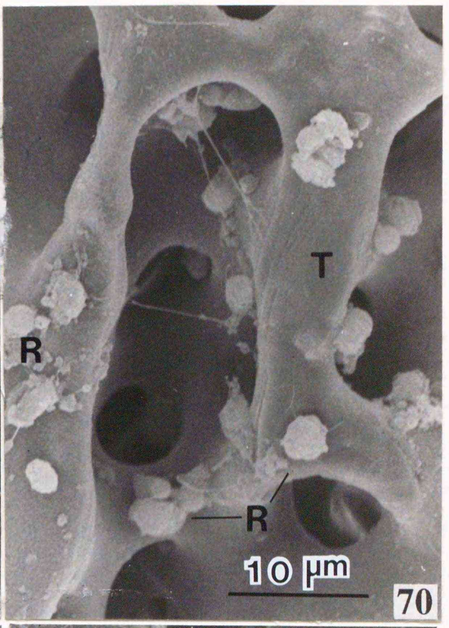

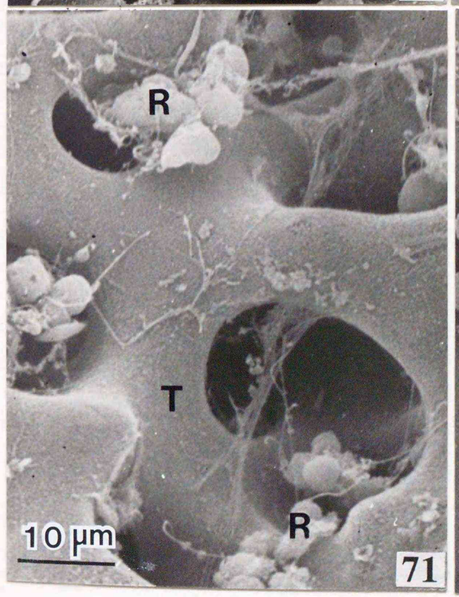

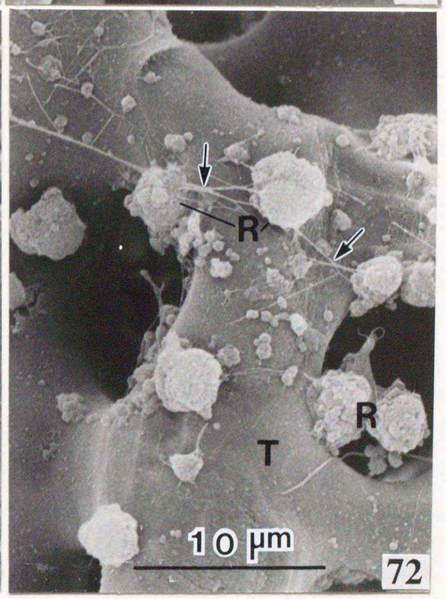

Figs. 73-76. SEM photographs of various phases of the round cells on the test stereom.

Fig. 73. Round cells (R) elongating their cytoplasmic processes (arrows) to chain other cells at a long distance. T: trabecula.

Fig. 74. Round cells (R) accumulated to surround the growing site (Gs) of the trabeculae with their cytoplasmic processes having bladder-like knots (Bk).

Fig. 75. Cytoplasmic processes (arrows) with bladder-like knots (Bk) of the round cells (R) attaching closely to the growing site (Gs) of the trabecula.

Fig. 76. Round cells (R) accumulated to enclose a growing trabecula (T) with their elongated cytoplasmic processes (arrow).

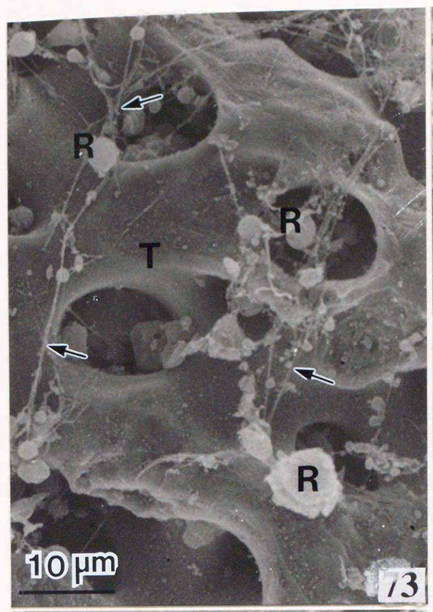

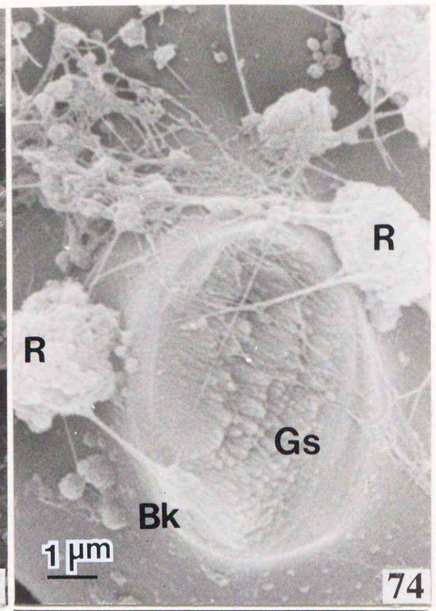

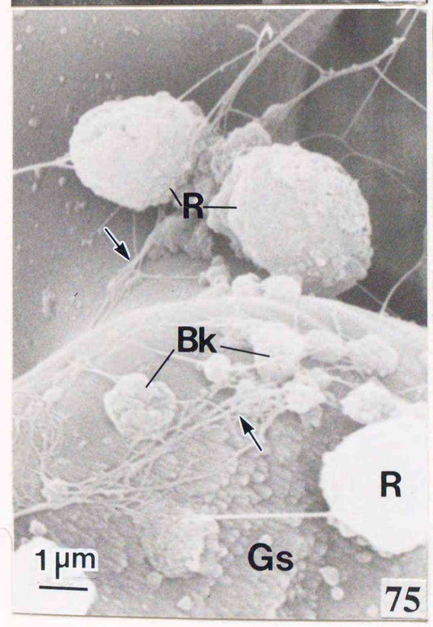

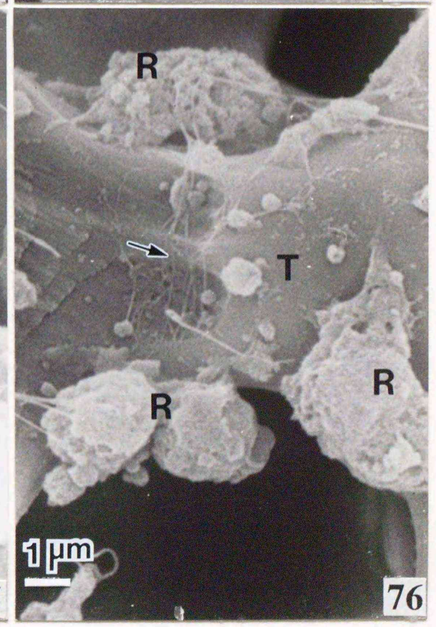

Figs. 77-79. SEM photographs of the flat cells on eroded trabecular surfaces.

Fig. 77. Flat cells (F) appearing on the eroded trabecular surface (arrows).

Fig. 78. Flat cell (F) aggregated to show a complicated contour at enlarged pore spaces of the stereom.

Fig. 79. Flat cells (F) aggregated to form bunches of grapes.

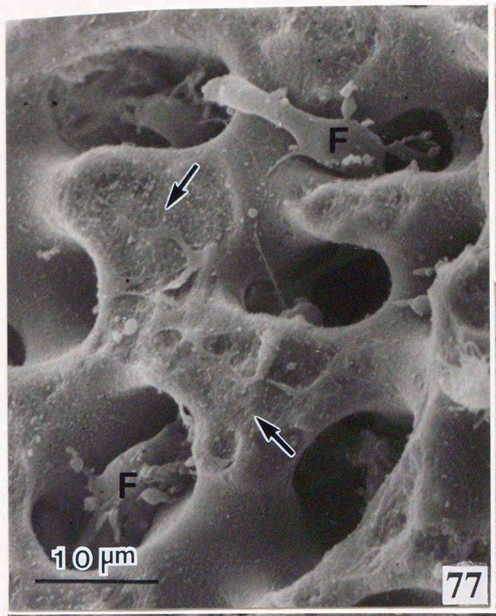

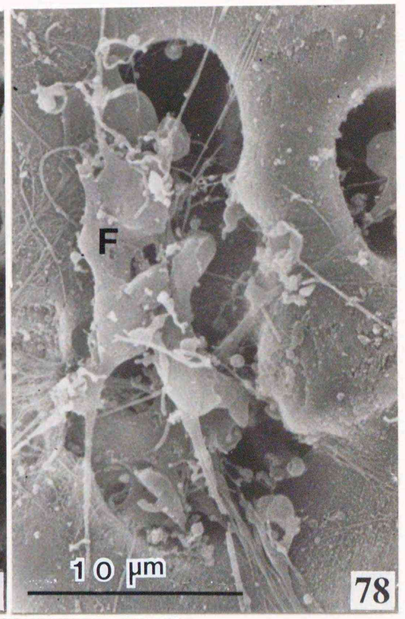

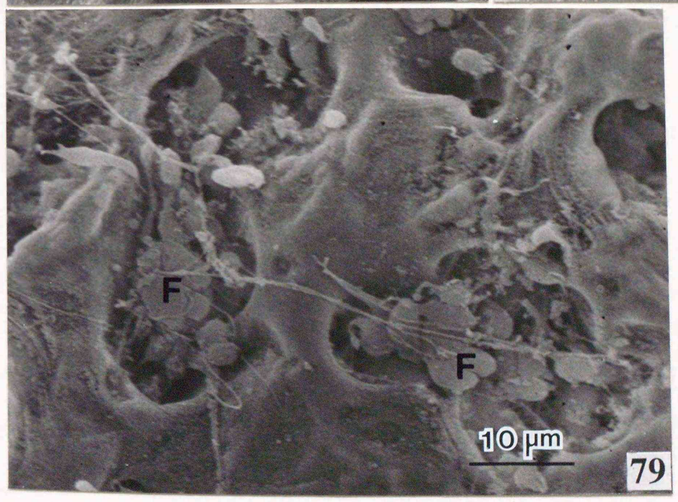

Figs. 80-82. SEM photographs of the flat cells at destructed trabeculae.

Fig. 80. Enlarged pore spaces sticked with flat cells (F) of complicated shapes.

Fig. 81. Caved surface (arrows) of the trabecula with a flat cell (F).

Fig. 82. Eroded trabecular surface (T) with fragmental structures of cytoplasmic processes probably of flat cells.

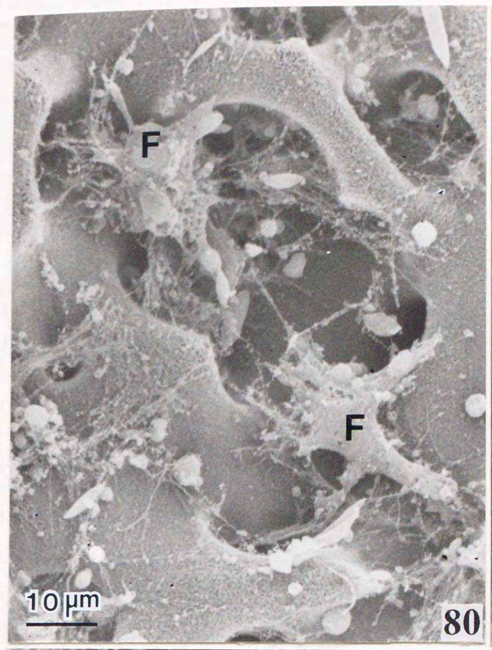

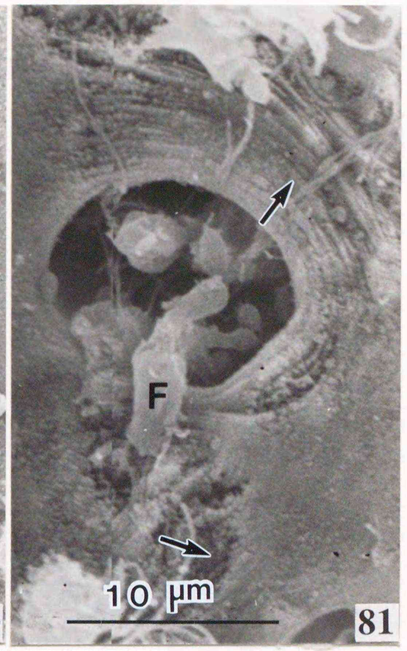

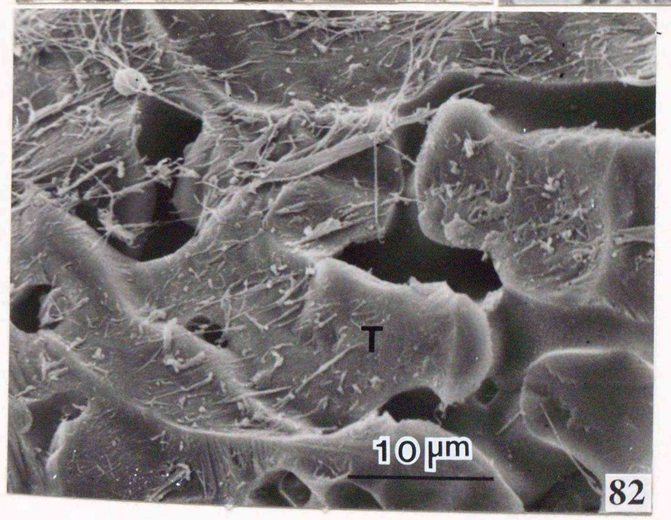

Figs. 83, 84. SEM photographs of cells having scrubbed brush-like structures.

Fig. 83. Cell having several scrubbed brush-like structures (sb). Portion anchored by the brush-like processes show an eroded appearance (arrow).

Fig. 84. Cell having a large, well-developed scrubbed brush-like structure (sb) on the eroded surface (arrow) of the trabecula.

Figs. 85-87. SEM photographs of the sutural area.

Fig. 85. Collagenous fibers (cf) localized abundantly at the organic stereom of the sutural area. T: trabeculae.

Fig. 86. Thick bundles of collagenous fibers (cf) localized at the sutural area. T: trabecula.

Fig. 87. Collagenous fibers (cf) interconnecting the neighboring plates at the suture (S).

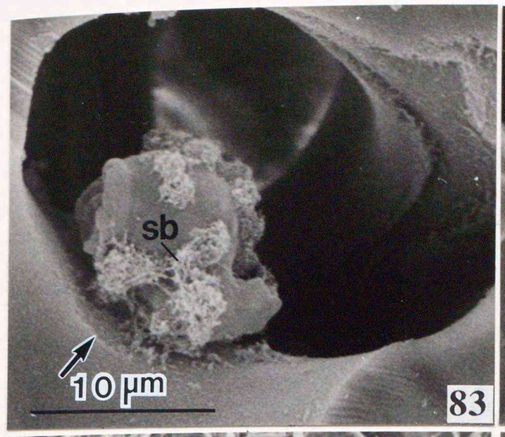

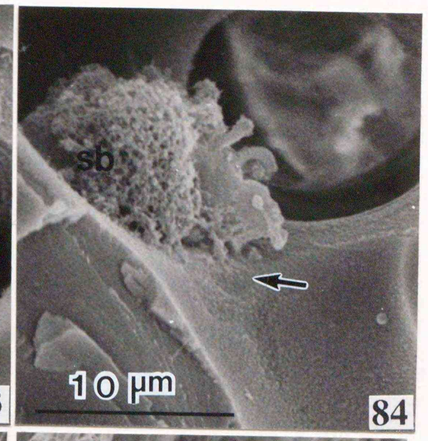

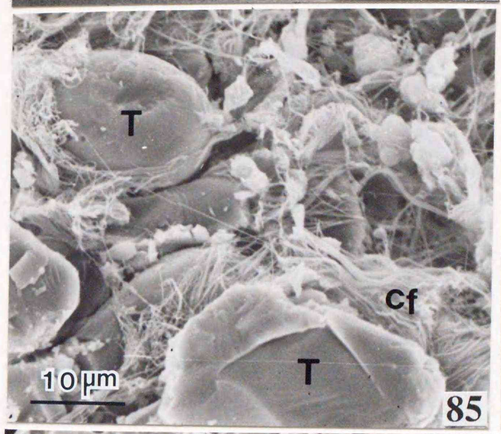

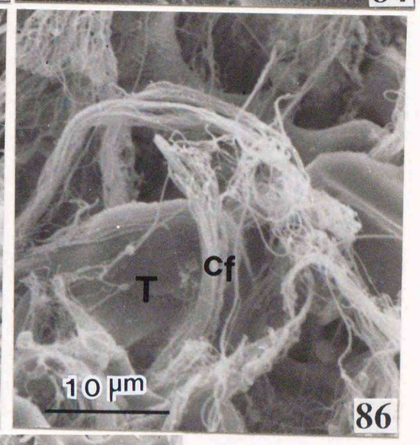

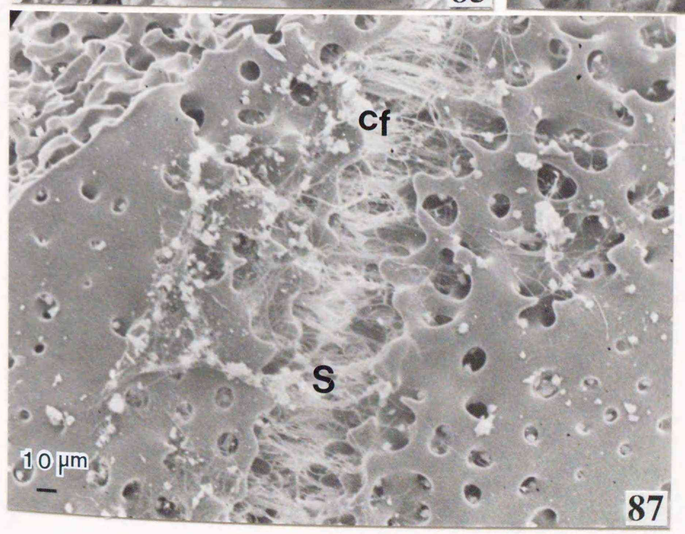

Figs. 88-91. SEM photographs of sutural areas of test plates of young sea urchins.

Fig. 88. Resorbed trabecular surfaces (arrows) showing caved and porous appearances.

Fig. 89. Round (R) and flat cells (F) distributed on the resorbed surface as shown in Fig. 88.

Fig. 90. Elongated cytoplasmic processes attached to the eroded trabecular surface (arrow).

Fig. 91. Cobweb-like meshwork (Ms) woven by cytoplasmic processes and fibrous elements covering the trabecular surface.

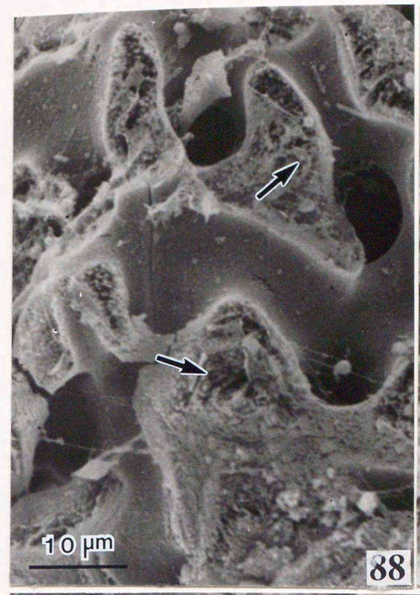

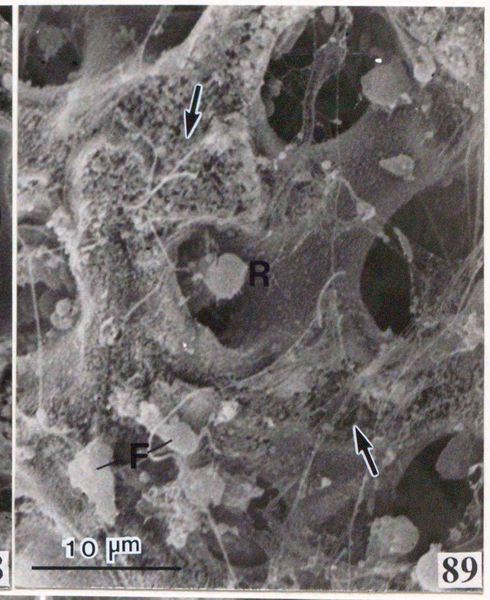

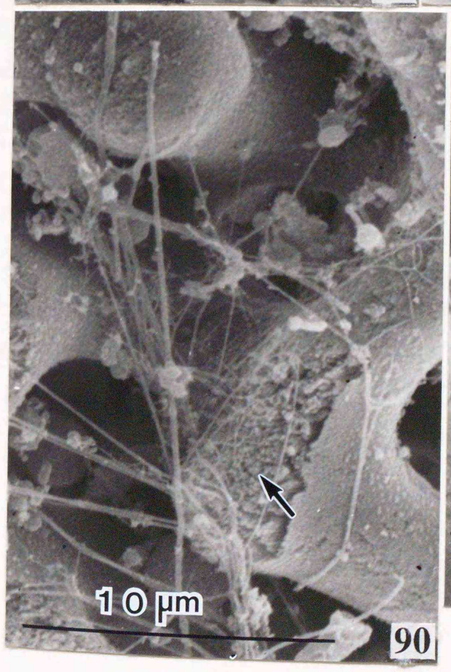

Fig. 92-95. SEM photographs of the sutural area.

Fig. 92. Cytoplasmic processes arranged circularly on a specific place (*) of the trabecular surface.

Fig. 93. Cytoplasmic processes appearing to fill a stereomal pore space (arrow).

Fig. 94. Amorphous material covering the trabecular surface coiled around with the cytoplasmic processes and fibers.

Fig. 95. Amorphous material covered compactly the trabecular surface coiled around with the cytoplasmic processes and fibers.

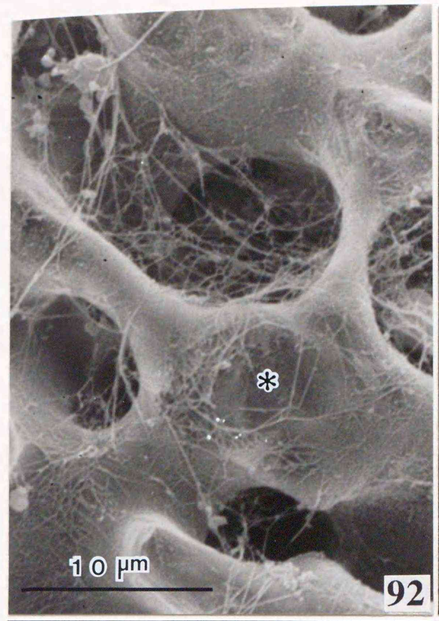

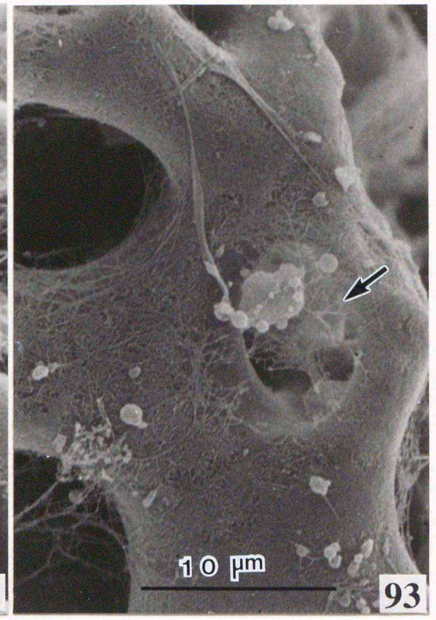

Figs. 96-98. SEM photographs of a rough surfaced stereom facing the inner test surface distant from the sutural area.

Fig. 96. Inner test surface exhibiting an eroded rough appearrance (arrows).

Fig. 97. Shallow crevices (arrows) around the stereomal holes at the eroded rough inner surface of a plate.

Fig. 98. Surface of the eroded trabecula covered with cytoplasmic processes (arrows) and fibers.

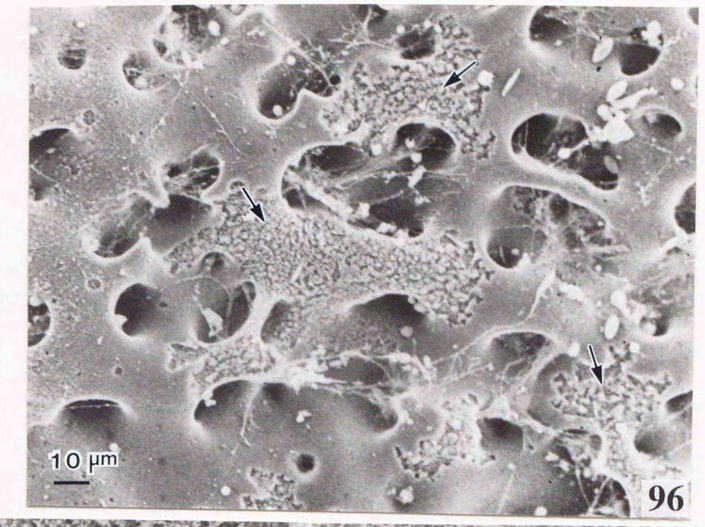

Figs. 99-102. SEM photographs of trabecular surface of sutural areas.

Fig. 99. Trabecular surface tightly covered by a membranous sheet woven by fibrous elements, which locked collagen fibers. On the membranous sheet, a cell with extended cytoplasm is observed. A cytoplasmic process is torn off from the cell body (arrow).

Fig. 100. High magnification of the membranous sheet covering the trabecular surface (arrow).

Fig. 101. Cytoplasmic processes torn off in places (arrows) to form succular vesicles.

Fig. 102. Many vesicles of round or irregular shapes distributed on the membranous sheet of the trabecular surface.

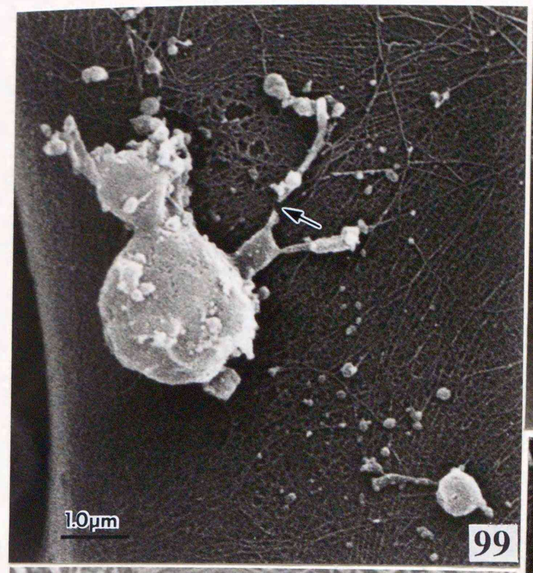

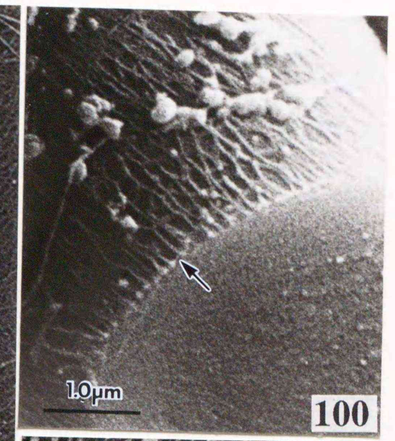

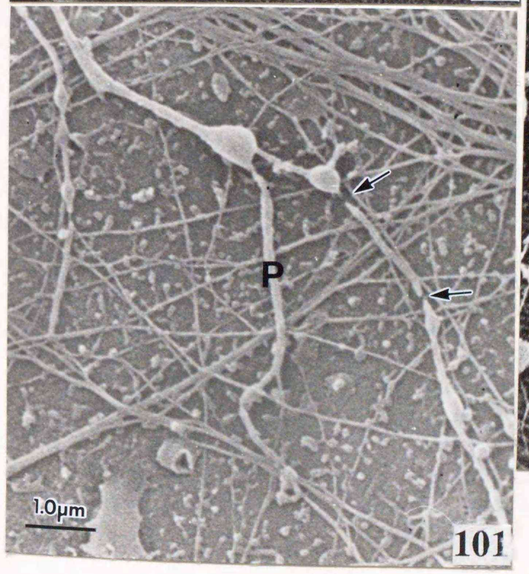

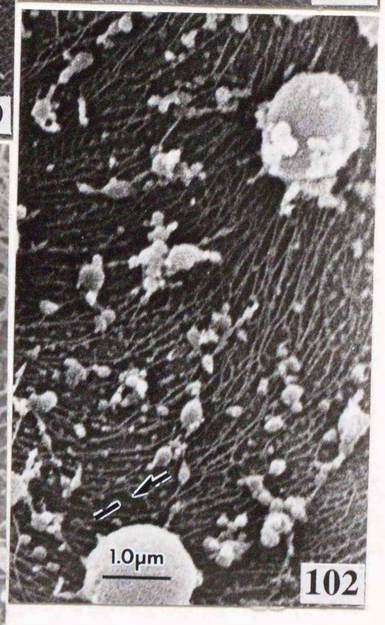

Figs. 103, 104. SEM photographs of the trabecular surface at a distant place from the sutural area.

Fig. 103. Numerous round to oval vesicles dotted on the trabecular surface.

Fig. 104. Cytoplasmic processes distributing around the trabeculae (T). v: vesicles shown in Fig. 103.

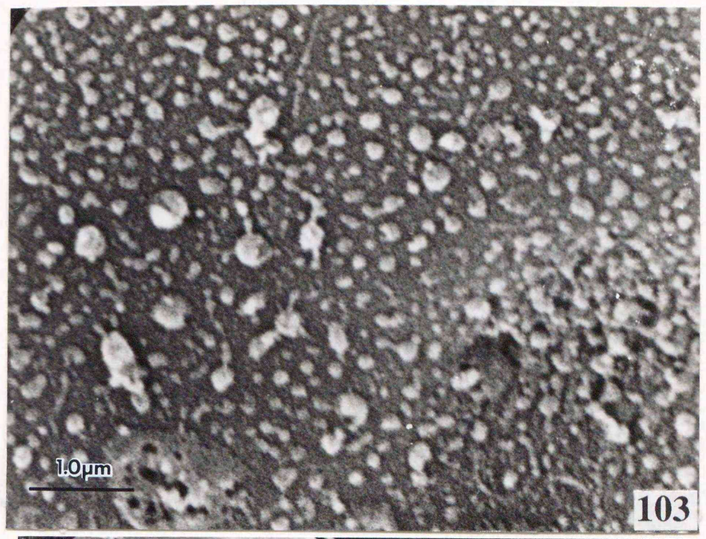

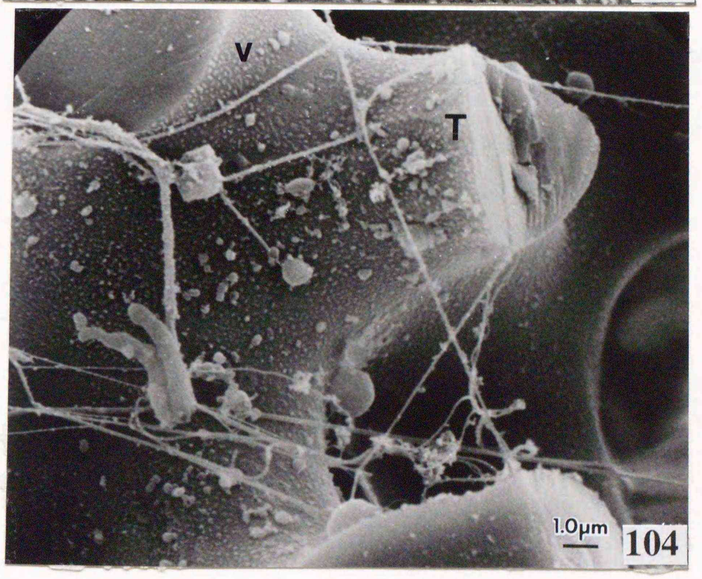

Figs. 105-107. SEM photographs of decalcified test plates.

Fig. 105. Membranous sheet forming a wall (Mw) between the trabecula and the organic stereom.

Fig. 106. High magnification of the membranous sheet. The calcified side (Cs) is smoother than the organic stereom side (Os) but shows the presence of granular materials and cytoplasmic processes.

Fig. 107. Membranous sheet in a weakly decalcified test plate. The granular materials and the cytoplasmic processes are observed on the sheet with disperced calcite crystals (C).

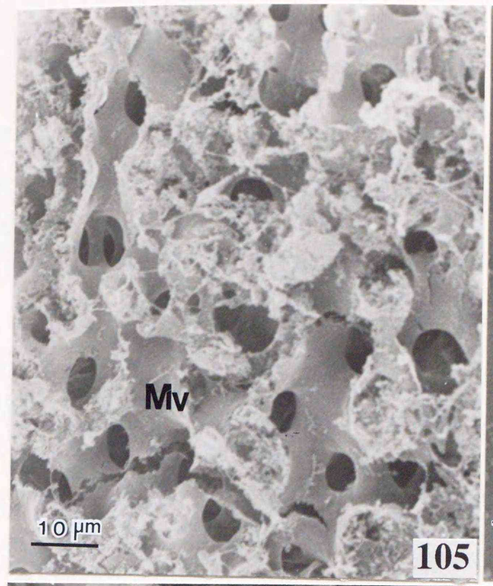

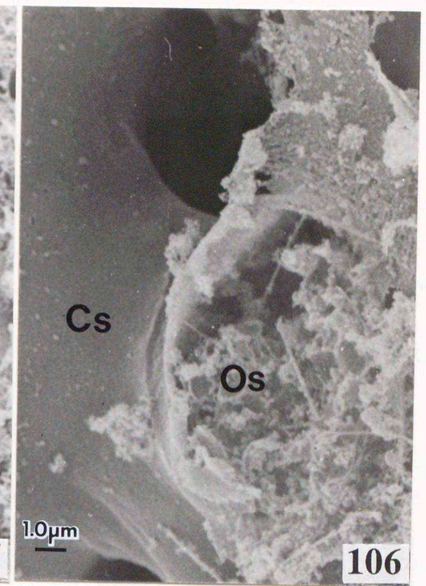

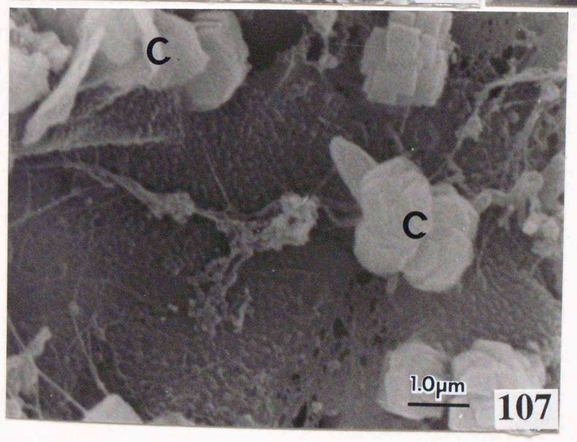

Figs. 108-111. SEM graphs of spines.

Fig. 108. Fractured plane of a spine showing large calcite crystals as "wedges" (W) and interposed "microspines" (Msp).

Fig. 109. Longitudinal wedges (W) of thick calcified pillars. Msp: "microspines"

Fig. 110. Numerous vesicles distributed on the surface of the spine skeleton. T: trabecula

Fig. 111. Interstitial organic spaces of the spine skeleton containing numerous cells with elongated cytoplasmic processes. T: trabeculae.

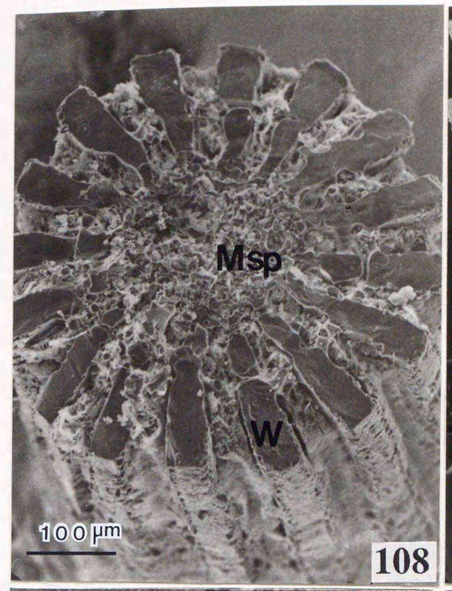

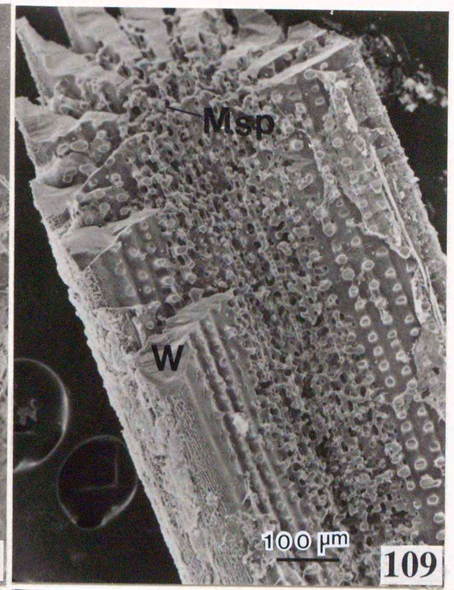

Figs. 112-114. SEM graphs of the spine stereom.

Fig. 112. Flat cell (F) showing a complicated contour on the spine trabecula (T).

Fig. 113. Cells distributed in the organic stereom of a spine. T: trabeculae

Fig. 114. Fine fibrillar elements of thin cytoplasmic processes twining around the trabeculae (T) and interconnecting the cells like a stretched cobweb.

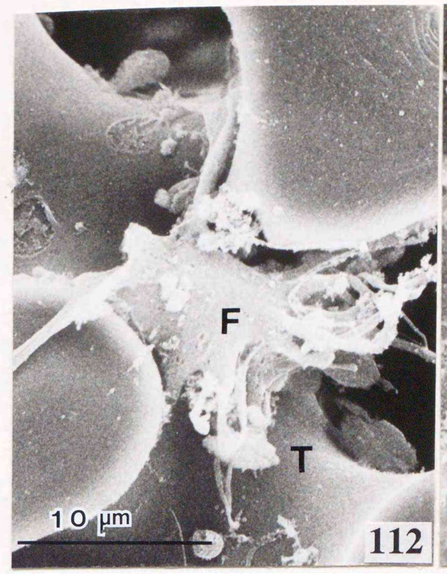

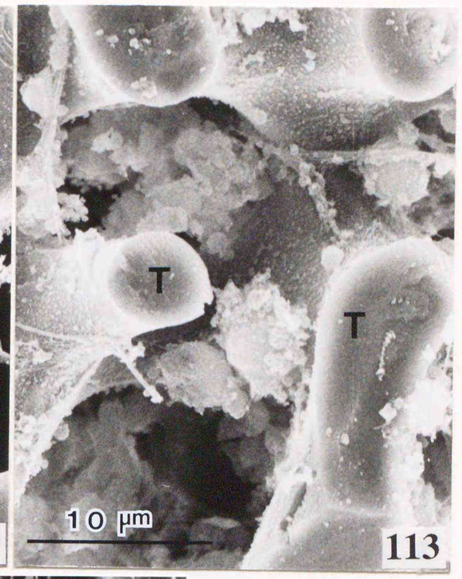

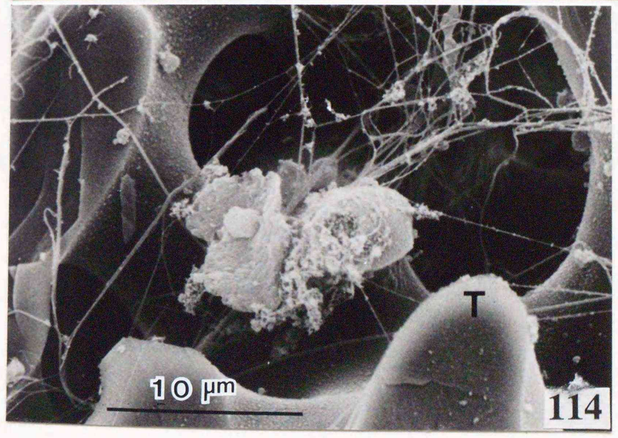

Fig. 115. LM photograph of bladder leucocytes. X 1700.

Fig. 116. LM photograph of filiform leucocytes. X 1250.

Fig. 117. LM photograph of coelomocytes in dish culture. X 800.

Fig. 118. TEM photograph of a filiform leucocyte. The cell elongates numerous cytoplasmic processes in every direction. X 6000.

Fig. 119. TEM photograph of a bladder leucocyte elongating the cytoplasmic processes to form large bladder-like envelopes. X 7200.

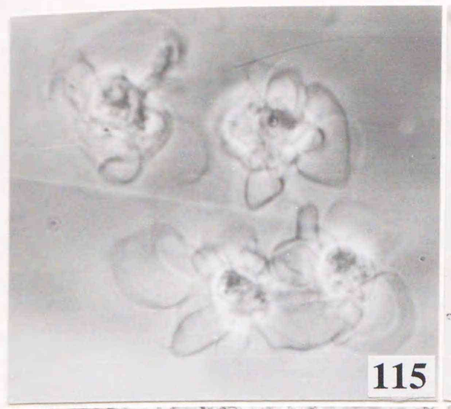
115

116

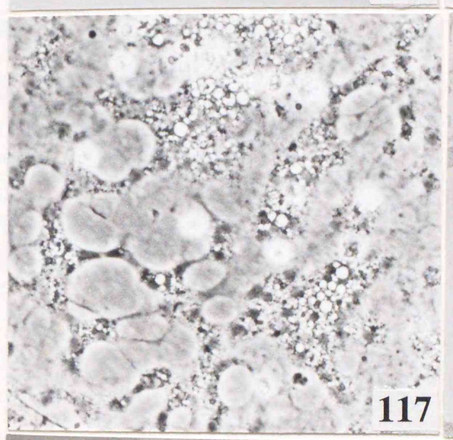
117

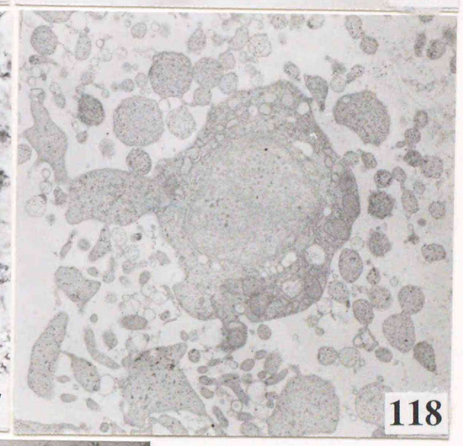
118

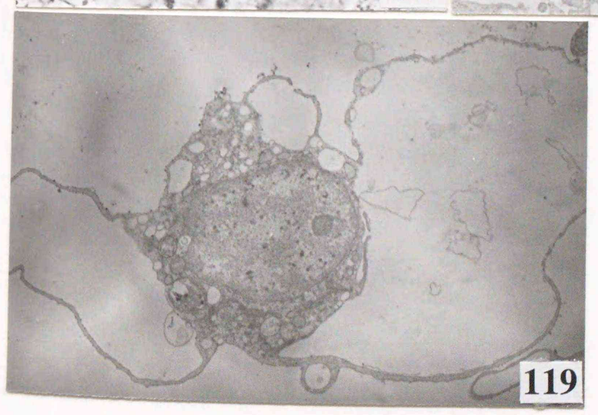
119

Figs. 120-123. TEM graphs of the phagocytic leucocytes in coelomic fuid.

Fig. 120. Bladder leucocyte (L) having many vacuoles of various sizes. X 5500.

Fig. 121. Bladder leucocyte (L) having well-developed Golgi complex, mitochondria, residual bodies and numerous vesicles. X 13500.

Fig. 122. Bladder leucocyte (L) ingesting a spherule cell (S). X 7000.

Fig. 123. Bladder leucocyte (L) holding a strange unknown structure (St). X 8000.

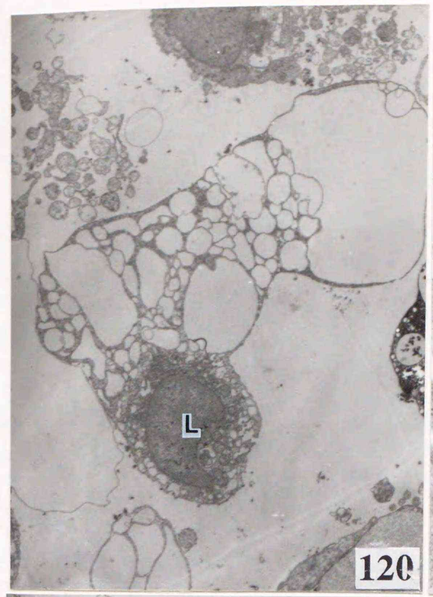

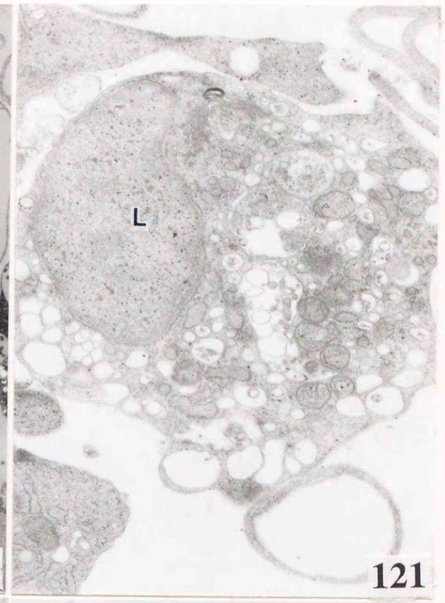

Fig. 124a. LM photograph of a spherule cell (S) in coelomic fluid. Methylene blue-azur II, X 1000.

Fig. 124b, TEM photographs of a spherule cell (S) in coelomic fluid. Three types of membrane-coated spherical inclusions are observed in the cytoplasm. X 9300.

Fig. 125. TEM photograph of a spherule cell having membrane-coated vesicular inclusions. Fine fibrous materials are observed in the spaces between the contents and the coating membrane. X 16000.

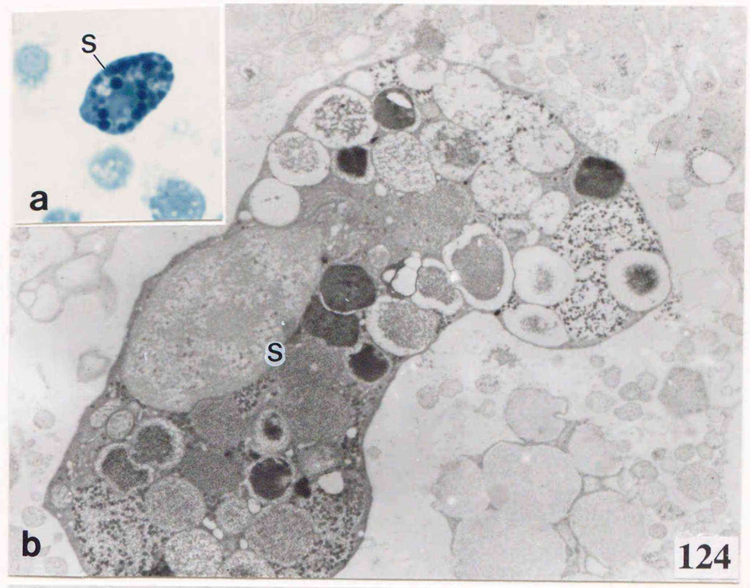

Figs. 126, 127. TEM photographs of the spherule cell in coelomic fluid.

Fig. 126. Spherical inclusions releasing the contents. X 15000.

Fig. 127. Spherule cell having emptied vacuoles. X 11000.

Figs. 128, 129. TEM photographs of the vibratile cell in coelomic fluid.

Fig. 128. Vibratile cell (V) occupied by many spherical iclusions. X 7200.

Fig. 129. High magnification of inclusions filled with finely fibrous and electron dense materials. X 13500.

126

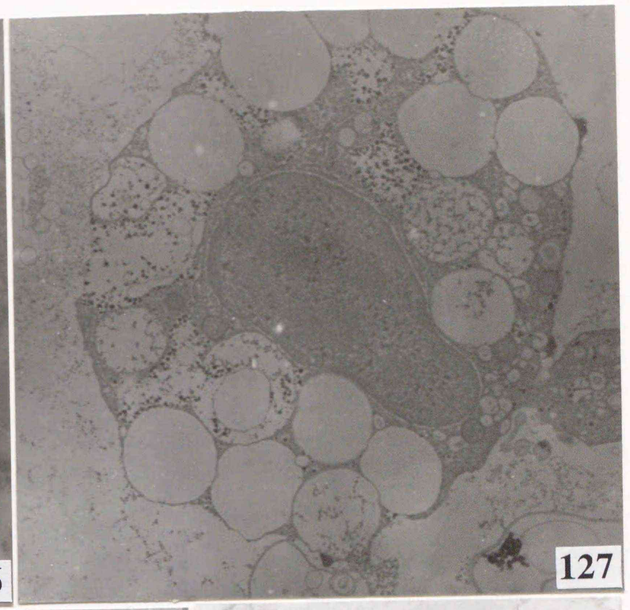
127

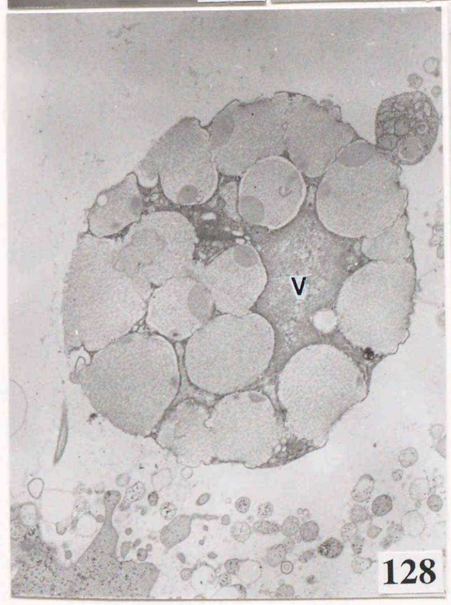

128

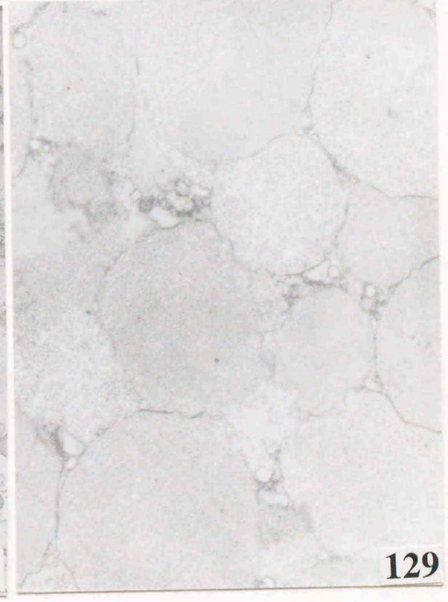
129

Fig. 130. TEM photograph of a hyaline cell in coelomic fluid. X 10800.

Figs. 131-133. TEM photographs of clotting coelomocytes <u>in vitro</u>.

Fig. 131. Leucocytes (L) are forming a delicate meshwork by their elongated cytoplasm and envelopes (E) X 4500.

Fig. 132. The delicate envelopes (E) extruded from the cytoplasmic processes of leucocytes (L). X 5400.

Fig. 133. Highly magnificated envelope (E) extruded from a cytoplsmic process of a leucocyte (L). X 24200.

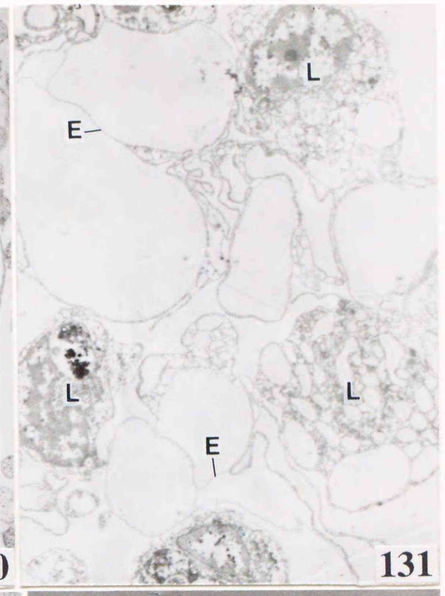

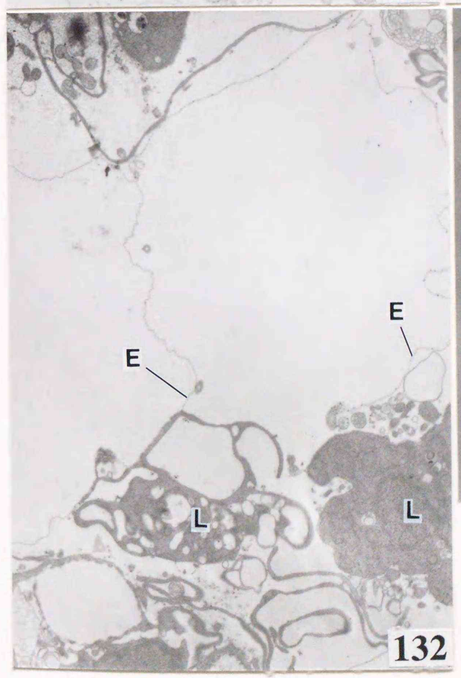

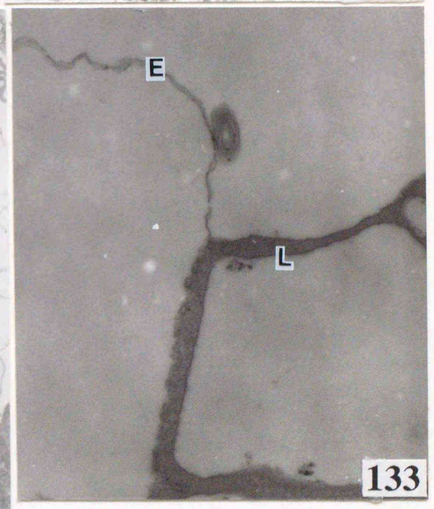

Figs. 134-137. TEM photographs of clotting coelomocytes in vitro.

Fig. 134. Fine granular or fibrous materials (*) in a space enclosed by envelopes (E) elongated from a leucocyte (L). X 18000.

Fig. 135. Bladder (B) and filiform (F) leucocytes trapped in a delicate framework of envelopes (E). X 5000.

Fig. 136. Cell having the dark-toned cytoplasm attached to cytoplasmic envelope (E) with its vacuolar membrane (arrow). X 8000.

Fig. 137. Spherule cell (S) trapped by the envelope (E), which attached closely to the cell membrane (arrow). X 7000.

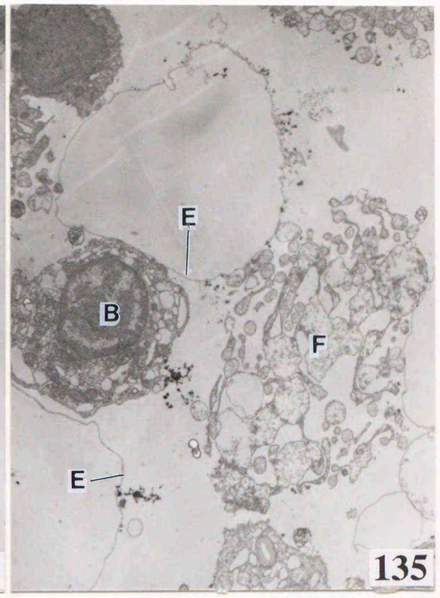

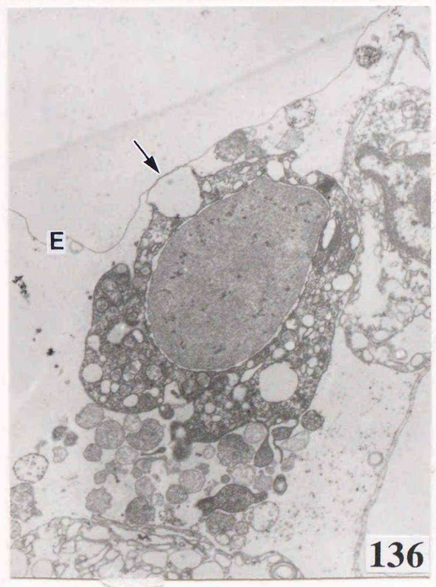

Fig. 138. TEM photograph of clotting coelomocytes <u>in vitro</u> showing an organic stereom-like structure consisted of various type cells and their debris. E: envelopes; L: leucocyte; S: spherule cells. X 4700.

Fig. 139. TEM photograph of a degenerating vibratile cell in a clot. The cell membrane (arrow) is fusing into a part of meshwork of envelopes (E). The cell inclusions are degrading in the internal space (*) of the meshwork. X 9000.

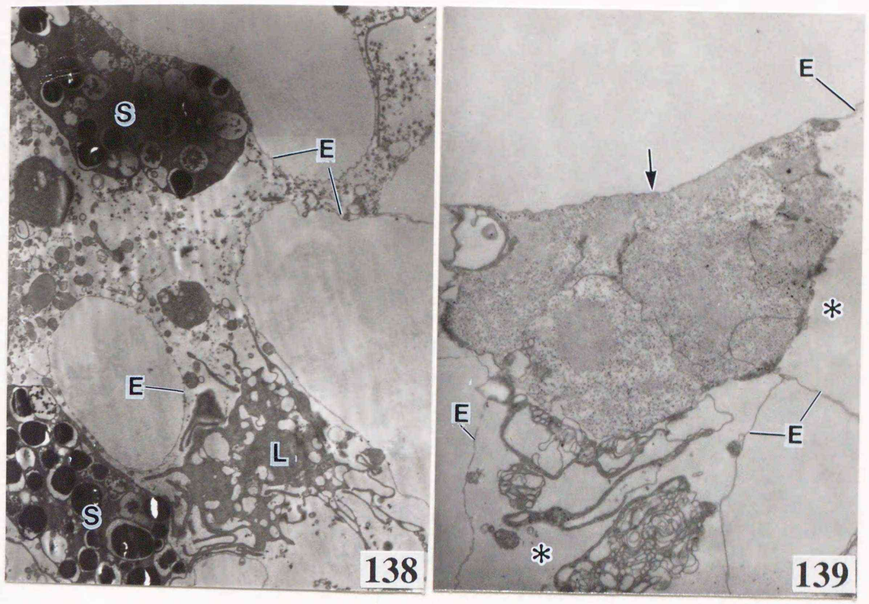

Fig. 140. LM photograph of test with a square window (*) made by removing the test fragment to induce the test regeneration. X 2.5.

Fig. 141. LM photograph of two-week-old blastema in the regenerating test plate. In the dermal connective tissue are the fibrous (f), the prestereomal (ps), and the stereomal(st) regions. The epidermis (ep) and the coelomic epithelium (cp) are seen covering the outer and the inner surfaces, respectively. Azan, X 210.

Fig. 142. TEM photograph of collagen fibers (cf) distributed at the prestereomal region. X 32000.

Fig. 143. TEM photograph of collagen fibers with calcifying vacuoles (cvo) appearing around them. X 20000

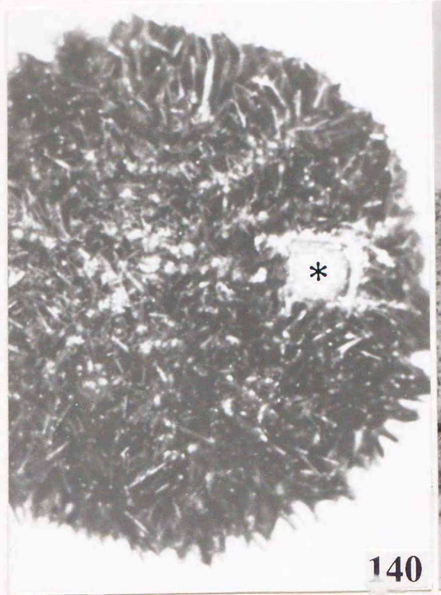

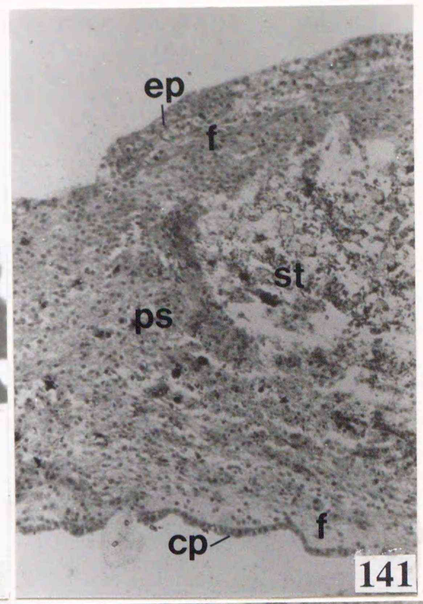

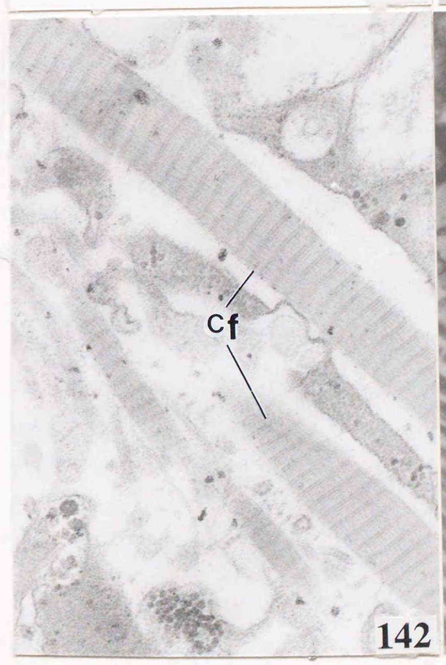

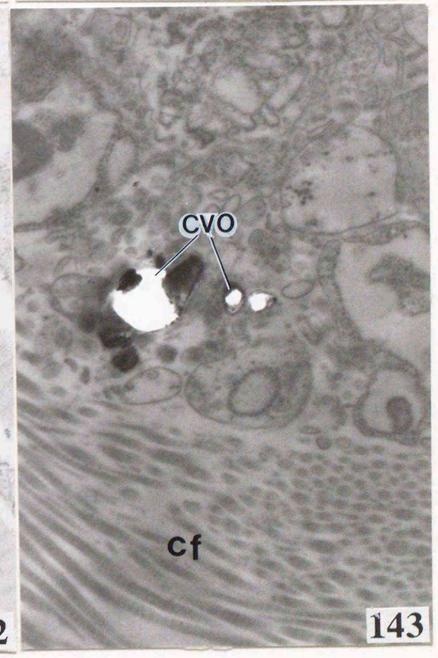

Fig. 144. LM photograph of prestereomal region near the fibrous region of the blastema. Spherule cells (s) and other coelomocytes are accumulating. Methylene blue-azur II, X 1000.

Fig. 145. TEM photograph of the area shown in Figure 144. There are still fibroblasts (Fb) among plasmodial cells. Finefibrils (ff) predominate in the intercellular spaces. X 5650.

Fig. 146. LM photograph of multinucleated cell (mc) indicating syncytium formation in the prestereomal region of the blastema. Methylene blue-azur II, X 1400.

Fig. 147. LM potograph of mineral deposits represented by holes (c) in a syncytial cell (sc). The cytoplasm shows intense azurophilia. Methylene blue-azur II. X 1460.

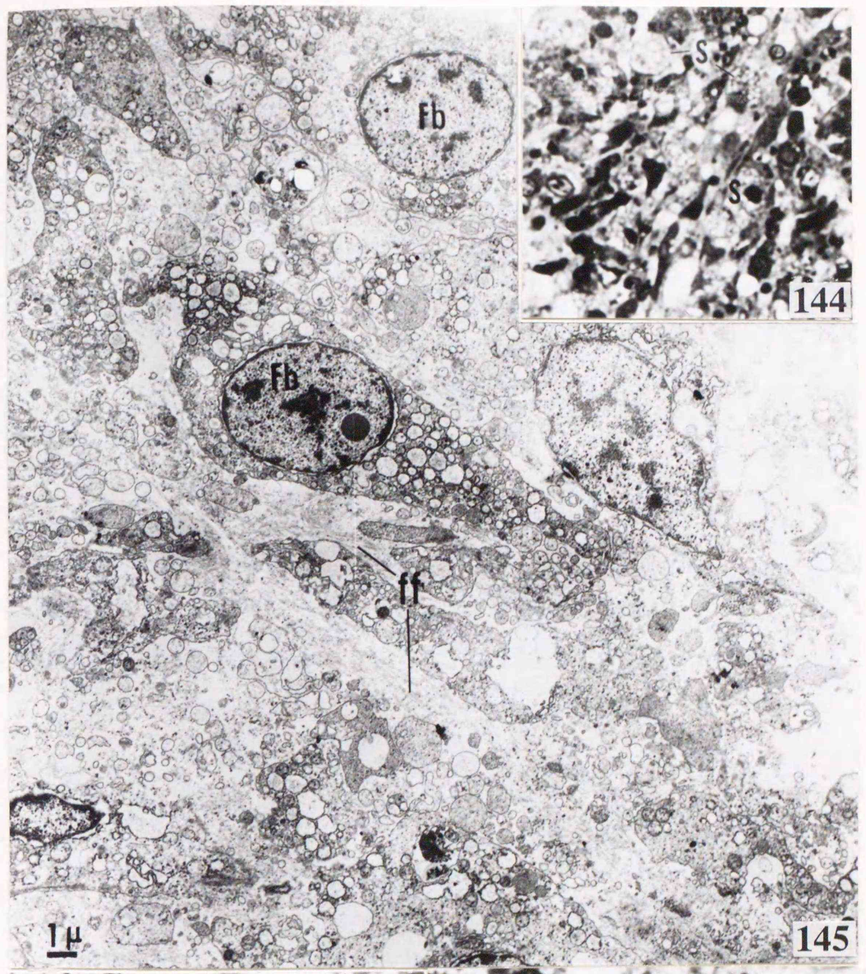

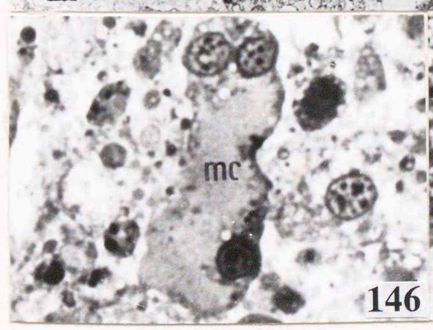

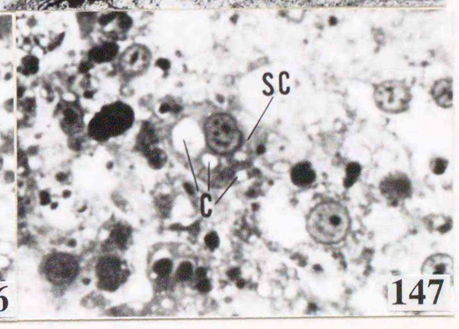

Fig. 148. LM phtograph of azurophilic granules (Ag) scattered in syncytial cells in the prestereomal region. Methylene blue-azur II, X 400.

Fig. 149. TEM photograph of a number of secondary lysosomes (L) appearing in the cytoplasm of a syncytium. Some membrane-bound bodies (mb) are associated with the cell body. G: Golgi complex; N: nucleus. X 8900.

Fig. 150. TEM photograph of abundant membrane-bound bodies (mb) found in the extracellular space of the prestereomal region. Electron-dense granules are noted in most of the bodies. X 13500.

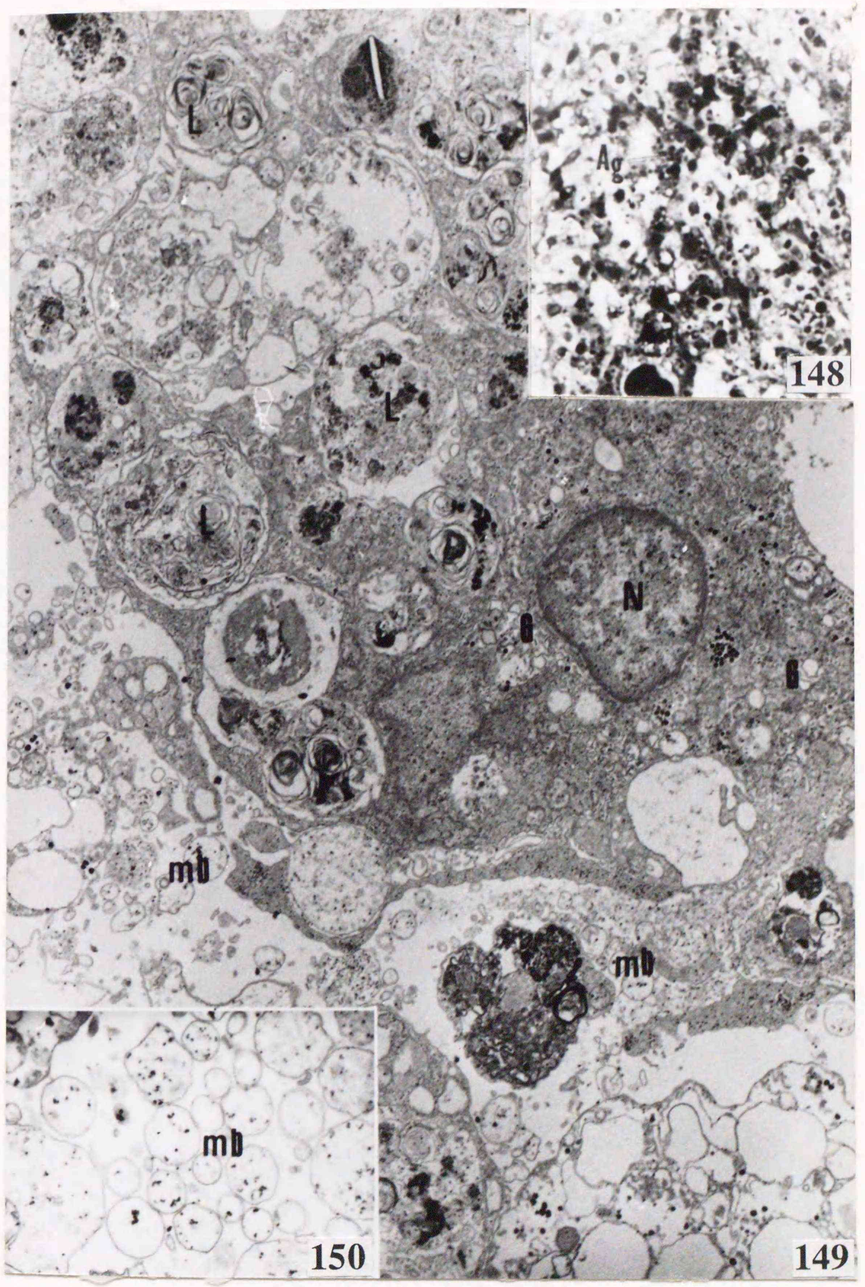

Fig. 151. TEM photograph of small crystalline concretions (c) developing in calcifying vacuoles (cvo). Mitochondria (Mt) and membrane-bound bodies (mb) reveal dense granules. L: lysosome; N: nucleus. X 11000.

Fig. 152. TEM photograph of sclerocyte having many calcifying vacuoles. X 11000.

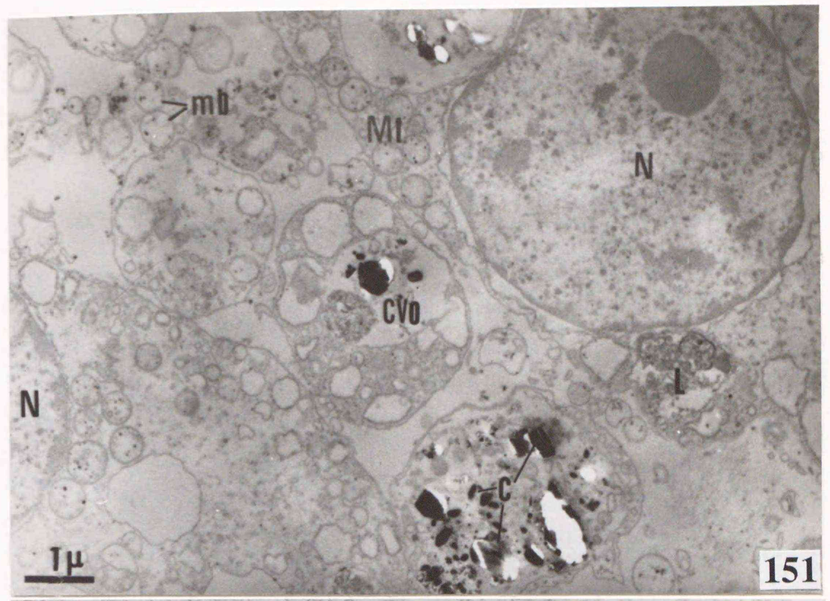

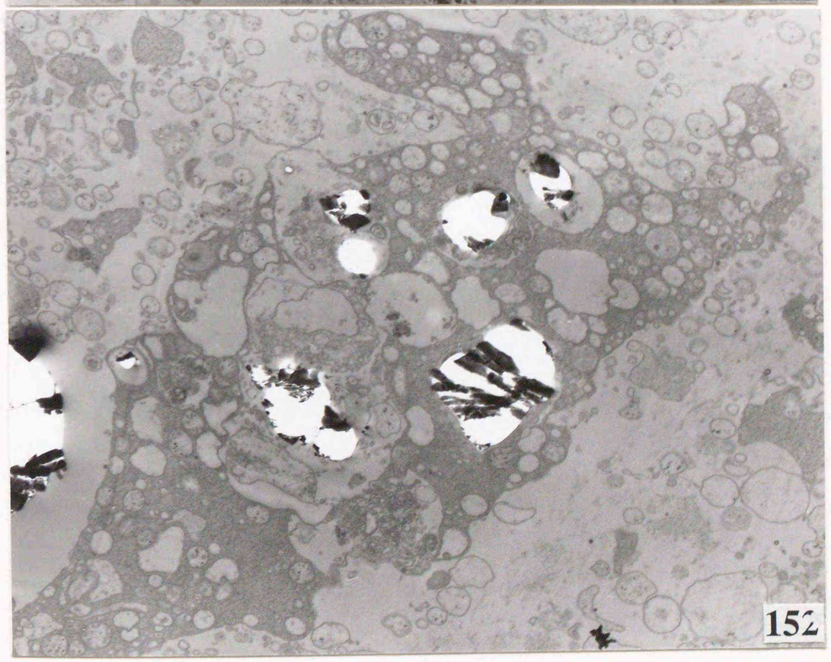

Figs. 153-157. TEM photographs of the regenerating test plate.

Fig. 153. Calcifying vacuole containing small polygonal crystallites (c) and moderaely dense vesicles (cv). Some of the vesicles are seen in close contact with crystallites (arrows). X 20000.

Fig. 154. Large crystal (c) left intact in the cytoplasm showing no membranous envelope. X 20000.

Fig. 155. Two crystalltes (c) enclosed by membrane (cvm) of a vacuole (cvo). Membranous structures are visible at the sites where the crystallites have been partly dissolved (arrows). Small vesicles (cv) and dense amorphous material are also contained in the vacuole. X 33500.

Fig. 156. Small calcifying vacuole containing polygonal crystallites (c), membrane-bound vesciles (cv), and amorphous material. X 29000.

Fig. 157. Small vesicles (cv) in close associatin with crystallites (c) which have been dissolved from the section. cvm: membrane of calcifying vacuole. X 39000.

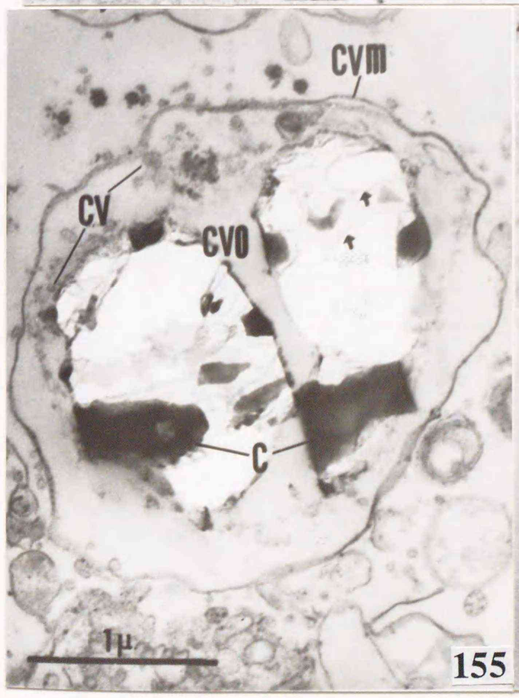

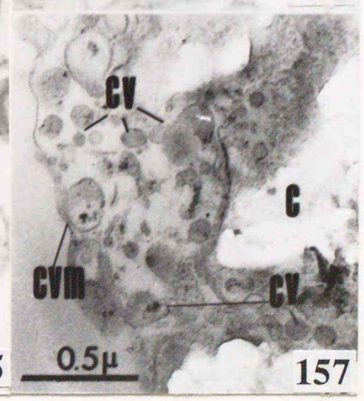

Figs. 158-160. TEM photograph of the regnerating test plate.

Fig. 158. A light sclerocyte having a calcifying vacuole (cvo) in close association with a Golgi complex (G). The cytoplasm is less compact. c: crystallite; cv: vesicles in calcifying vacuole; Mt: mitochondria; N: nucleus. X 25600.

Fig. 159. Calcifying vacuole containing small vesicles (cv) and granular material. Vesicles just contiguous to the crystallite (c) are indicated by an arrow. Mitochondria (Mt) having dense granules are seen at the outside of the vacuole (cvo). cvm: membrane of calcifying vacuole. X 35600.

Fig. 160. Triangular crystallite (c) developed to the nearly utmost extent of the calcifying vacuole (cvo). Membranous structures in parallel array are left after the crystallite has been dissolved (short arrows). Mt: mitochondria. X 25600.

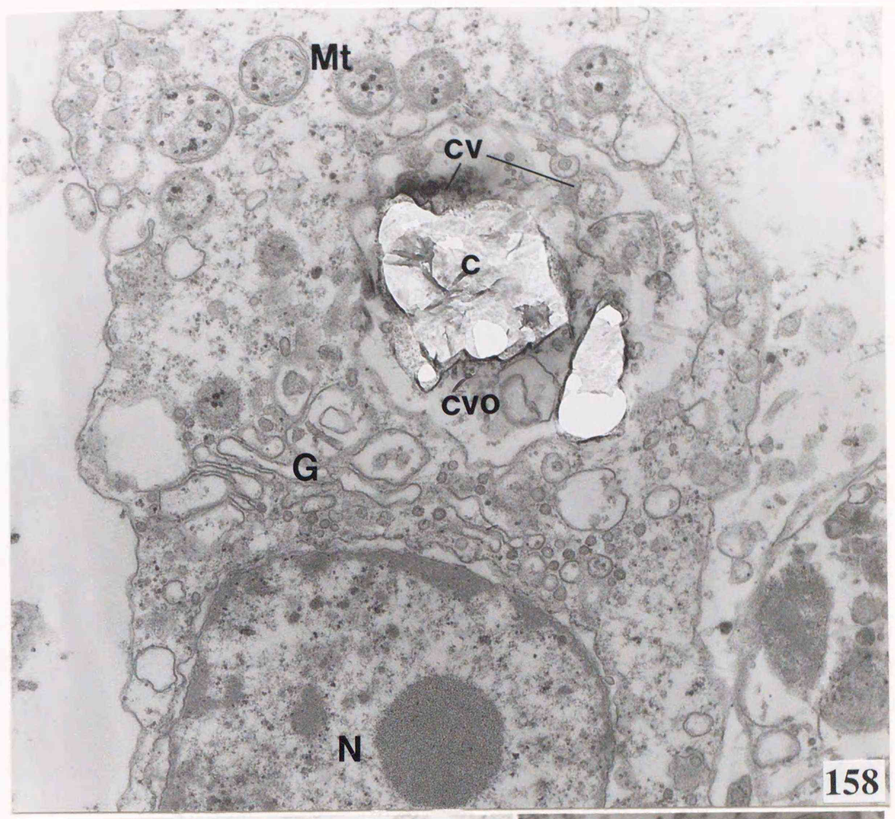

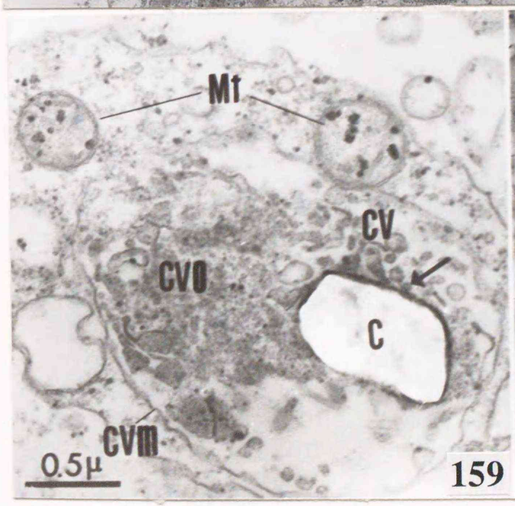

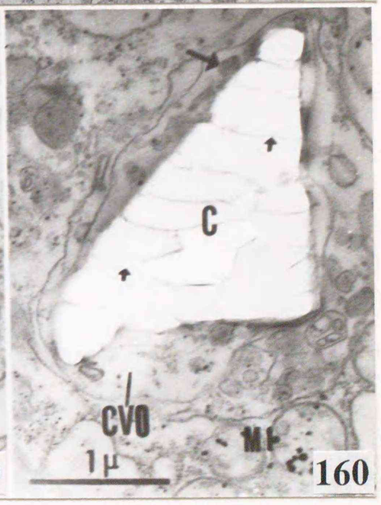

Figs. 161-163. TEM photographs of the regenerating test plate.

Fig. 161. Dark syncytial sclerocyte. cvo: calcifying vacuole; ff: fine fibrils; L: lysosome: mb: membrane-bound bodies; Mt: mitochndria; N: nucleus. X 7200.

Fig. 162. Gycogen field (Gl) found in a dark sclerocyte. mb: membrane-bound bodies. X 11000.

Fig. 163. Golgi complex in a dark sclerocyte. Gl: glycogen granules; Gv: Golgi vesciles; Gvo: Golgi vacuoles; Mt: mitochondria. X 33000.

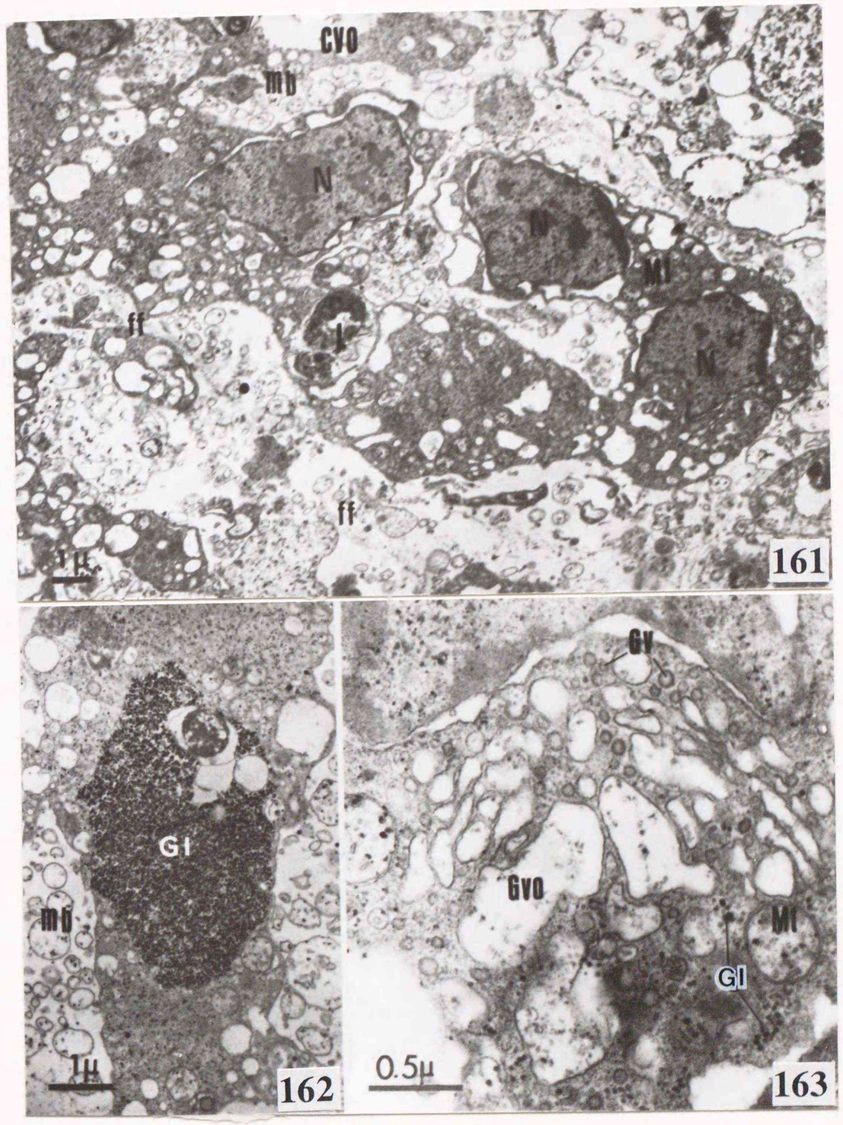

Figs. 164-167. LM photographs of semithin sections.
Methylene blue-azur II.

Fig. 164. Growing crystals (c) in a syncytium or syncytia. s: spherule cell. X 1320.

Fig. 165. Growing stereomal structure (st) enclosed by the prestereomal region (ps). c: crystals. X 350.

Fig. 166. Nearly completed stereomal structure in a three-week-old regenerate. s: spherule cell. X 550.

Fig. 167. Stereom of the normal test. s: spherule cells. X 550.

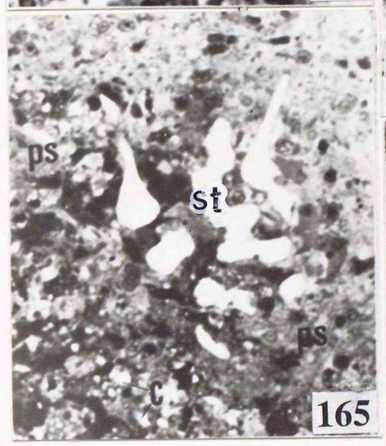

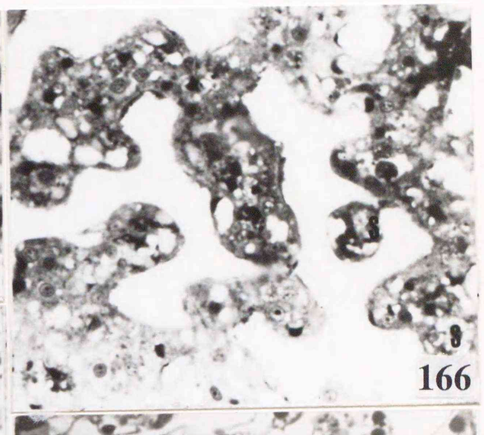

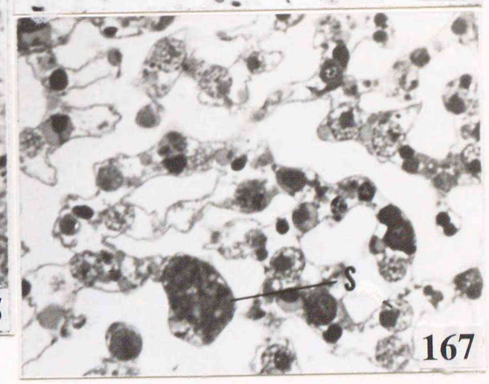

Fig. 168. LM photograph of a two-week-old regeneratig spine showing a prevalent accumulation of cells with many small crystals (c) visible as holes in the tip region. B: basal region; ep:epidermis; ct: connective tissue. Methylene blue-azur II, X 330.

Figs. 169, 170. TEM photographs of sclerocytes.

Fig. 169. Spine sclerocyte containing crystals (c) in calcifying vacuoles (cvo). L: lipid-like granules; N: nucleus. X 8000.

Fig. 170. Spine sclerocyte having well-developed Golgi complex (G). c: crystal; cvo: calcifying vacuole; Mt: mitochondria; N. nucleus. X 20000.

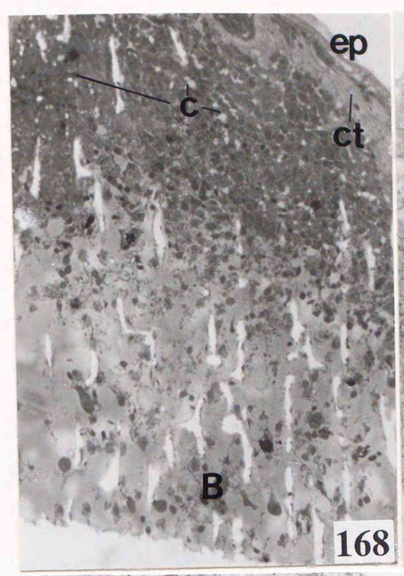

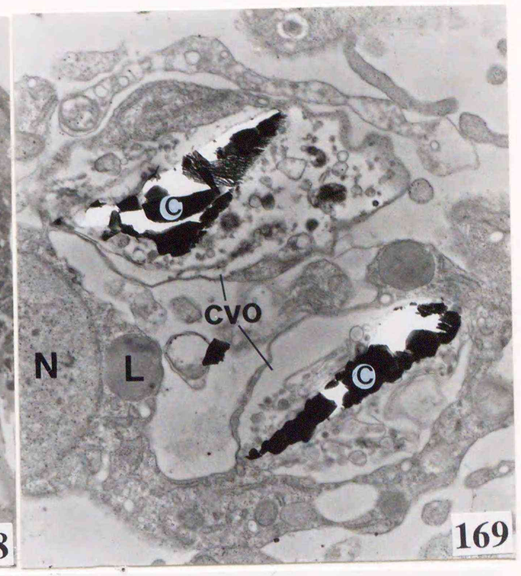

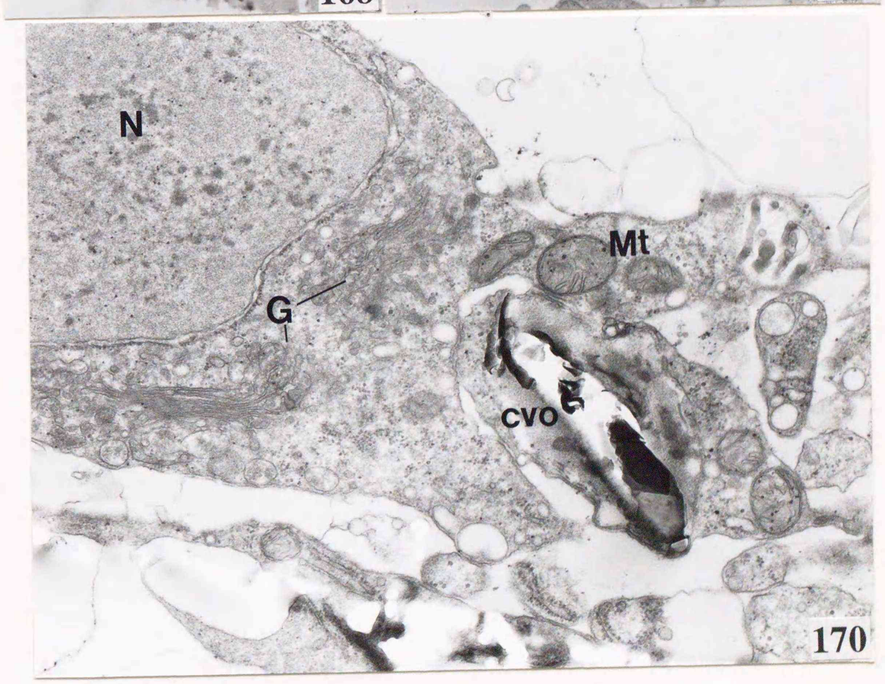

Figs. 171, 172. TEM photographs of spine sclerocytes.

Fig. 171. Cytoplasm of the sclerocyte (S) having crystal (c) of several microns. The cytoplasm enclosing the crystal has nemerous vescicular structures. X 11000.

Fig. 172. Cytoplasm with the crystal (c) having multivesicular bodies and residual bodies. S: spine sclerocyte. x 12000.

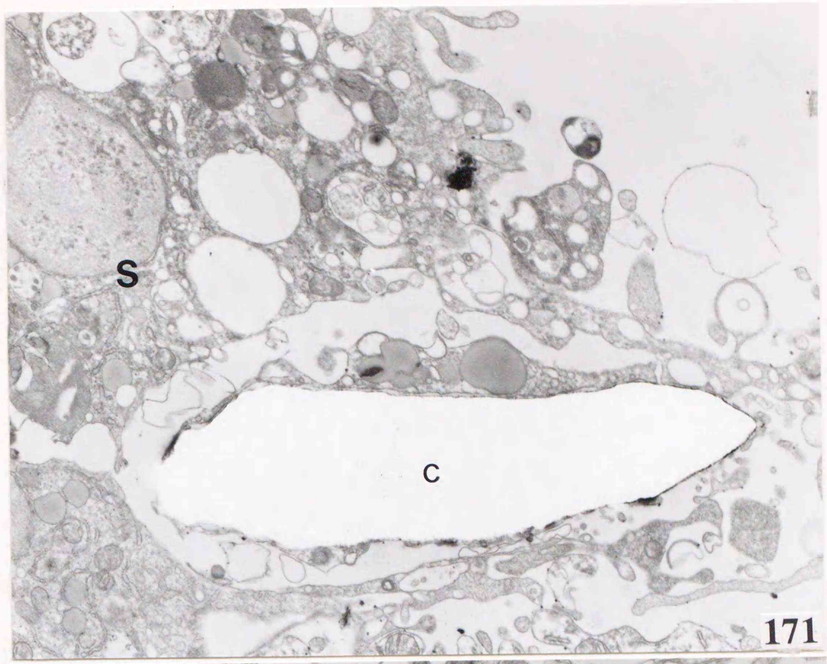

171

172

Figs. 173-175. TEM graphs of regenerating spines.

Fig. 173. Regenerating spine tissue into which ruthenium red (RR) was introduced. No RR particles are visible inside the calcifying vacuole (cvo). X 8700.

Fig. 174. Large extravacuolar crystal (c) covered by elongated thin cytoplasmic extensions of spine sclerocytes (S). The cytoplasmic envelop is indistinct in some parts (arrows). X 2700.

Fig. 175. Large crystal (c) enclosed by a large space between the cytoplasmic extensions. A part of the crystal surface in contact with only the plasma membrane is indicated by arrow. X 8500.

173

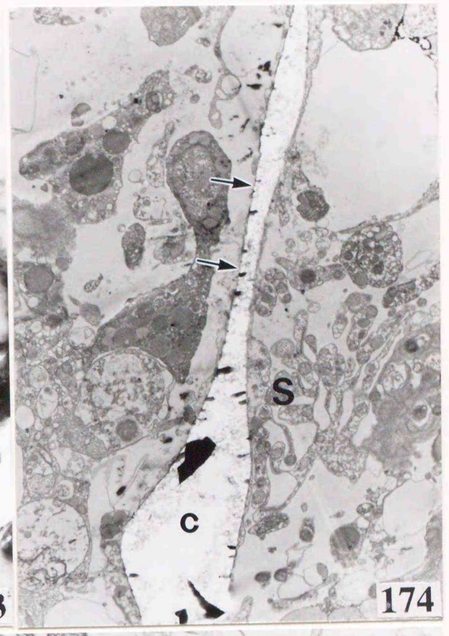

174

175

Figs. 176-179. TEM photographs of the regenerating spine.

Fig. 176. Spine sclerocyte (S) attached to a large crystal (c) by an extension of the loose cytoplasm with a number of vesicular structures of various sizes. X 6500.

Fig. 177. Surface of a large crystal (c) covered by a thin cytoplasmic extension (E) of a spine sclerocyte (S). X 7800.

Fig. 178. Part of a large crystal (c) having no cytoplasmic envelop on the surface. Vesicles (V) of various sizes are aligned along the crystal surface. X 45000.

Fig. 179. Ruthenium red particles (RR) found in the interstitial space and on the crystal (c) surface where only vesicles (V) are aligned as shown in Fig. 178. X 19000.

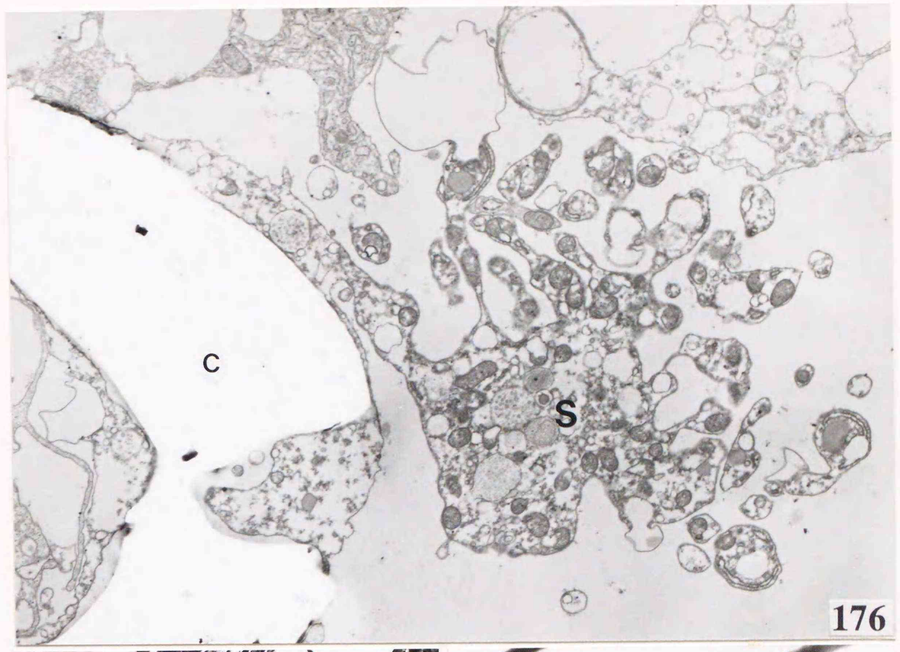

176

177

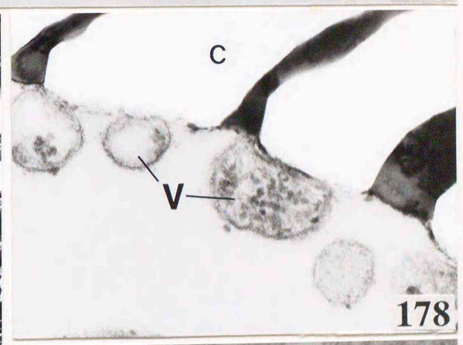

178

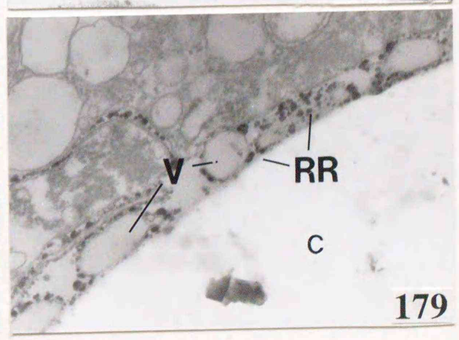

179

Fig. 180. TEM photograph of a sclerocyte (S) and a presclerocyte (PS). The preosclerocyte is contiguous to the cytoplasm of a matured spine sclerocyte covering large crystal (c). G: Golgi complex. X 17000.
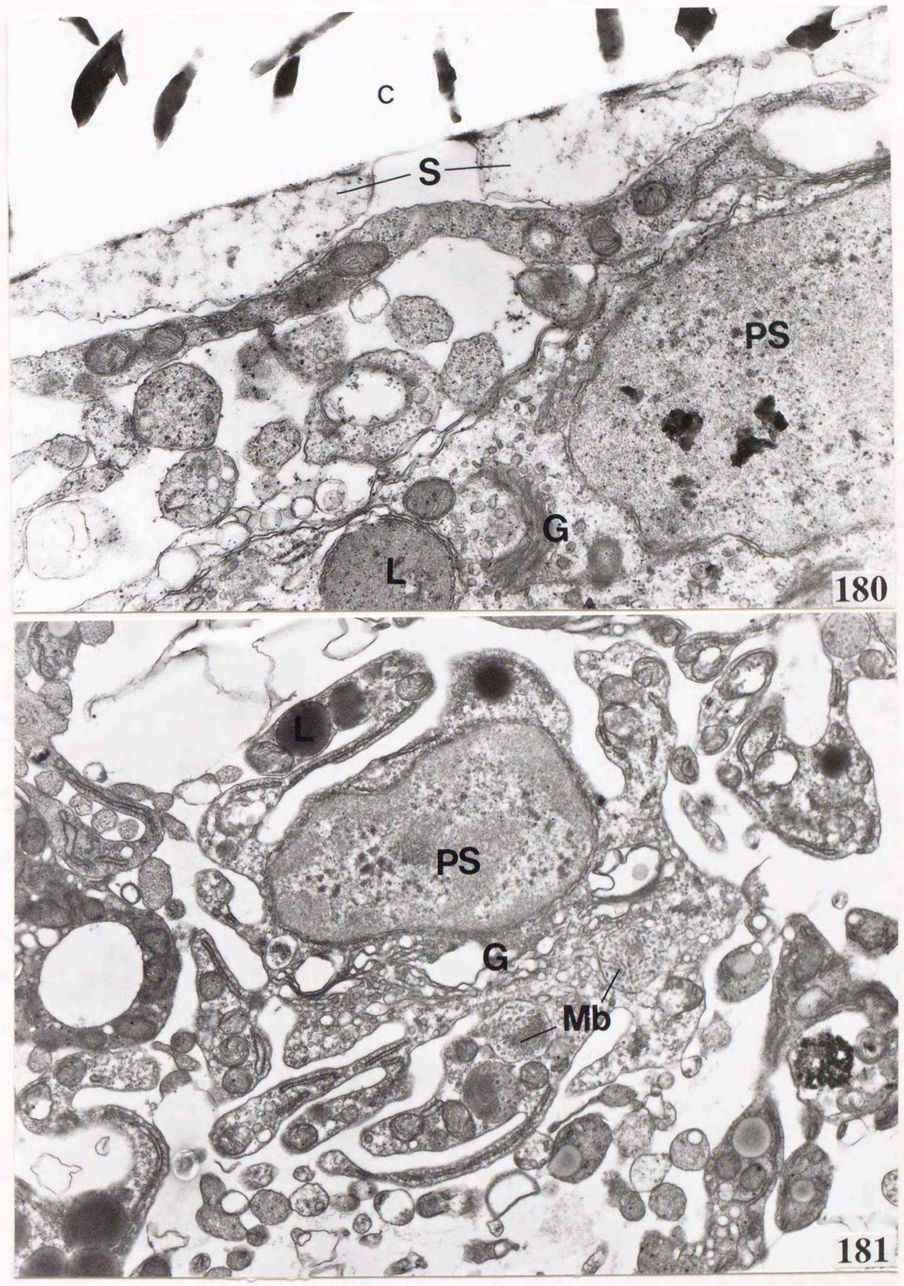
Fig. 181. TEM photograph of a presclerocyte. The presclerocyte (PS) of the regenerating spine showing numerous cytoplasmic extensions. G: Golgi complex; Mb: multivesicular bodies; L: lipid-like granule. X 10000.